

กำเนิดศิลาของหินแอมฟิโบไลต์ในพื้นที่อำเภอวังน้ำเขียว จังหวัดนครราชสีมา

นางสาววนัชรวรรณ ฮั่นเย็ก

วิทยานิพนธ์นี้เป็นส่วนหนึ่งของการศึกษาตามหลักสูตรปริญญาวิทยาศาสตรมหาบัณฑิต

สาขาวิชาธรณีวิทยา ภาควิชาธรณีวิทยา

คณะวิทยาศาสตร์ จุฬาลงกรณ์มหาวิทยาลัย

ปีการศึกษา 2555

ลิขสิทธิ์ของจุฬาลงกรณ์มหาวิทยาลัย

บทคัดย่อและแฟ้มข้อมูลฉบับเต็มของวิทยานิพนธ์ตั้งแต่ปีการศึกษา 2554 ที่ให้บริการในคลังปัญญาจุฬาฯ (CUIR)

เป็นแฟ้มข้อมูลของนิสิตเจ้าของวิทยานิพนธ์ที่ส่งผ่านทางบัณฑิตวิทยาลัย

The abstract and full text of theses from the academic year 2011 in Chulalongkorn University Intellectual Repository (CUIR)

are the thesis authors' files submitted through the Graduate School.

PETROGENESIS OF AMPHIBOLITES IN AMPHOE WANG NAM KHIAO AREA,
CHANGWAT NAKHON RATCHASIMA

Miss Vanachawan Hunyek

A Thesis Submitted in Partial Fulfillment of the Requirements
for the Degree of Master of Science Program in Geology

Department of Geology

Faculty of Science

Chulalongkorn University

Academic Year 2012

Copyright of Chulalongkorn University

Thesis Title Petrogenesis of Amphibolites in Amphoe Wang Nam Khiao Area,
Changwat Nakhon Ratchasima

By Miss Vanachawan Hunyek

Field of Study Geology

Thesis Advisor Assistant Professor Chakkaphan Sutthirat, Ph.D.

Accepted by the Faculty of Science, Chulalongkorn University in Partial
Fulfillment of the Requirements for the Master's Degree

.....Dean of the Faculty of Science
(Professor Supot Hannongbua, Dr. rer. nat.)

THESIS COMMITTEE

.....Chairman
(Associate Professor Montri Choowong, Ph.D.)

.....Thesis Advisor
(Assistant Professor Chakkaphan Sutthirat, Ph.D.)

.....Examiner
(Associate Professor Punya Charusiri, Ph.D.)

.....External Examiner
(Mr. Suvapak Imsamut, M.Sc.)

วันชววรรณ ฮันเย็ก : กำเนิดศิลาของหินแอมฟิโบไลต์ในพื้นที่อำเภอวังน้ำเขียว จังหวัดนครราชสีมา (PETROGENESIS OF AMPHIBOLITES IN AMPHOE WANG NAM KHIAO AREA, CHANGWAT NAKHON RATCHASIMA). อ.ที่ปรึกษาวิทยานิพนธ์
หลัก : ผศ.ดร.จักรพันธ์ สุทธิรัตน์, 92 หน้า.

หินแอมฟิโบไลต์ในพื้นที่ศึกษาอำเภอวังน้ำเขียวกระจายตัวเป็นหย่อมๆ กลุ่มพื้นที่กว่า 65 ตร.กม. ในบริเวณบ้านยุบอีปุ่นและบ้านหนองไม้แดง ตัวอย่างหินทั้งหมดกว่า 40 ตัวอย่าง ถูกนำมาใช้ศึกษาสัณฐานวิทยา วิเคราะห์ธรณีเคมีและเคมีแร่ สามารถแบ่งหินได้เป็น 3 กลุ่ม คือ หินแอมฟิโบไลต์เนื้อเม็ดผลึกหยาบหินแอมฟิโบไลต์ชั้นสลับ และหินแอมฟิโบไลต์มีกมาไทต์ สำหรับการศึกษาด้านธรณีเคมี พบว่าหินแอมฟิโบไลต์อาจมีต้นกำเนิดหินอัคนีชนิดเมฟิกที่พบเป็นส่วนหนึ่งของแผ่นเปลือกโลกมหาสมุทร โดยลักษณะทางเคมีระบุว่าหินกลุ่มนี้มีองค์ประกอบเริ่มต้นจาก E-MORB ที่มีความสัมพันธ์กับแนวภูเขาไฟโค้งจากผลการศึกษาดูร่องรอยและธาตุหายากก็ระบุว่าหินแอมฟิโบไลต์มีต้นกำเนิดมาจาก E-MORB นอกจากนี้การคำนวณอุณหภูมิและความดันพบว่าจัดอยู่ในชุดหินแปร ที่มีอุณหภูมิและความดันประมาณ 686 ± 32 องศาเซลเซียส 4.2 ± 1 กิโลบาร์

ภาควิชา.....ธรณีวิทยา..... ลายมือชื่อ.....
สาขาวิชา.....ธรณีวิทยา..... ลายมือชื่อ อ.ที่ปรึกษาวิทยานิพนธ์หลัก.....
ปีการศึกษา.....2555.....

##5272516023 : MAJOR Geology

KEYWORDS : AMPHIBOLITES, ARC, E-MORB, PETROGENESIS

VANACHAWAN HUNYEK : PETROGENESIS OF AMPHIBOLITES IN
 AMPHOE WANG NAM KHIAO AREA, CHANGWAT NAKHON
 RATCHASIMA. ADVISOR : ASST. PROF. CHAKKAPHAN SUTTHIRAT, Ph.D.,
 92 pp.

Amphibolites around Ban Yup I Pun and Ban Nong Mai Daeng in Wang Nam Khiao area have sparsely exposed within an area of about 65 km². Over 40 rock samples were collected from various amphibolite exposures, for petrographic investigation, whole-rock geochemical and mineral chemistry analyses. Based on petrographic features, these rock samples can be classified as coarse-grained granular amphibolites, layered amphibolites and migmatitic amphibolites. Geochemically, these amphibolites appear to have mafic igneous origin with a signature of oceanic remnant; moreover, indication of E-MORB-type within arc affinities is also observed for their initial provenance. Chondrite-normalized rare earth element (REE) and other trace element patterns supported that amphibolites should have been derived from island arc-related E-MORB. Regarding to P-T calculations, these amphibolites clearly belong to amphibolites facies with estimated P-T of about 686±32°C and 4.2± 1 Kbar.

Department.....Geology..... Student's Signature.....

Field of Study.....Geology..... Advisor's Signature.....

Academic Year.....2012.....

ACKNOWLEDGEMENTS

This research project has been supported by 90th Year Chulalongkorn Scholarship. The authors would like to give a deep appreciation to Assist. Prof. Dr. Chakkaphan Sutthirat and Assist. Prof. Veerote Daorerk for advices and suggestions in this study. Thank for Piyaphong Chainrai, Jensarin Vivatpinyo, Chutima Nudam and all geology students at Chulalongkorn University who have assisted in the field investigation and sample collection. Special thank is given to Apichart Piyarom from Department of Mineral Resources for RTP-map training and Tawatchai Chualaowanich from Department of Mineral Resources for PT-condition training. Sample preparations and laboratory works were supported by Prajin Thongchum, Suriya Chokmoh, Jiraprapa Neampan, Bunchong Puangthong and Sopit Poompuang. Finally, the first author would like to thank for the Development and Promotion of Science and technology Talents project (DPST) for scholarship during her study in MSc program at Department of Geology, Faculty of Science, Chulalongkorn University.

CONTENTS

	page
ABSTRACT IN THAI.....	iv
ABSTRACT IN ENGLISH	v
ACKNOWLEDGEMENTS.....	vi
CONTENTS.....	vii
LIST OF TABLES.....	x
LIST OF FIGURES	xi
CHAPTER I INTRODUCTION	1
1.1 General Statement	1
1.2 Scope of Work.....	5
1.3 Objective	9
1.4 Methodology	9
CHAPTER II GENERAL GEOLOGY	11
2.1 Geologic Setting	11
2.2 Tectonic Evolution.....	13
CHAPTER III PETROGRAPHY	16
3.1 Granular Amphibolites	18
3.2 Migmatitic Amphibolites.....	23

3.3 Layered Amphibolites	26
3.4 Other Associated Rocks.....	27
CHAPTER IV WHOLE-ROCK GEOCHEMISTRY AND MINERAL CHEMISTRY	29
4.1 WHOLE-ROCK GEOCHEMISTRY	29
4.1.1 Major Oxides	29
4.1.2 Trace Elements.....	34
4.1.3 Rare Earth Elements	41
4.2 MINERAL CHEMISTRY	46
4.2.1 Amphiboles.....	46
4.2.2 Plagioclase	49
4.2.3 Pyroxene	53
CHAPTER V DISCUSSIONS AND CONCLUSIONS	58
5.1 Protolith and Initial Provenance of Amphibolite.....	58
5.2 Metamorphism	63
5.3 Ancient Tectonic Setting.....	67
5.4 Conclusions.....	69
REFERENCES.....	71
APPENDICES.....	78
Appendix A.....	79

page

Appendix B.....	80
Appendix C.....	88
Appendix D.....	89
BIOGRAPHY	92

LIST OF TABLES

Table	page
3.1 Mineral assemblages of amphibolites investigated under this study.	19
4.1 Whole-rock analyses of amphibolites and pyroxenite from Wang Nam Khiao, Nakhon Ratchasima. Major and minor oxides (% wt) yielded from XRF analysis and trace elements (ppm) obtained from ICP-MS analysis.....	32
4.2 Representative EPMA analyses of amphiboles in rock samples collected from Wang Nam Khiao Area.	48
4.3 Representative EPMA analyses of feldspars found in various rock samples from Wang Nam Khiao Area.	52
4.4 Representative EPMA analyses of pyroxene found in different rock types collected from Wang Nam Khiao Area, Nakhon Ratchasima.	55
5.1 P-T estimation of amphibolites from Wang Nam Khiao Area, using Amp-TB of Ridolfi et al. (2009).....	65

LIST OF FIGURES

Figure	page
1.1 Geologic map showing emery and silimanite ores associated with hornblendite (redescribed as amphibolite in this study) in Ban Yup I Pun area (after Kumalachan and Yoemniyom, 1978).	5
1.2. Map of Thailand showing main tectonic blocks and their related sutures indicated by some crucial rocks; the study area is located in red rectangular (modified after Sutthirat, 2009).	7
1.3. Topographic map of the study area and localities of sample collection.	8
1.4 Reduction to the pole magnetic map (RTP-map) showing magnetic anomaly of the study area and sample localities (pink pentagons). This map was used to initiate boundary of the study area and to plan for sample collection.....	8
1.5 Flowchart showing methodology of this study.	10
2.1 Geologic map of study area and adjacency (after Putthaphiban et al., 1989).....	13
2.2 Schematic model of ophiolite suites (Monroe et al., 2007).	15
3.1. Topographic map (sheet 5337I and 5337IV) showing locations of rock sampling around Ban Nong Mai Daeng and Ban Yup I Pun areas in Amphoe Wang Nam Khiao, Changwat Nakhon Ratchasima.	16
3.2 Map of rock boundaries after topographic map and geologic map with cross section in the study area.	17

Figure	page
3.3 Coarse-grained amphibolites: A) mining quarry is a sample locality; B) a black specimen with very coarse-grained crystals; C) photomicrograph showing subhedral amphiboles with perfect cleavages and triple-junction boundary (XPL); D) subhedral plagioclase laths with obvious twining (XPL).....	20
3.4 Plagioclase-rich granular amphibolites: A) an outcrop showing clearly crystals of greenish black amphibole and white plagioclase that is typical feature of this rock group; B) a hand specimen presenting the mixing compositions between amphibole and plagioclase mostly show nematogranoblastic crystals; C and D) photomicrographs showing mineral compositions of plagioclase (Pl) and amphibole (Amp) with about 40-50% mode each (PPL).	22
3.5 Medium-grained granular amphibolites: A) a natural outcrop and its specimen (B) taken for this study; C) photomicrograph (PPL) showing medium-grained short nematoblastic amphiboles (Amp) are greenish color and clearly show cleavages and plagioclases (Pl) that have the same size with amphibole crystals; D) pyroxene (Pyx) with obvious right-angle cleavages is rarely found in this rock (XPL).....	23
3.6 A natural outcrop of migmatitic amphibolites (dark layers) interbedded white coarse-grained marble layers with usually about 30-50 cm thick.	24
3.7 Migmatitic amphibolites specimen (left). Photomicrographs (PPL) showing orientation of tiny pale green nematoblastic amphiboles (Amp) and white grey plagioclases (Pl) but the ratio between amphibole and plagioclase in each zone are different in each zone A, B and C.	25

Figure	page
3.8 Layered amphibolites: A) an outcrop showing clearly layers between black greenish minerals (amphibole) and white minerals (mostly plagioclase) that is typical feature of this rock group; B) a hand specimen presenting the layers of minerals; C) photomicrograph showing the layers between amphibole (Amp) and plagioclase (Pl) under cross-polarized (XPL)	27
3.9 Pyroxenite: A) outcrop is mostly weathered; B) highly altered specimen of serpentinite. Photomicrographs (C) showing highly alteration of medium-grained serpentine (Ser) (XPL) and D) relict grains of plagioclase (Plg) (XPL).....	28
4.1 Variation diagrams of major elements plotted against magnesium number (#Mg = $\text{MgO}/(\text{MgO}+\text{FeO})$) of amphibolites and pyroxenite from Wang Nam Khiao Area, Nakhon Ratchasima	33
4.2. Variation diagrams of selective trace elements plotted against magnesium number (#Mg) of amphibolites and pyroxenite from Wang Nam Khiao Area, Nakhon Ratchasima	38
4.3 Chondrite-normalized spider diagrams of granular amphibolites and pyroxenite from Wang Nam Khiao Area (chondrite's composition and patterns of E-MORB and OIB after Sun and McDonough, 1989)	39
4.4. Chondrite-normalized spider diagrams of migmatitic amphibolites from Wang Nam Khiao Area (chondrite's composition and patterns of E-MORB and OIB after Sun and McDonough, 1989)	39

Figure	page
4.5. Chondrite-normalized spider diagrams of layered amphibolites from Wang Nam Khiao Area (chondrite's composition and patterns of E-MORB and OIB after Sun and McDonough, 1989).....	40
4.6. Chondrite-normalized REE plots of granular amphibolites and pyroxenite from Wang Nam Khiao Area (chondrite's composition and patterns of E-MORB and OIB after Sun and McDonough, 1989).....	44
4.7. Chondrite-normalized REE plots of migmatitic amphibolites from Wang Nam Khiao Area (chondrite's composition and patterns of E-MORB and OIB after Sun and McDonough, 1989)	44
4.8. Chondrite-normalized REE plots of layered amphibolites from Wang Nam Khiao Area (chondrite's composition and patterns of E-MORB and OIB after Sun and McDonough, 1989).....	45
4.9. Atomic Mg-Fe-Ca plots showing compositions of amphiboles from various rock types collected from Wang Nam Khiao area, Nakhon Ratchasima (classification after Eyuboglu et al., 2011).	49
4.10. Plots of albite–anorthite–orthoclase end-members showing various compositions of plagioclases found in each rock type collected from Wang Nam Khiao area, Nakhon Ratchasima (compositional fields after Deer et al., 1992).	53
4.11. Atomic Ca-Mg-Fe plots showing wide compositions (diopside-augite range) of pyroxenes in various rock types collected from Wang Nam Khiao area, Nakhon Ratchasima (fields of classification after Morimoto et al., 1989).....	56

Figure	page
5.1. TAS diagram (Le Bas et al., 1986) showing compositional plots of whole-rock chemistry of samples collected from Wang Nam Khiao Area, Nakhon Ratchasima.	59
5.2. Triangular MgO-FeO-Alkali plots (after Irvine and Baragar, 1971) applied to indicate initial magma series of rock samples from Wang Nam Khiao Area, Nakhon Ratchasima.	59
5.3. Ti-V plots of tectono diagram (after Jian et al., 2009) indicating potentially initial magma series of rock samples from Wang Nam Khiao Area, Nakhon Ratchasima.	60
5.4. Th-Zr-Nb tectono-diagram (after Wood, 1980) indicating significantly most whole-rock analyses of amphibolites geochemically associated with arcbasalt. ..	60
5.5. Chondrite-normalized REE patterns (chondrite composition after Sun and McDonough, 1989) of granular amphibolites and pyroxenite collected from Wang Nam Khiao Area compared to shaded pattern of normal amphibolites occurred in oceanic domain (after Castro et al., 1996).	62
5.6. Chondrite-normalized REE patterns (chondrite composition after Sun and McDonough, 1989) of migmatitic amphibolites from Wang Nam Khiao Area compared to shaded pattern of normal amphibolites occurred in oceanic domain (after Castro et al., 1996).	62
5.7. Chondrite-normalized REE patterns (chondrite composition after Sun and McDonough, 1989) of layered amphibolites from Wang Nam Khiao Area	

Figure	page
compared to shaded pattern of normal amphibolites occurred in oceanic domain (after Castro et al., 1996).....	63
5.8 ACF diagram showing whole-rock chemical plots against essential mineral assemblages found in each rock type significantly suggesting amphibolite facies.	64
5.9 Plots of pressure and temperature (P-T) of amphiboles available under this study in correlation with metamorphic facies after Cambeses (2011)..	67
5.10 Ancient tectonic model of the study area.....	68

CHAPTER I

INTRODUCTION

1.1 General Statement

Amphibolite is one type of high grade metamorphic rocks which may have been originated from mafic igneous rocks, i.e., basalt and gabbro. However, amphibolites can be classified, based on the parental rocks, into two groups, i.e., ortho-amphibolite and para-amphibolite. Ortho-amphibolite is given for prograde metamorphosed basalts. This rock type includes amphibole (mostly hornblende), plagioclase, epidote, zoisite, chlorite, quartz, sphene, leucosene, ilmenite and magnetite (Winter, 2001). On the other hand, para-amphibolite may have same equilibrium mineral assemblage as ortho-amphibolite but it usually includes more biotite, more quartz, and more albite with calcite or wollastonite depending on the protolith (Winter, 2001). Some previous studies show that amphibolites may be associated with sutures (Qasim, 1988; Orberger et al., 1995; Koroteev et al., 2007; Wang et al., 2007; Sutthirat, 2009). Oceanic basalts lain between two continents may be the initial rock of amphibolite occurred during collision. The other processes such as metamorphism in the deep continental crust which contained mafic igneous rocks may take place and turn these rocks to amphibolite. However, mafic and ultramafic rocks and their related rocks in Thailand have not much been studied in detail because most exposures are highly weathered due to the hot and humid weather in this region. This research is aimed to study types and origin of rocks as well as ancient geotectonic setting within this area.

Metamorphic amphibolites have been found rarely in Thailand. Salyapongse (2002) reported that metamorphic rocks in Thailand can be subdivided into four belts

elongated in the north-south direction. They are characterized from west to east by Abukuma Facies Series Belt, Barrovian Facies Series Belt, Blueschist-Greenschist Facies Series Belt and Unclassified Greenschist Facies Belt. Abukuma Facies Series Belt is significantly occupied by Precambrian rocks comprising granitic to granodioritic gneisses, mica to hornblende schists, calc-silicate to marble with local quartzite. Barrovian Facies Series Belt, or lower greenschist Abukuma Facies belt, compose of lower grade of Greenschist facies to higher grade of Amphibolite facies rocks. There are volcaniclastic rocks, calc-silicate, rhyolitic to andesitic rocks, phyllitic tuffs with some marble lens and are unconformed by younger Jurassic red bed. (suggested that the study area is in Barrovian Facies Series Belt) For Blueschist-Greenschist Facies Series Belt, mafic lava (subduction-related metamorphism) also found with associated rocks. Last, for Unclassified Greenschist Facies Belt, this belt exposed only in Loei province. Volcanogenic sequence and fossiliferous limestone are mainly exposed with chert beds. Metaandesite were metamorphosed to the Greenschist Facies are rare. All metamorphic belts are related to tectonic settings of Thailand.

Charusiri et al. (1997) suggested that Thailand consists of some geological sutures including Chiang Mai suture situated between Lampang - Chiang Rai volcanic belt and Shan–Thai micro-continent, Nan suture lain along Lampang - Chiang Rai volcanic belt and Nakhon Thai plate, Sa Kaeo suture expected to continue from Nan suture, Loei suture located along Nakhon Thai plate and Indochina micro-continent and Pattani suture between Shan - Thai and Indochina micro-continents in the south (see Figure1.1).

However, only a few works have been carried out for rocks related to the suture in Thailand. For example, Orberger et al. (1995) studied ultramafic and chromititic rocks collected from Nan-Uttaradit ophiolite suite which is distributed along Shan - Thai and

Indo-China micro-continents in the NE-SW direction. The ophiolite can be grouped into two ages; Permo-Triassic and Carboniferous age. Sixty samples of these rocks and related volcanic rocks were analyzed; consequently, this rock sequence was proven to be related to subduction zone. Moreover, chromititic rocks in this area have two origins, boninites and transitional boninites. Some parts of the ophiolite suite seem to be originated in supra-subduction zone. Their protoliths appear to be harzburgites and dunites.

Ueno and Hisada (2001) studied Paleotethys as indicated by fossils. The evidences showed that Nan-Uttaradit-Sa Kaeo suture is unlike boundary between Indochina micro-continent and Sibumasu block. It should be notified that Sibumasu is comparable to Shan-Thai micro-continent reported by Charusiri et al. (1997). This suture is only a part of the small ancient sea that is not a Paleotethys. On the other hand, mafic rocks and amphibolites that are scattered along Chiang Rai being the remnants of Paleotethys.

Seusutthiya and Maopth (2001) studied on petrography and geochemistry of ultramafic rocks at Ban Ban Tan, King Amphoe Suwankuha in Changwat Nong Bua Lumphu. The rock unit was classified into three groups including Pre-Devonian strongly altered more-mafic rocks (serpentinite and hornblendite), Devonian pelagic rocks (metacherts and phyllite) and Post-Devonian unaltered less-mafic rocks (gabbros, diabase and granitic rock). The results indicated the pelagic sediments are lying above more-mafic rocks, which have undergone retrograde metamorphism, likely a part of ophiolite suites.

Hisada et al. (2004) studied on the ophiolite that is disappeared in Mae Yuam Fault, using chromium spinel. The chromium spinels were associated with Triassic Mae

Sa Reang Group. They can be divided into three groups including high Ti, low Ti and high Cr. Three different origins, i.e., volcanic rocks, peridotites (from the ocean floor) and chromitite were then suggested.

Chutakositkanon and Hisada (2008) studied the evolution of collision between Indochina micro-continent and the oceanic plate around Sa Kaeo-Chanthaburi accretionary complex (SKCB-AC); consequently, they divided the study area into five units including Khao Hleam unit, Khao Prik unit, Ban Nong Bon unit, Soi Dao unit and Pong Nam Ron Formation. Khao Hleam unit and Soi Dao unit consist of reddish brown chert, pillow lavas, pyroclastic rocks and serpentinites that appear to be parts of ophiolitic mélangé.

Sutthirat (2009) studied mafic and ultramafic rocks along the suspected sutures in the country (Figure 1.1). These rocks have been reported as parts of ophiolite suite which contains sea floor sediments, mafic and ultramafic igneous rocks.

Kumalachan and Yoemniyom (1978) reported occurrences of iron ore associated with emery in Prachinburi area. The emery was in red-soil that weathered from coarse-grained hornblende in Ban Non Sout Ae and Ban Yup I Pun areas (Figure 1.1.) In Ban Yup I Pun area, a part of this study area, outcrops could be divided into six zones, i.e., corundum-emery zone, spinel-silimanite zone, silimanite zone, garnet-silimanite zone, calc-silicate zone and marble zone. However, detailed study on amphibolites in Ban Yup I Pun, Amphoe Wang Nam Khiao, Changwat Nakhon Ratchasima has never been reported prior to starting of this research study (see also Figure 1.2). Many outcrops are spreading over and can be easily surveyed. Geological maps scale 1:50,000 (sheets 5337 I and IV) of the Department of Mineral

Resources show exposures of hornblendite spreading over the center of study area; therefore, it was selected for this thesis.

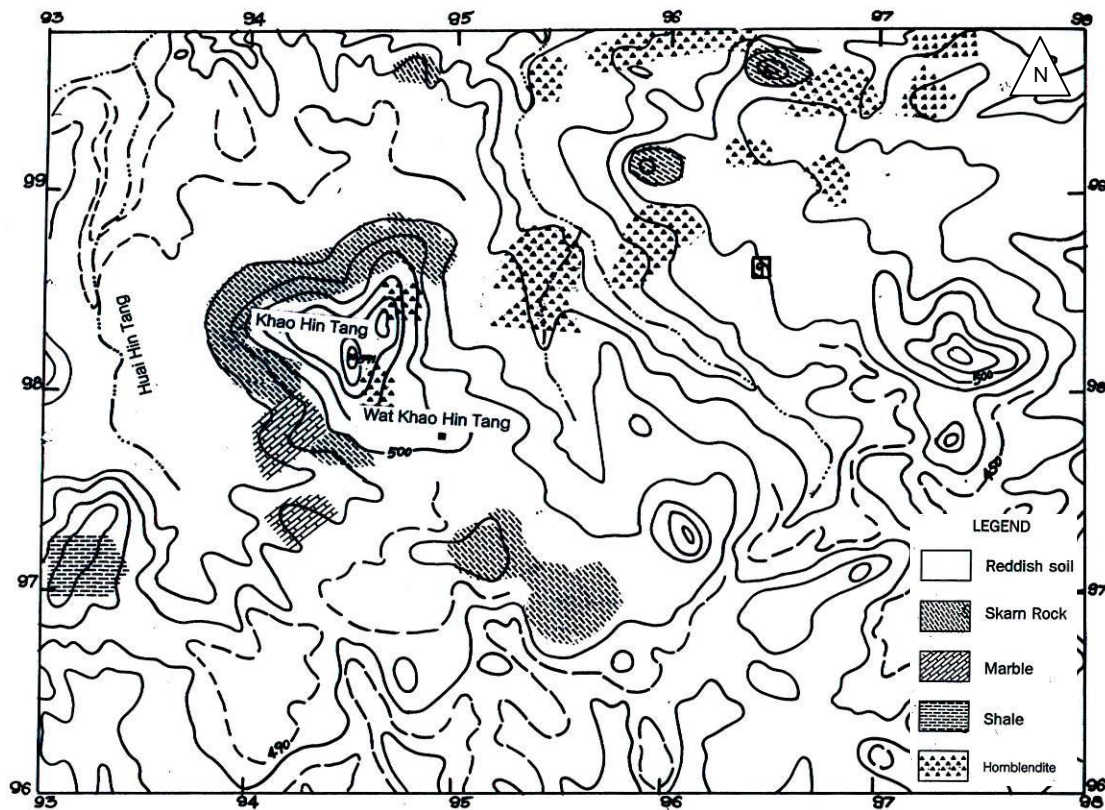


Figure 1.1. Geologic map showing emery and silimanite ores associated with hornblendite (redescribed as amphibolite in this study) in Ban Yup I Pun area (after Kumalachan and Yoemniyom, 1978).

1.2 Scope of Work

The study area is located at Ban Yup I Pun and Ban Nong Mai Daeng areas in Amphoe Wang Nam Khiao, Changwat Nakhon Ratchasima (Figure1.3). The area can be accessed using Highway 304 (Kabinburi-Bangkok), then turn to the local road number 2082 at km 79 to Ban Tha Wang Sai, Ban Yup I Pun and Ban Nong Mai Daeng.

According to the topographic map sheets 5337IV and 5337 I, it is reported that topography in this area is mostly high. The highest peak (949 meters above mean sea level, msl) is located on a ridge of the mountain range in Khao Yai National Park. The northern area is mountainous while the southern area is flatland. The central area is the study area is ripples areas. Many exposures of mafic igneous rocks, which were suspected to be amphibolites, have been extensively found. Field study and sample collection were taken place initially. The samples were prepared as slabs, thin sections and polished-thin sections for petrographic work and mineral chemical analysis and as rock powder and rock solutions for whole-rock chemical analysis. Rock powders were taken to X-ray Fluorescence (XRF) Spectrometry analysis for determination of major and minor elements whereas Inductively Coupled Plasma-Mass Spectrometer (ICP-MS) was used to analyze trace elements and rare earth elements from rock solutions. Moreover, Electron Probe Micro-Analyzer (EPMA) was engaged to analyze mineral chemical analysis using polished thin sections.

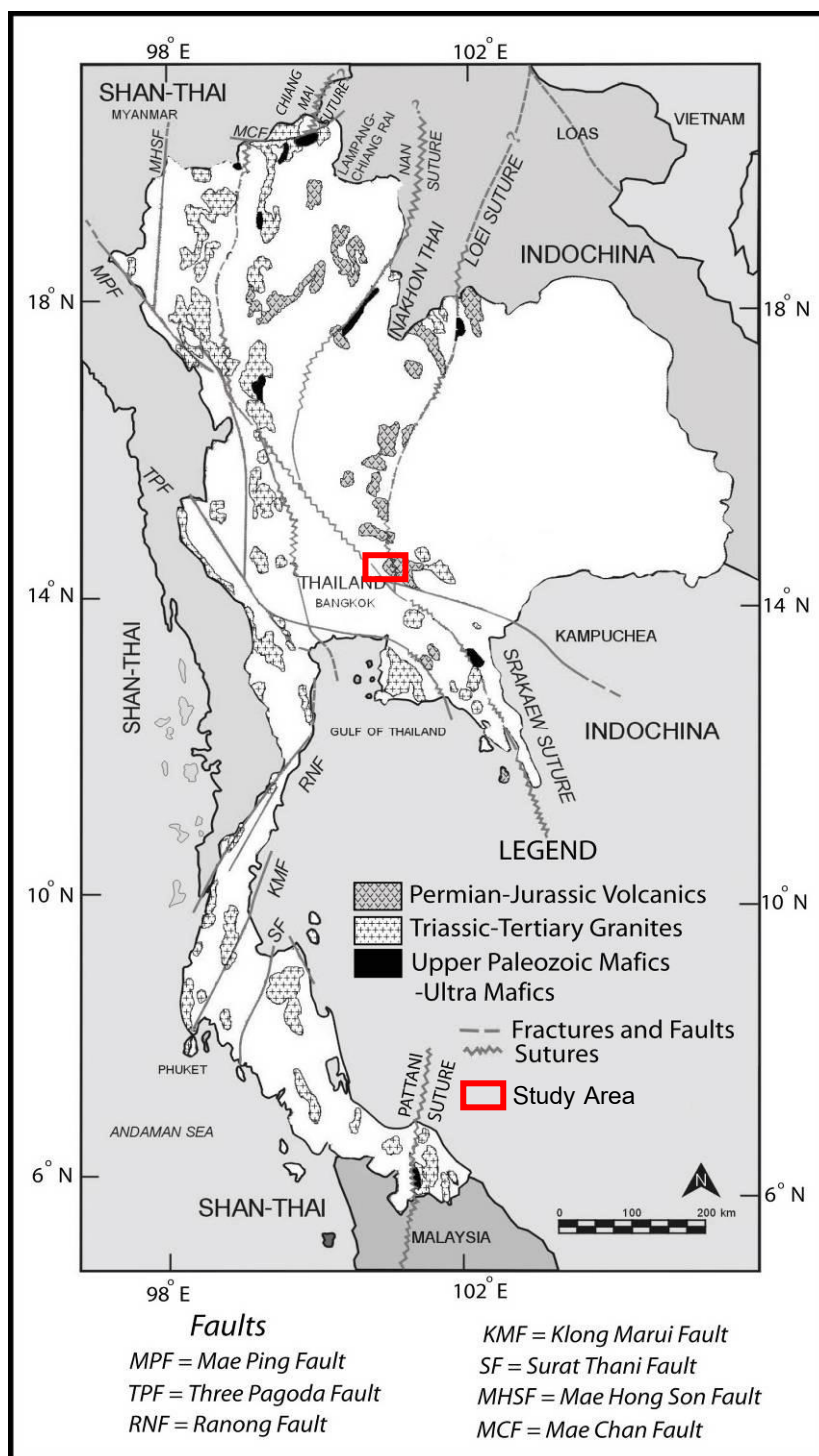


Figure 1.2. Map of Thailand showing main tectonic blocks and their related sutures indicated by some crucial rocks; the study area is located in red rectangular (modified after Sutthirat, 2009).

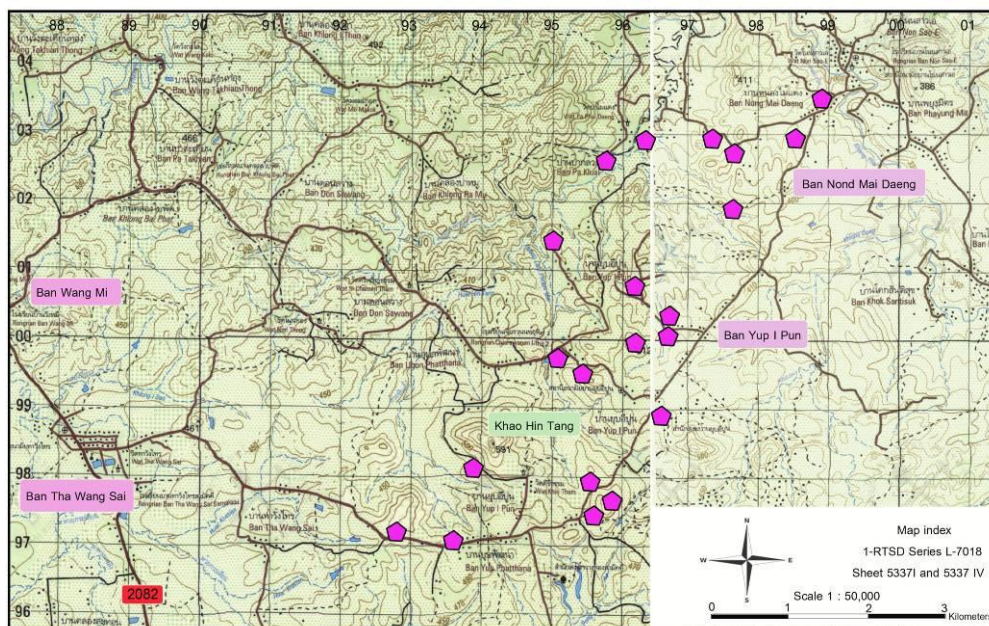


Figure1.3. Topographic map of the study area and localities of sample collection indicated by pink pentagons.

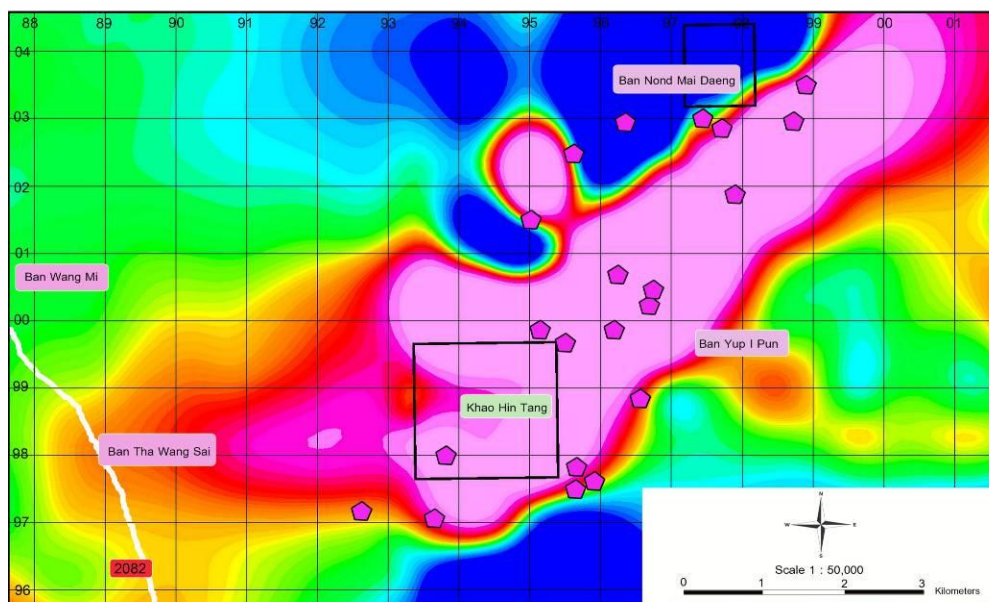


Figure1.4. Reduction to the pole magnetic map (RTP-map) showing magnetic anomaly of the study area and sample localities (pink pentagons). This map was used to initiate boundary of the study area and to plan for sample collection.

1.3 Objective

The main objective of this study is to carry out petrochemistry of the amphibolites exposed in Amphoe Wang Nam Khiao, Changwat Nakhon Ratchasima. All data analyzed from this study could be used to interpret the rock origins and ancient tectonic settings of the study area.

1.4 Methodology

Method of study is shown in Figure 1.5. Previous studies and geological maps were initially reviewed. However, data of amphibolites in the study were rarely reported even there are many outcrops of them spreading over the area, particularly at Ban Yup I Pun and Ban Nong Mai Daeng. Subsequently, RTP-map (Reduction to the Pole-map; Figure 1.4) prepared and interpreted from magnetic anomaly data were used for field work and sampling plans. The red-color zone is set for high magnetic anomaly whereas the blue-color zone is low magnetic. Therefore, amphibolites should response as along the red zones in which exposures may be occurred.

During the fieldwork and sample collection, 40 samples were collected from 21 stations as shown in pinky pentagons (Figure 1.3). Subsequently, all samples were cut to slabs, thin sections, polished-thin sections, rock powders and solutions were prepared for appropriate laboratories. Specimens and slabs were used for rough description such as color and main compositions to differentiate types of rock. Subsequently, petrographic investigation was carried out using 59 thin sections under a polarizing microscope. X-ray Fluorescence (XRF) Spectrometer, Bruker AXS S4 PIONEER, operated at a condition of 220/380V, 50Hz and 8kVA, was engaged for whole-rock geochemical analyses, major and minor elements. In addition, loss on

ignition (LOI) and FeO content were also determined by weighting and titration-technique, respectively. Inductively Coupled Plasma-Mass Spectrometer (ICP-MS), Perkin Elmer Optima 5300DV and Elan 6100, was used to analyze rock solutions for trace elements and rare earth elements (REE). This instrument is based at the mineral and geological services by SGS (Thailand) Limited. Electron Probe Micro-Analyzer (EPMA), JEOL JXA-8100, with operating condition of focused beam, 15kV and about 2nA was used to analyze chemical compositions of main mineral phases using polished-thin sections. Finally all analyzed data were discussed and concluded for report writing and preparing manuscript.

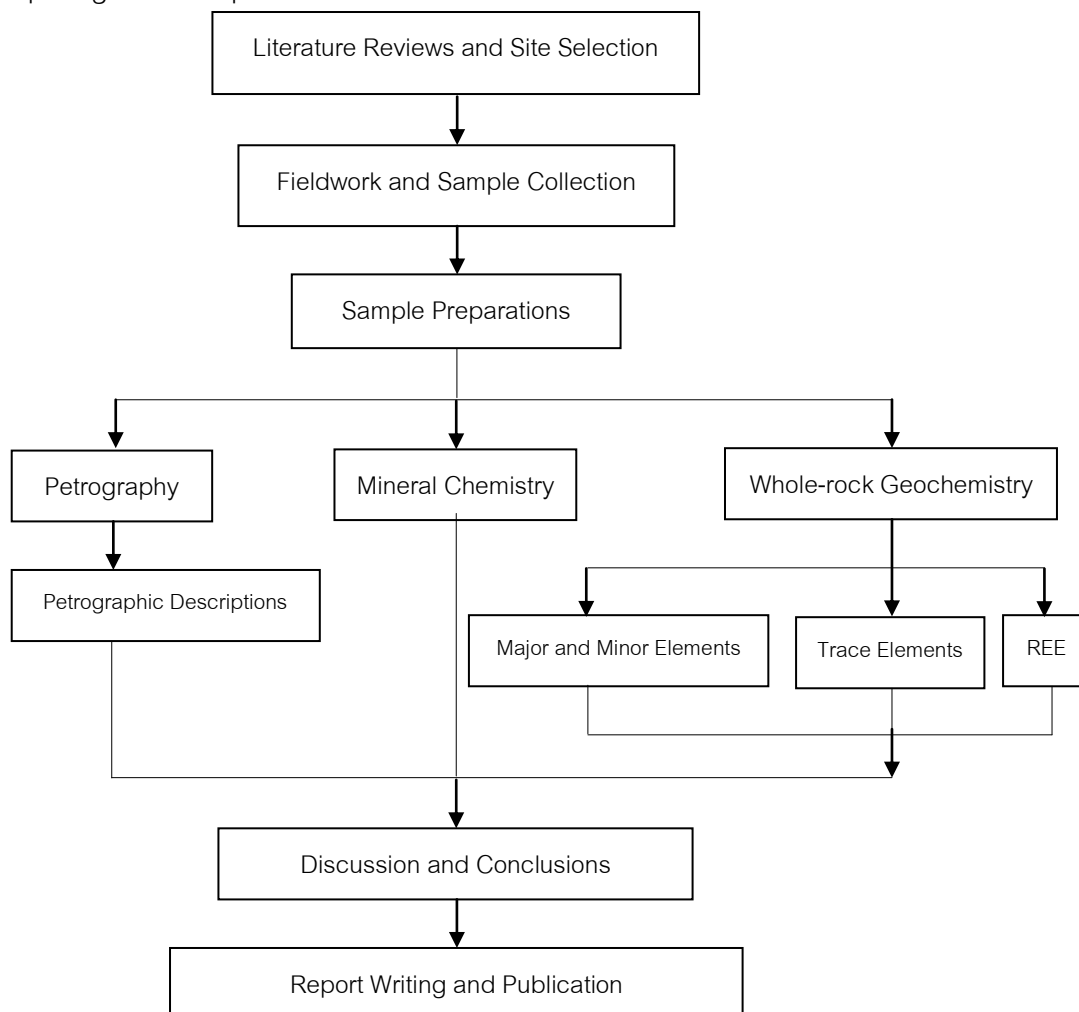


Figure1.5. Flowchart showing methodology of this study.

CHAPTER II

GENERAL GEOLOGY

2.1 Geologic Setting

The main geologic structure of this area is confined by the northwest-southeast direction parallel to the main fold axis of a large syncline with slightly dipping into the south. Permian and Permo-Triassic rocks are more metamorphosed than the Khorat Group (Putthaphiban et al., 1981; 1989). Some faults are clearly defined along the northwest-southeast direction which usually formed features of cliff. The other faults are additionally in the northeast-southwest and east-west directions. Salyapongse (2002) reported that the study area is located in a narrow elongate belt belonging to Barrovian Facies Series Belt. This belt varies from lower grade of Greenschist facies to higher grade of Amphibolite facies. In general, it usually indicates boundary between Shan-Thai and Indochina microcontinents.

According to the Putthaphiban et al. (1981; 1989), the regional area consists of mostly sedimentary and igneous rocks with less abundance of metamorphic rocks. The ages of rocks are ranging from Permian to Quaternary. The older rocks are exposed in the central part while the younger ones are surrounding that is called window structure.

Sedimentary Rocks

- Saraburi Group (Permian): is the oldest rock in this area. They include shale, siltstone, sandstone chert and limestone. Some were metamorphosed to phyllite, slate, quartz-schist, hornfels, marble and quartzite.

- Khorat Group (Mesozoic): consists of Phu Kradung Formation, Phra Wihan Formation and Sao Khua Formation. They mainly consist of siltstone, sandstone and conglomerate. These rocks mostly found along the mountain ranges excepted the northwestern range.

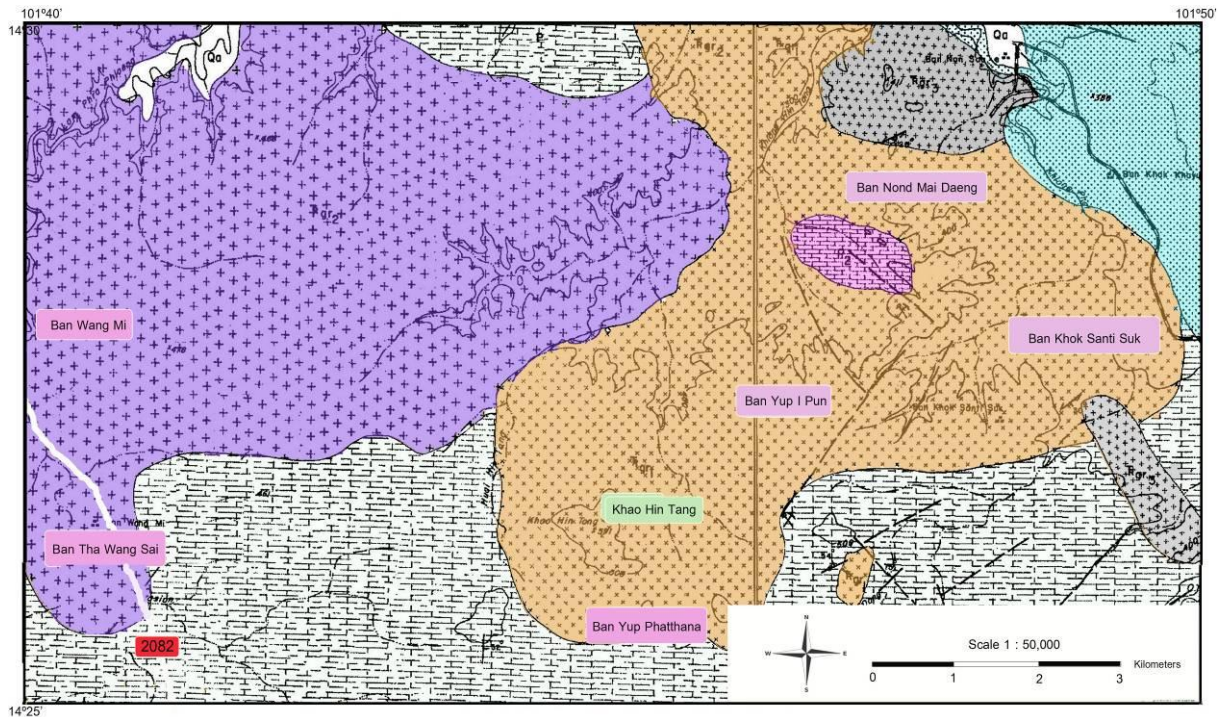
- Quarternary sediments: are mainly characterized by colluviums and alluviums.

Igneous Rocks

- Plutonic rocks: in this area are characterized by mafic- to felsic-rocks including hornblendite, gabbro, diorite, tonalite, alamelite and granite. They are crucially oriented in the northwest-southeast direction. These rocks appear to be older than the Phu Kra Dung Formation because they are covered by Phu Kra Dung Formation with unconformity.

- Volcanic rocks: are composed of rhyolite, andesite, agglomerate and tuff. These volcanic rocks underlaid the Phu Kra Dung Formation with the disconformity and angular unconformity.

The igneous rocks in this area could be divided after Putthaphiban et al. (1981; 1989) into many groups as shown with different colors in Figure 2.1. For this study, amphibolites or black greenish color rocks are also mapped with other gray to black, medium- to coarse- grained, equigranular texture, hornblende-rich igneous rocks as shown by the orange area in Figure 2.1. However, they are reclassified, based on petrographic information gained from this study, as metamorphic amphibolites which are reported in the nest chapters.



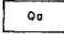

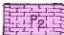
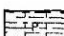



-  Quaternary alluvial deposit
-  Jurassic micaceous-, calcareous siltstone, sandstone, locally basal conglomerate
-  Triassic-Permian recrystalline argillaceous limestone with nodular chert, phylitic shale
-  Permian phylitic shale, siltstone, sandstone, bedded gray chert, hornfels and quartzite
-  Biotite-hornblende granite
-  Granite, biotite-muscovite-tourmaline granite
-  Hornblende granite, hornblende diorite, hornblende gabbro and hornblendite

Figure 2.1. Geologic map of the study area and adjacency (after Putthaphiban et al., 1989).

2.2 Tectonic Evolution

Thailand consists of two micro-continents, named as Shan Thai and Indochina (see Figure 1.2) which they appear to have undergone four steps of tectonic evolution

(Charusiri et al., 1997). Begin with Archeotectonic stage, Pre-Cambrian high-grade metamorphosed core complexes show that Shan-Thai was a part of Gondwana supercontinent while Indochina was a part of Pan-Cathaysia supercontinent. Shan-Thai and Indochina began to move and rotate closer and began moving apart in Devonian of Paleotectonic stage leading to formations of two new small blocks including Nakhon-Thai ocean floor expected to be a part of the ancient sea (Paleotethys) and Lampang-Chiang Rai volcanic arc. Nakhon-Thai block was lying on the west of Indochina microcontinent while Lampang-Chiang Rai volcanic arc was lying on the east of Shan-Thai. In Mesotectonic stage, four blocks had been uplifting and suturing while the paleotethys as some parts of the eastern Shan-Thai microcontinent had closed in late Triassic. Subsequently, Neotectonic stage started from the collision of Indian plate and Eurasian plate in the southwest of Thailand. Then the collision led to development of main faults in Thailand within three directions, i.e., northwest-southeast, northeast-southwest and north-south.

Moreover, the collision of Shan-Thai and Indochina in the past would generate geologic suturing (Charusiri et al., 1997). These sutures are called Chaing Mai suture (between Lampang-Chiang Rai volcanic arc and Shan-Thai), Nan suture (between Lampang-Chiang Rai volcanic arc and Nakhonthai ocean floor), Srakeaw suture (expected to continue from Nan suture), Loei suture (between Nakhonthai ocean floor and Indo-China) and Pattani suture (between Shan-Thai and Indochina). These sutures and related rocks were studied by a few researchers. For example, Sutthirat (2009) studied mafic and ultramafic rocks along the Chiang Mai suture, Sa Kaeo-Pattani suture and Loei suture. The research was concluded that both mafic and ultramafic rocks are part of ophiolite suite (see Figure 2.2) which consists of sea floor sediments, mafic and ultramafic igneous rocks. However, the detailed study of these rocks in many areas has

not been reported due to high weathering caused by the tropical climate in Southeast Asia.

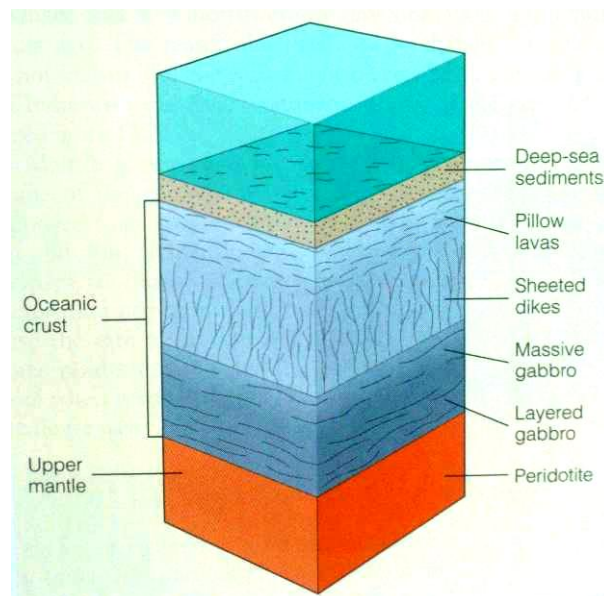


Figure 2.2. Schematic model of ophiolite suites (Monroe et al., 2007).

In addition, Hutchison (1975) suggested that ophiolites were parts of oceanic lithosphere which have mostly been found as incomplete sequences. In Thailand, ophiolitic sequences are crucially found in the northern area extending to Laos. These ophiolitic sequences consist of gabbro, pyroxenite, diabase, andesite, tuff and metabasite (amphibolites) in Lampang-Houei Sai. They also consist of serpentized pyroxenite, gabbro, diorite, dolerite in Uttaradit-Luang Prabang (Hutchison, 1975). However, information of the other areas including this study area is rarely reported.

CHAPTER III

PETROGRAPHY

More than 40 samples were collected from 23 stations around the study area (see Figure 3.1). Subsequently, all samples were prepared as slabs and thin sections used for petrographic description prior to classification of rock types. Detailed petrographic investigation was carried out using more than 50 thin sections under a polarizing microscope.

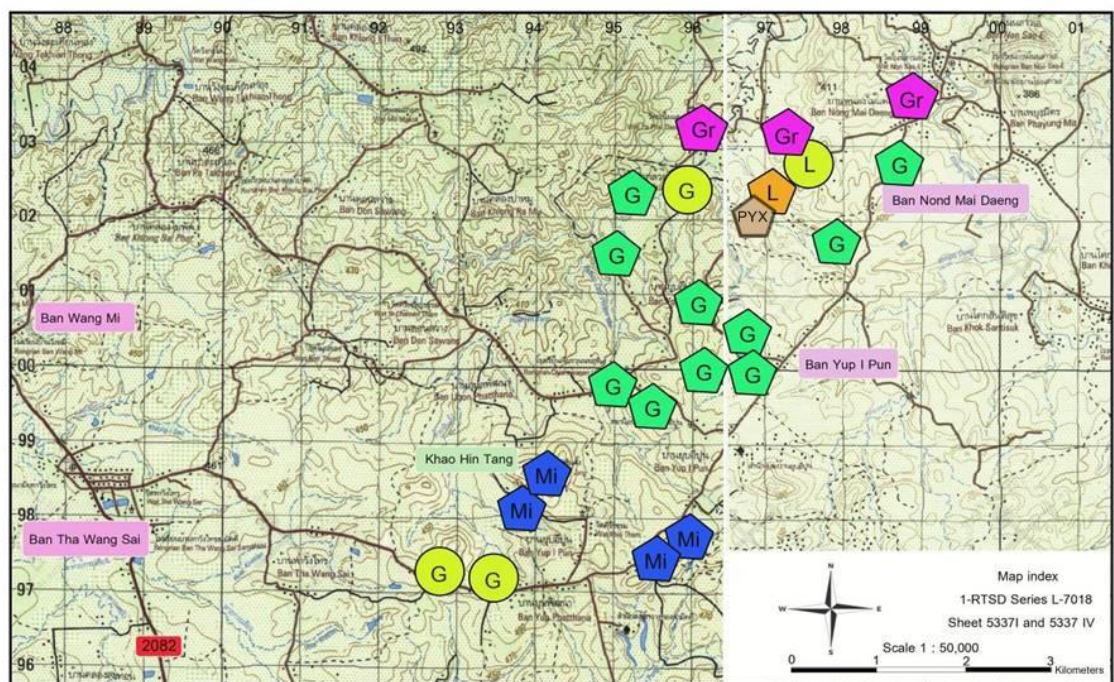


Figure 3.1. Topographic map (sheet 5337I and 5337IV) showing locations of rock sampling around Ban Nong Mai Daeng and Ban Yup I Pun areas in Amphoe Wang Nam Khiao, Changwat Nakhon Ratchasima (G = Granular Amphibolites; Mi = Migmatitic Amphibolites; L = Layered Amphibolites; Gr = Granite; PYX = Pyroxenite; ○ loose block; ◡ outcrop).

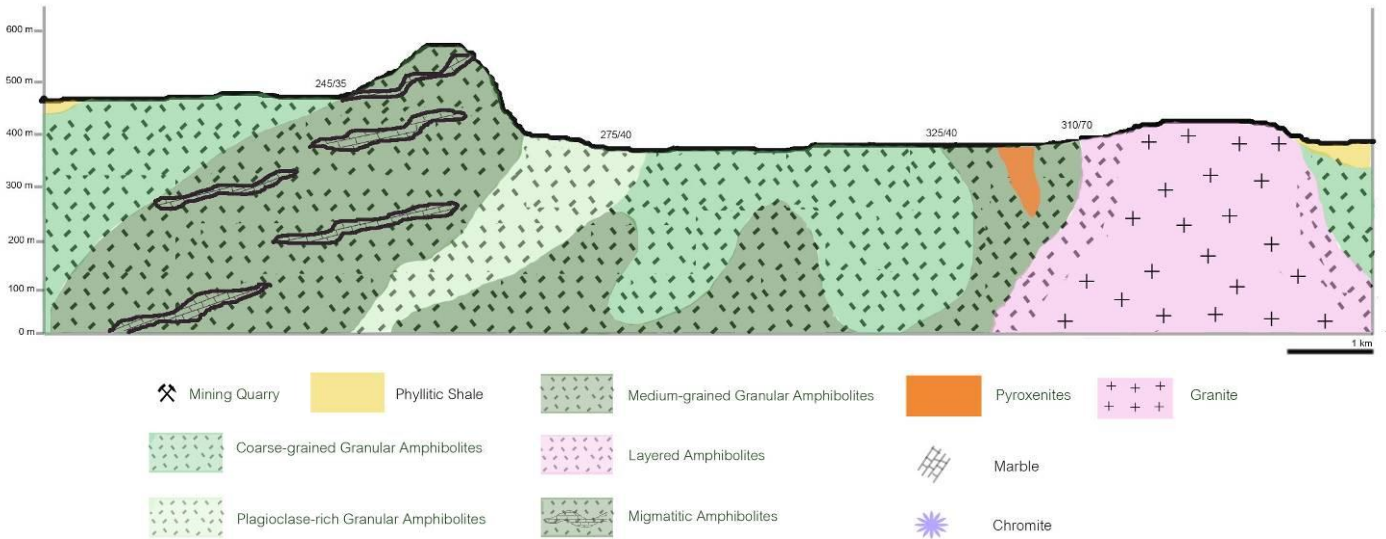
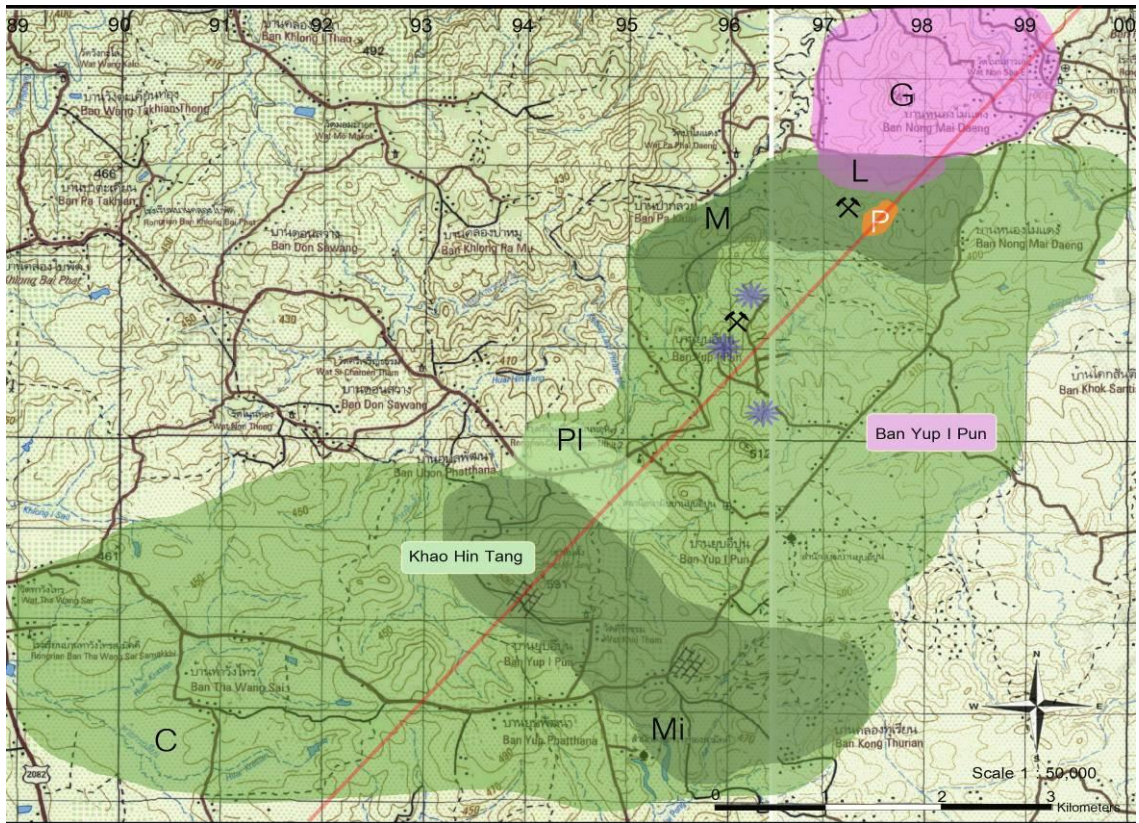


Figure 3.2. Map of rock boundaries after topographic map and geologic map with cross section in the study area. (C = Coarse-grained granular amphibolites; PI = Plagioclase-rich granular amphibolites; M = Medium-grained granular amphibolites; Mi = Migmatitic amphibolites; L = Layered Amphibolites; G = Granite; P = Pyroxenite).

In general, these samples are categorized into three groups, based on physical properties, including granular amphibolites, layered amphibolites and migmatitic amphibolites. Moreover, a few associated rocks including pyroxenite and pink granite were also investigated in this study. Details of these rocks are reported in Figure 3.1 and Figure 3.2.

3.1 Granular Amphibolites

Granular amphibolites are used to describe amphibolites containing large grains of minerals clearly observed in hand specimens. Granular amphibolites were sampled from 10 locations in which are usually characterized by greenish black outcrops. The outcrops are natural exposures and mining quarries. The natural outcrops have spread throughout the study area; on the other hand, mining quarry is also found only in the northwestern part as shown in Figure 3.2. These samples clearly contain amphibole crystals. Mineral compositions are mostly composed of amphiboles with some feldspar; besides, pyroxene, chlorite, quartz and opaque minerals are also found as small crystals with less abundance. Holocrystalline and pandiocrystalline granoblastic textures with triple-junction boundaries are commonly observed in these rocks (Figure 3.3). However, these granular amphibolites can be subdivided into three groups, based on grain size (0.5 cm) and mineral compositions, including coarse-grained amphibolite, plagioclase-rich amphibolite and medium-grained amphibolite. Although, they have similar features and mineral assemblages their petrographic details are somewhat different as reported below.

Table 3.1 Mineral assemblages of amphibolites investigated under this study.

Classification		Sample	Mineral Assemblages					
			Amp	Pyx	Pl	Qz	Chl	Ser
Granular Amphibolites	Coarse-grained	QB_1	****		**			
		QC	****		**			
	Plagioclase-rich	HT_2	****	*	***		*	
		PYX_3	****		***	*		
		PYX_8	****	*	***	*		
	Medium-grained	QB_4	***		***			
		PYX_2	****	*	**			
		PYX_7	****		**			
		SC	****		*			
		QF	****	*	**			
N	****		**	*				
Migmatitic Amphibolites	GU_1	****	*	**	*			
	GU_2	****		***	*			
	GU_3	****		****				
	GU_4	****		**				
	GU_5	****		***				
	GD_2	****	**	****				
	GD_3	***	*	****				
	GD_4	****		****				
	GD_5	****		**				
Layered Amphibolites	PYX_4	****		**	*			
	PYX_5	**		****	*			
	PYX_6	**		****	*			
Pyroxenite	PYX_1	*	**	*			****	

Remark: Amp = Amphibole; Pyx = Pyroxene; Pl = Plagioclase; Qz = Quartz; Chl = Chlorite; Ser = Serpentine; **** significantly found; *** often found; ** found; * rarely found

Coarse-Grained Amphibolite: Their specimens are usually greenish black color and clearly contain coarse-grained amphibole crystals (>0.5 cm in diameter) as shown in Figure 3.3. Amphiboles (about 80-90% mode) clearly show euhedral crystals usually forming triple junction boundaries. Plagioclase feldspars are also recognized usually with small amount (av. 5-10% mode). Plagioclases are usually anhedral to subhedral lath shape with about 1 mm long and they are strongly altered to sericite. Anhedral quartz and opaque minerals are rarely found in this group.

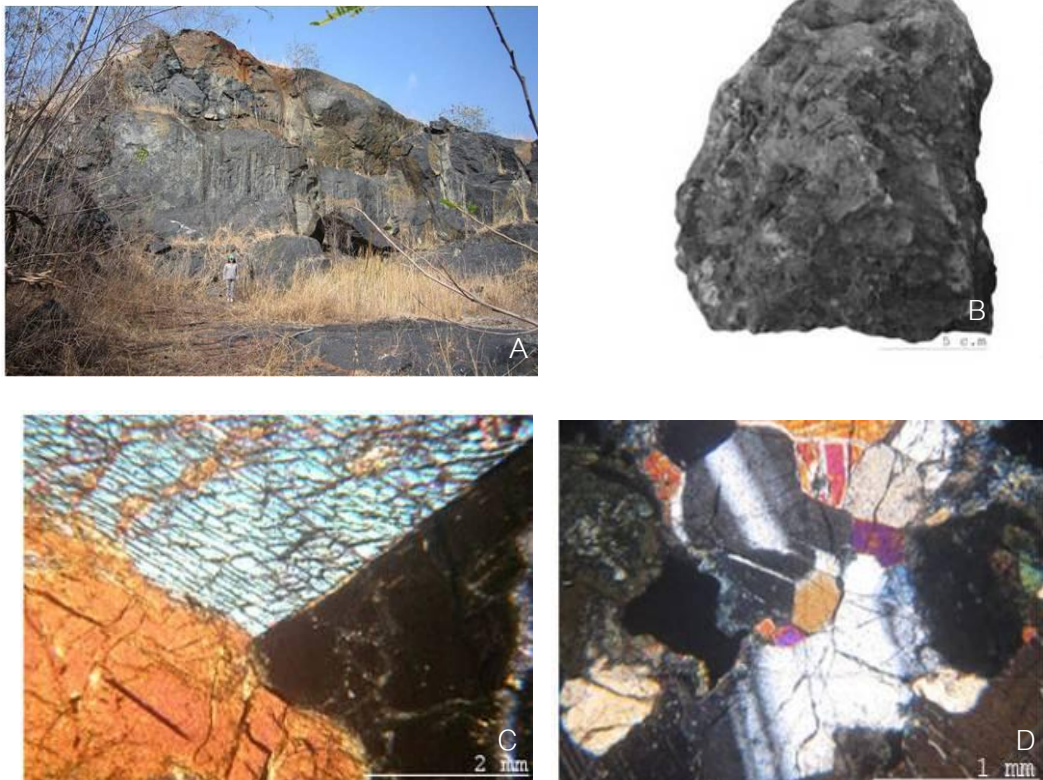


Figure 3.3. Coarse-grained amphibolites: A) mining quarry is a sample locality (scale 160 meters high); B) a black specimen with very coarse-grained crystals; C) photomicrograph showing subhedral amphiboles with perfect cleavages and triple-junction boundary (XPL); D) subhedral plagioclase laths with obvious twinning (XPL).

In addition, a few chromite and iron mining quarries have been operated in zones of coarse-grained amphibolites as shown in Figure 3.2. It should be noted that chromite is typically deposited in ophiolite suite and associated with oceanic plate (Leblanc, 1989; Ravikant et al., 2004 and Shi et al., 2012).

Plagioclase-Rich Amphibolites: These samples are greenish black color with white spots. They are highly weathered; however, their fresh parts clearly show green amphibole and white plagioclase feldspar (Figure 3.4). Amphiboles (av. 60-80% mode) are coarse-grained (>0.5 cm) anhedral-subhedral crystals showing typically perfect cleavages which have been turned to oblique cleavages, clearly. Plagioclases usually contain about 20-40% mode. They mostly present anhedral to subhedral lath shapes, similar to nematogranoblasts, with more than 0.5 cm long. These plagioclases are also strongly altered to sericite. In addition, pyroxene, anhedral quartz and some opaque minerals are also found with very small amounts.

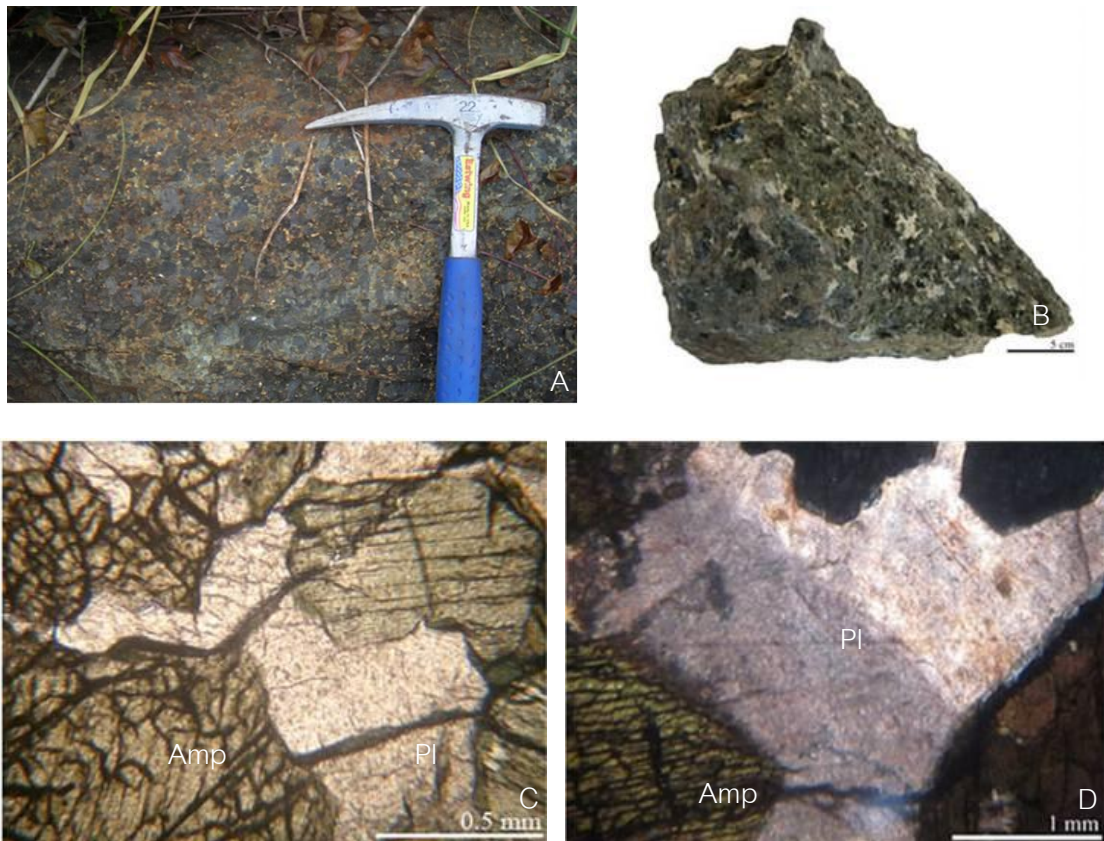


Figure 3.4. Plagioclase-rich granular amphibolites: A) an outcrop showing clearly crystals of greenish black amphibole and white plagioclase that is typical feature of this rock group; B) a hand specimen presenting the mixing compositions between amphibole and plagioclase mostly show nematogranoblastic crystals; C and D) photomicrographs showing mineral compositions of plagioclase (Pl) and amphibole (Amp) with about 40-50% mode each (PPL).

Medium-Grained Amphibolite: These specimens are greenish black color and contain mainly medium-grained crystals (smaller than 0.5 cm). Amphiboles with short nematoblastic crystals are still the main component (av. 60-90% mode). Plagioclases (av. 5-10% mode) usually present small anhedral to subhedral lath shapes (short nematoblasts) with less than 0.5 cm long. They usually have white gray to gray colors. Pyroxenes are also rarely found (less than 5% mode) (Figure 3.5).

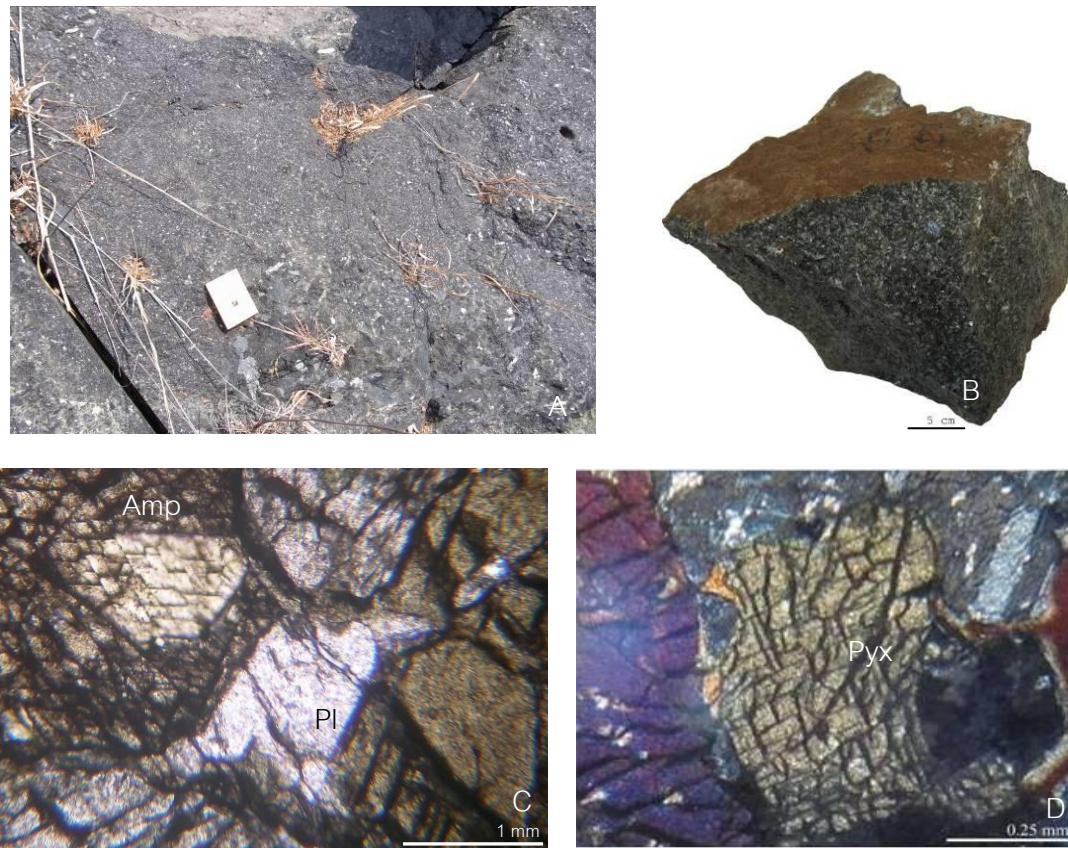


Figure 3.5. Medium-grained granular amphibolites: A) a natural outcrop and its specimen (B) taken for this study; C) photomicrograph (PPL) showing medium-grained short nematoblastic amphiboles (Amp) are greenish color and clearly show cleavages and plagioclases (Pl) that have the same size with amphibole crystals; D) pyroxene (Pyx) with obvious right-angle cleavages is rarely found in this rock (XPL).

3.2 Migmatitic Amphibolites

Migmatitic amphibolites are indicated by migmatite-like features which contain irregular white bands situated in dark green matrix. Their outcrops are also present strongly folding (Figure 3.6) and also contain layers of coarse-grained marbles (Figure 3.6) that usually show sutured textures under microscope. Dark green matrix consists mainly of tiny nematoblastic amphibole crystals (av. 80% mode) with average grain size

<1 mm whereas irregular white layer usually contains tiny nematoblastic plagioclase (av. 15% mode) and pyroxene (less than 5% mode). Moreover, some quartz crystals and rare opaque minerals are also observed (Figure 3.7) in these samples.



Figure3.6. A natural outcrop of migmatitic amphibolites (dark layers) interbedded white coarse-grained marble layers with usually about 30-50 cm thick.

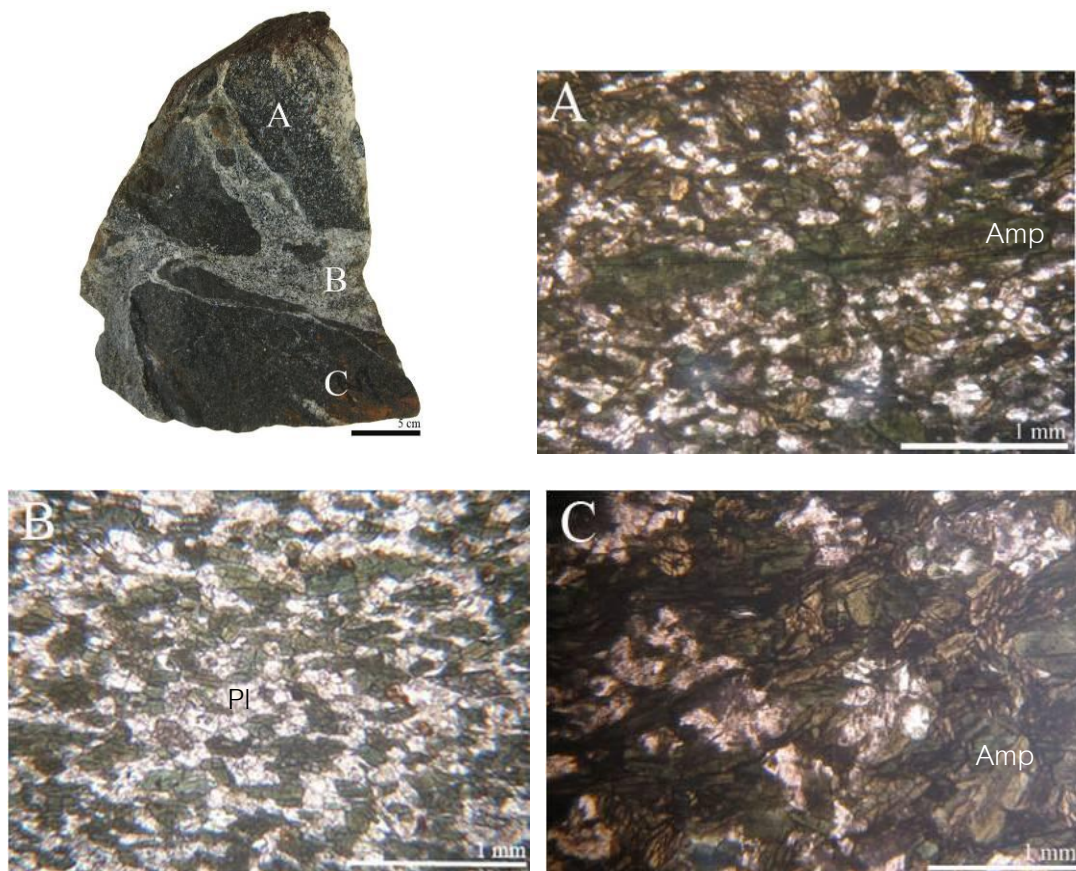


Figure 3.7 Migmatitic amphibolites specimen (left). Photomicrographs (PPL) showing orientation of tiny pale green nematoblastic amphiboles (Amp) and white grey plagioclases (PI) but the ratio between amphibole and plagioclase in each zone are different in each zone A, B and C.

Microscopically, they usually show lineament of amphibole and plagioclase. Their textures could be classified, based on ratio of mineral compositions, into 3 zones. *Zone A* is composed of dark green minerals that are mainly amphibole crystals (av. 50% mode) with average grain size <1 mm whereas white minerals mostly contain plagioclase (av. 45% mode) (Figure 3.7). Moreover, pyroxene (less than 5% mode) with some quartz and rare opaque minerals are also observed. Regarding to mineral

compositions, they are quite similar to those found in the granular amphibolites. For *Zone B* and *Zone C*, the compositions and textures are similar to *Zone A* but ratios between dark green minerals (amphibole) and white mineral (mostly plagioclase) are different. *Zone B* has the amphibole/plagioclase ratio of about 3:7 while that of *Zone C* is about 7:3 as shown in Figure 3.7 B and C, respectively.

However, migmatitic amphibolites usually contain coarse-grained marble layers which appear to have been volatilized during metamorphism. The volatilization of particular CO₂ may lead to higher gas pressure and partially melting of these amphibolites.

3.3 Layered Amphibolites

Layered amphibolites have exposed locally in the northern part of the study area in which is associated closely with pink granite as shown in Figure 3.1. This outcrop is a part of mining quarry with about 5 m high and 3 m wide (Figure 3.8). It typically shows layers alternated between white and dark minerals. However, whole mineral compositions are similar to those of plagioclase-rich granular amphibolite. Although, its outcrop is strongly altered, layers are clearly observed on hand specimens (Figure 3.8). Dark layer consists mostly of greenish amphiboles (av. 80% mode) with size <1 mm in diameter whereas white layer contain mainly plagioclase (about 80% mode) with size of about 0.5-1 mm. Moreover, some anhedral quartz and rare opaque minerals are also observed (Figure 3.8) as lepidoblastic textures.



Figure 3.8. Layered amphibolites: A) an outcrop showing clearly layers between black greenish minerals (amphibole) and white minerals (mostly plagioclase) that is typical feature of this rock group; B) a hand specimen presenting the layers of minerals; C) photomicrograph showing the layers between amphibole (Amp) and plagioclase (Pl) under cross-polarized (XPL)

3.4 Other Associated Rocks

Although the study area is mostly occupied by amphibolites, the other related rocks were found in the northern part as shown in Figure 3.2. There are pyroxenite (highly altered to serpentinite) and pink granite. In addition, phillitic shale (as shown in Figure 2.2) with some loose blocks of gabbro is also found around the study area. However, only pyroxenite is taken into this study as described below.

Pyroxenite is found as a road-cut outcrop while ping granite also found as a natural outcrops. Only pyroxenite is considered for this study because it may have originated from the same provenance of amphibolite. A road-cut outcrop with size of about 2X6 square meters is found near the medium-grain amphibolites (Figure3.2). The outcrop is mostly weathered and altered to serpentine with some asbestos as shown in Figure 3.9 B. Microscopically, they consist of less than 0.5 cm pyroxene and plagioclase crystals that are mostly strongly altered. Serpentine is characterized by fibrous feature (Figure 3.9C). About 50% mode serpentine are composed in these samples with some relict minerals of pyroxene crystals are about 30-40% mode as shown in Figure 3.9D

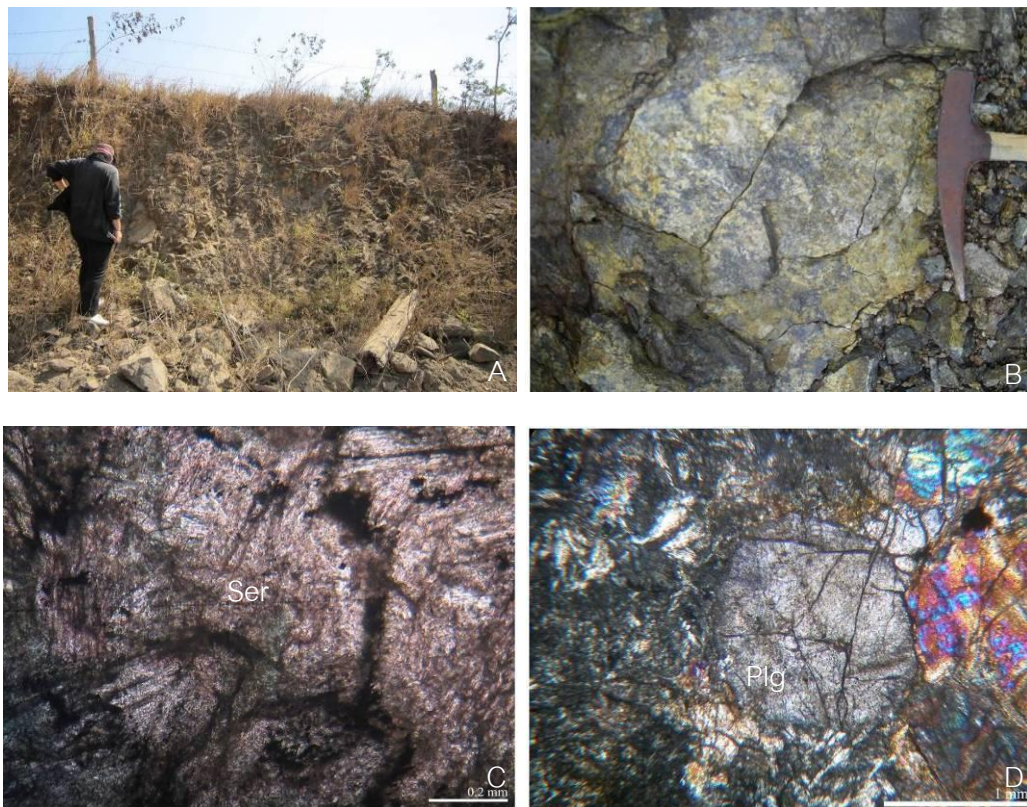


Figure3.9 Pyroxenite: A) outcrop is mostly weathered; B) highly altered specimen of serpentinite. Photomicrographs (C) showing highly alteration of medium-grained serpentine (Ser) (XPL) and D) relict grains of plagioclase (Plg) (XPL).

CHAPTER IV

WHOLE-ROCK GEOCHEMISTRY AND MINERAL CHEMISTRY

4.1 WHOLE-ROCK GEOCHEMISTRY

The whole-rock geochemistry of amphibolites and related rocks are investigated to carry out their characteristics and relations which can lead to interpretation on tectonic processes involved with their geneses. Major and minor oxides as well as trace compositions of these rocks were analyzed using X-ray Fluorescence (XRF) and Inductively Coupled Plasma-Mass Spectrometer (ICP-MS) as reported in Chapter 1. These analyses are correlated with each other rocks and compared with published data of known tectonic occurrences. General idea of their initial source and tectonic setting is constructed from these data. Moreover, mineral chemistry of crucial assemblages of each rock type is also carried out for investigation of metamorphic equilibriums as reported in the following section. Subsequently, chemical compositions of main metamorphic minerals are taken for P-T estimation of possible peak metamorphism. Results gained from this chapter will be therefore discussed along with previous publications for tectonic model of the study area and regional area.

4.1.1 Major Oxides

Major and minor oxides of rock samples obtained from XRF are selected and summarized in Table 4.1 and all analytical data are collected in Appendix A.

For granular amphibolites, the coarse-grained granular amphibolites consist of 45.01-45.45 wt% SiO₂ (av. 45.23%), 10.92-11.12 wt% Al₂O₃ (av. 11.02%), 0.05-1.40 wt%

Fe_2O_3 (av. 9.52%), 8.32-10.72 wt% FeO (av. 0.73%), 13.00-14.08 wt% MgO (av. 13.54%), 13.26-13.94 wt% CaO (av. 13.60%), 0.10-0.11 wt% MnO (av. 0.11%), 0.72-0.78 wt% K_2O (av. 0.75%), 1.77-1.89 wt% Na_2O (av. 1.83%), 1.92-2.05 wt% TiO_2 (av. 1.99%) and about 0.02 wt% P_2O_5 . Plagioclase-rich granular amphibolites consist of 48.76-50.96 wt% SiO_2 (av. 49.99%), 5.37-13.47 wt% Al_2O_3 (av. 8.53%), 0.02-0.06 wt% Fe_2O_3 (av. 0.03%), 7.53-9.55 wt% FeO (av. 8.55%), 7.21-14.18 wt% MgO (av. 11.21%), 11.76-21.33 wt% CaO (av. 17.87%), 0.11-0.22 wt% MnO (av. 0.14%), 0.15-1.02 wt% K_2O (av. 0.50%), 0.16-3.86 wt% Na_2O (av. 1.49%), 0.59-1.10 wt% TiO_2 (av. 0.76%) and 0.04-0.29 wt% P_2O_5 (av. 0.16%). The medium-grained granular amphibolites contain 46.82-49.31 wt% SiO_2 (av. 48.17%), 9.52-15.72 wt% Al_2O_3 (av. 11.57%), 0.02-1.43 wt% Fe_2O_3 (av. 0.50%), 8.17-12.02 wt% FeO (av. 9.97%), 7.12-16.56 wt% MgO (av. 11.92%), 9.72-17.68 wt% CaO (av. 12.97%), 0.10-0.15 wt% MnO (av. 0.14%), 0.53-2.39 wt% K_2O (av. 1.10%), 1.26-2.14 wt% Na_2O (av. 1.51%), 0.62-1.34 wt% TiO_2 (av. 1.07%) and 0.04-0.32 wt% P_2O_5 (av. 0.17%).

Migmatitic amphibolites are composed of 48.53-49.65 wt% SiO_2 (av. 48.96%), 9.56-12.25 wt% Al_2O_3 (av. 10.49%), 0.10-1.11 wt% Fe_2O_3 (av. 0.68%), 6.29-11.08 wt% FeO (av. 9.47%), 5.98-13.07 wt% MgO (av. 10.34%), 12.10-18.17 wt% CaO (av. 14.75%), 0.13-0.19 wt% MnO (av. 0.16%), 0.21-0.94 wt% K_2O (av. 0.65%), 1.30-2.32 wt% Na_2O (av. 1.69%), 0.78-1.07 wt% TiO_2 (av. 0.93%) and 0.07-0.84 wt% P_2O_5 (av. 0.46%).

Layered amphibolites yield 61.53-73.61 wt% SiO_2 (av. 68.97%), 14.18-19.70 wt% Al_2O_3 (av. 16.61%), 0.00-0.16 wt% Fe_2O_3 (av. 0.12%), 1.54-3.02 wt% FeO (av. 2.26%), 0.43-1.15 wt% MgO (av. 0.68%), 0.85-2.28 wt% CaO (av. 1.33%), about 0.03 wt% MnO , 0.40-3.92 wt% K_2O (av. 2.31%), 0.36-0.49 wt% Na_2O (av. 0.43%), about 0.06 wt% TiO_2 and 0.69-1.27 wt% P_2O_5 (av. 1.06%).

Pyroxenite, which is closely related to amphibolites, reveals 42.90 wt% SiO₂, 11.75 wt% Al₂O₃, 0.05 wt% Fe₂O₃, 12.90 wt% FeO, 19.26 wt% MgO, 12.18 wt% CaO, 0.21 wt% MnO, 0.06 wt% K₂O, 0.22 wt% Na₂O and 0.34 wt% TiO₂.

Table 4.1. Whole-rock analyses of amphibolites and pyroxenite from Wang Nam Khiao, Nakhon Ratchasima. Major and minor oxides (% wt) yielded from XRF analysis and trace elements (ppm) obtained from ICP-MS analysis.

Name	Granular Amphibolites								Migmatitic Amphibolites			Layered Amphibolites			Pyroxenite
	Coarse-grained		Plagioclase-rich			Medium-grained			GU_1	GU_3	GU_5	PYX_4	PYX_5	PYX_6	PYX1
	QB_1	QC	HT_2	PYX_3	QB_4	PYX_7	SC	QF							
SiO ₂	45.45	45.01	48.76	50.16	50.08	47.49	46.82	49.31	48.53	49.65	48.70	61.53	73.61	71.76	42.90
Al ₂ O ₃	11.12	10.92	9.31	5.37	13.47	9.52	10.78	10.25	9.56	12.25	9.67	19.70	14.18	15.95	11.75
Fe ₂ O ₃	10.72	8.32	8.58	7.53	9.55	12.02	9.72	8.17	11.05	6.29	11.08	3.02	1.54	2.22	12.90
FeO	0.05	1.40	0.02	0.02	0.06	0.05	0.02	1.43	0.82	1.11	0.10	0.00	0.21	0.16	0.05
MgO	13.00	14.08	9.83	14.18	7.21	12.88	11.11	16.56	13.07	5.98	11.96	1.15	0.43	0.46	19.36
CaO	13.26	13.94	21.21	21.33	11.76	13.22	17.68	9.27	12.10	18.17	13.99	4.04	2.28	0.85	12.18
MnO	0.10	0.11	0.11	0.13	0.09	0.15	0.10	0.14	0.19	0.13	0.16	0.03	bdl	bdl	0.21
K ₂ O	0.72	0.78	0.21	0.15	1.02	0.88	0.60	2.39	0.80	0.21	0.94	0.40	2.60	3.92	0.06
Na ₂ O	1.77	1.89	0.16	0.54	3.86	1.26	1.30	1.34	1.45	2.32	1.30	9.38	4.31	3.94	0.22
TiO ₂	1.92	2.05	0.75	0.59	1.10	1.31	1.34	0.62	0.95	0.78	1.07	0.45	0.36	0.49	0.34
P ₂ O ₅	bdl	0.02	0.04	bdl	0.29	bdl	0.04	0.16	0.07	0.84	bdl	0.06	bdl	bdl	bdl
LOI	1.40	0.61	1.15	0.76	1.90	1.42	0.79	2.04	1.71	1.39	1.89	0.69	1.27	1.23	0.89
Total	99.51	99.13	100.13	100.76	100.39	100.20	100.30	101.68	100.30	99.12	100.86	100.45	100.79	100.98	100.86
Elements (ppm)															
Ba	75.80	77.10	2.70	87.00	327.00	93.40	50.10	256.00	83.10	21.50	97.00	221.00	761.00	1600.00	113.00
Ce	4.10	6.20	9.20	16.30	18.70	11.00	5.50	19.00	17.90	28.00	15.20	60.70	42.40	76.00	2.20
Co	78.90	77.30	48.40	49.50	48.70	69.60	68.40	72.40	70.90	40.30	66.40	18.30	61.00	99.80	87.50
Cr	290.00	190.00	60.00	580.00	260.00	430.00	20.00	1600.00	700.00	bdl	770.00	10.00	bdl	bdl	220.00
Cu	83.00	129.00	8.00	7.00	25.00	115.00	70.00	7.00	47.00	19.00	64.00	207.00	13.00	12.00	286.00
Dy	2.87	3.53	2.15	3.86	3.10	3.94	2.65	1.88	2.97	3.87	2.78	4.83	3.43	4.94	1.40
Er	1.50	1.97	1.14	2.01	1.94	2.29	1.37	1.05	1.94	1.90	1.62	3.14	1.88	2.92	0.80
Eu	0.79	0.86	0.65	0.98	1.01	1.16	0.73	0.53	0.99	1.53	0.97	1.94	0.88	1.54	0.33
Ga	13.00	14.00	22.00	10.00	16.00	15.00	13.00	14.00	17.00	18.00	15.00	18.00	10.00	17.00	8.00
Gd	2.80	3.60	2.19	3.78	3.38	3.80	2.37	2.03	3.26	4.51	2.76	4.51	3.82	5.25	1.11
Hf	bdl	bdl	1.00	1.00	2.00	1.00	bdl	2.00	2.00	1.00	1.00	6.00	4.00	6.00	bdl
Ho	0.56	0.71	0.42	0.74	0.63	0.82	0.52	0.35	0.61	0.74	0.55	1.02	0.67	0.98	0.26
La	1.10	1.80	3.60	5.30	8.30	3.40	1.80	9.60	6.50	10.70	6.10	33.10	22.80	40.50	0.80
Lu	0.17	0.22	0.15	0.31	0.28	0.30	0.18	0.15	0.26	0.27	0.21	0.47	0.25	0.44	0.10
Nb	bdl	1.00	1.00	2.00	2.00	2.00	bdl	1.00	2.00	4.00	2.00	7.00	7.00	9.00	bdl
Nd	5.50	7.40	7.30	13.20	12.50	11.30	5.90	9.80	12.60	18.90	10.10	24.40	17.60	32.70	2.60
Ni	112.00	67.00	42.00	84.00	75.00	178.00	24.00	462.00	99.00	11.00	108.00	15.00	11.00	10.00	245.00
Pr	0.92	1.25	1.44	2.72	2.77	2.01	1.04	2.38	2.66	4.19	2.18	6.69	4.79	8.94	0.43
Rb	1.70	2.00	0.20	5.00	15.10	8.10	2.10	52.20	8.70	0.70	10.70	2.90	37.80	92.90	0.70
Sc	89.00	103.00	37.00	54.00	32.00	47.00	80.00	21.00	49.00	21.00	72.00	15.00	bdl	9.00	41.00
Sm	2.20	2.70	1.80	3.40	3.00	3.50	2.10	2.00	2.80	4.70	2.40	4.90	3.80	6.00	0.90
Sr	278.00	219.00	438.00	102.00	497.00	187.00	257.00	251.00	192.00	642.00	278.00	489.00	196.00	187.00	129.00
Tb	0.47	0.54	0.34	0.57	0.51	0.64	0.40	0.28	0.50	0.66	0.45	0.72	0.59	0.79	0.23
Th	0.10	0.10	1.00	0.60	1.30	0.40	0.10	3.00	1.10	1.50	0.60	8.00	12.30	11.20	0.10
Ti	287.71	8391.59	143.86	95.90	383.62	287.71	95.90	8583.40	4891.10	6665.32	575.42	0.00	1246.75	959.04	287.71
Tm	0.18	0.25	0.16	0.31	0.28	0.31	0.17	0.14	0.28	0.31	0.24	0.51	0.28	0.41	0.10
V	557.00	680.00	382.00	253.00	329.00	390.00	525.00	197.00	336.00	182.00	394.00	75.00	13.00	bdl	192.00
W	139.00	83.00	243.00	93.00	103.00	98.00	141.00	52.00	76.00	219.00	58.00	213.00	572.00	938.00	64.00
Y	14.10	17.60	10.50	19.40	17.20	19.80	12.60	9.80	16.90	17.60	14.50	29.40	18.60	26.20	6.60
Yb	1.10	1.50	1.00	1.90	1.80	1.90	1.00	0.90	1.80	1.50	1.40	3.50	1.80	2.70	0.60
Zn	36.00	74.00	43.00	95.00	52.00	102.00	38.00	243.00	95.00	89.00	75.00	11.00	26.00	54.00	69.00
Zr	13.30	18.00	27.20	32.70	54.10	29.70	18.80	50.20	47.60	31.50	32.20	199.00	127.00	210.00	9.40

* bdl = below detection limit

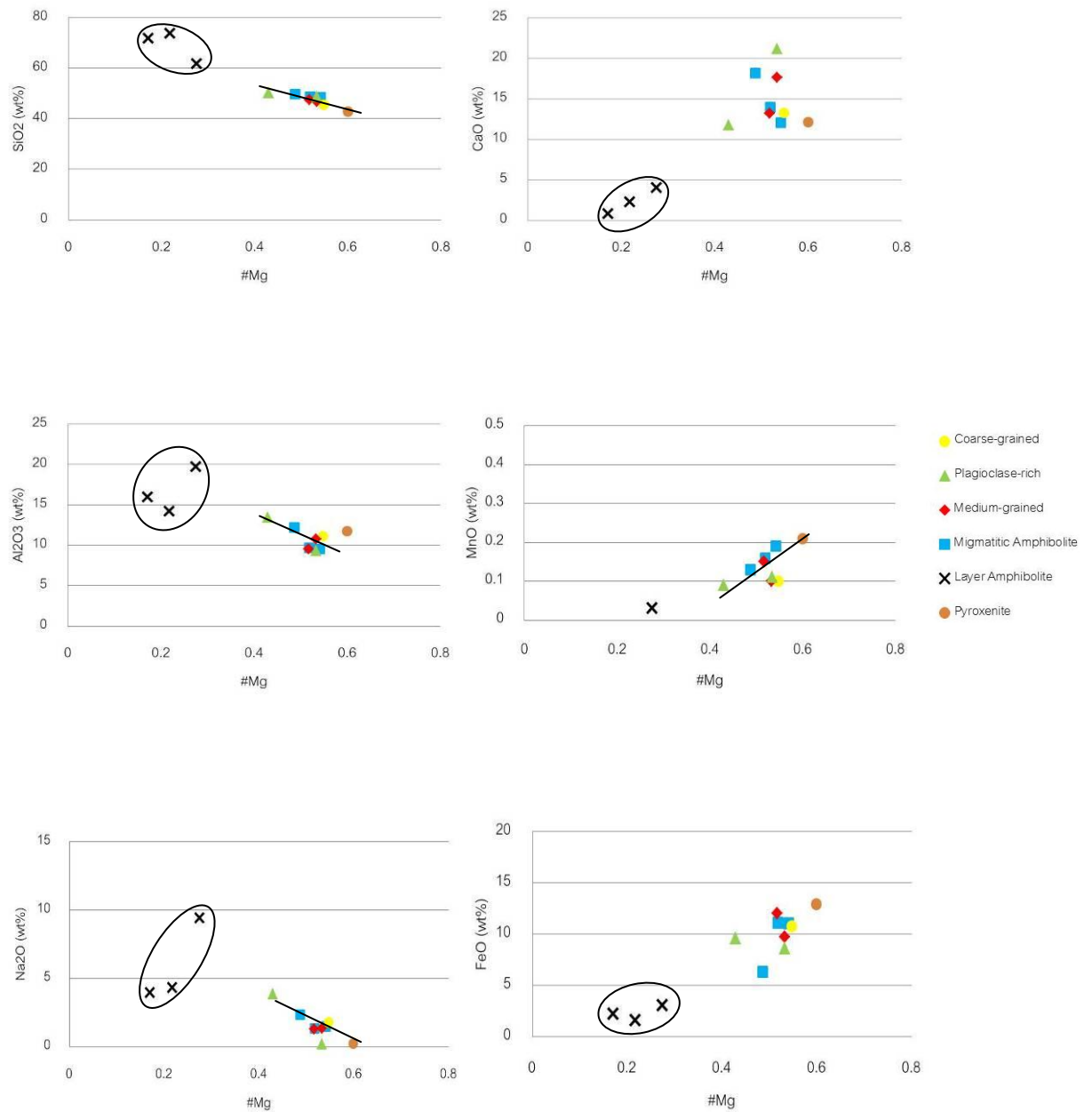


Figure 4.1. Variation diagrams of major elements plotted against magnesium number (#Mg = $\text{MgO}/(\text{MgO}+\text{FeO})$) of amphibolites and pyroxenite from Wang Nam Khiao Area, Nakhon Ratchasima

Major and minor oxides are plotted in Harker-type variation diagrams as shown in Figure 4.1. In general, granular amphibolites and migmatitic amphibolites fall within the same ranges of major and minor oxides. For layer amphibolites, they appear to have higher SiO_2 , Al_2O_3 and Na_2O contents with lower FeO and CaO contents than those of the other amphibolite groups. This may indicate that layered amphibolites have been influenced chemically by pink granite exposed in the north of the study area. On the other hand, pyroxenite (only one analysis available) reveals the same compositions of main amphibolite groups but appear to have higher MgO and FeO content as shown by magnesium number or #Mg (see Figure 4.1). SiO_2 , Al_2O_3 and Na_2O contents decreasing against higher Mg numbers (as black line) are recognized from plagioclase-rich granular amphibolites towards migmatitic amphibolites and pyroxenite, respectively; however, these trends are not clearly distinguished in coarse-grained and medium grained granular amphibolites. For MnO and FeO contents, all groups appear to have increasing trends towards higher Mg numbers. This can assume that these rock samples may have mafic composition increasing from plagioclase-rich granular amphibolites to migmatitic amphibolites, medium- and coarse-grained granular amphibolites and pyroxenite, respectively.

4.1.2 Trace Elements

Trace elements, usually present in rocks with very low concentrations of less than 0.1 wt% (1000 ppm), were analyzed using Inductively Coupled Plasma-Mass Spectrometer (ICP-MS) in this study. Trace elements with preference to combine in the mineral phase are described as compatible, whereas elements with preference to remain in the melt are described as incompatible (Rollinson, 1993). The incompatible elements can be subdivided, based on charge/size ratio, into high field strength (HFS)

such as Sc, Y, Th, U, Pb, Zr, Hf, Ti, Nb and Ta and low field strength (large ion lithophile elements) (e.g., Cs, Rb, K and Ba). Study of trace elements may lead to understanding of geological processes controlled distribution of these elements.

Coarse-grained granular amphibolites consist of barium (Ba) 75.80-77.10 ppm (av. 76.45 ppm), cobalt (Co) 78.90-77.30 ppm (av. 78.10 ppm), chromium (Cr) 190.00-290.00 ppm (av. 240.00 ppm), copper (Cu) 83.00-129.00 ppm (av. 106.00 ppm), niobium (Nb) 1.00-2.00 ppm (about 1.50 ppm), nickel (Ni) 67.00-112.00 ppm (av. 89.50 ppm), rubidium (Rb) 1.70-2.00 ppm (av. 1.85 ppm), scandium (Sc) 89.00-103.00 ppm (av. 96.00 ppm), strontium (Sr) 219.00-278.00 ppm (av. 248.50 ppm), thorium (Th) about 0.1 ppm, vanadium (V) 557.00-680.00 ppm (av. 618.50 ppm), yttrium (Y) 14.10-17.60 ppm (av. 15.85 ppm), zinc (Zn) 36.00-74.00 ppm (av. 55.00 ppm) and zircon 13.00-18.00 ppm (av. 15.50 ppm).

Plagioclase-rich granular amphibolites consist of barium (Ba) 2.70-327.00 ppm (av. 138.90 ppm), cobalt (Co) 48.40-49.50 ppm (av. 48.87 ppm), chromium (Cr) 60.00-580.00 ppm (av. 300.00 ppm), copper (Cu) 7.00-25.00 ppm (av. 13.33 ppm), hafnium (Hf) 1.00-2.00 ppm (av. 1.33 ppm), niobium (Nb) 1.00-2.00 ppm (av. 1.67 ppm), nickel (Ni) 42.00-84.00 ppm (av. 67.00 ppm), rubidium (Rb) 0.20-15.10 ppm (av. 6.77 ppm), scandium (Sc) 32.00-54.00 ppm (av. 41.00 ppm), strontium (Sr) 102.00-497.00 ppm (av. 345.67 ppm), thorium (Th) 0.60-1.30 ppm (av. 0.97 ppm), vanadium (V) 253.00-382.00 ppm (av. 390.00 ppm), yttrium (Y) 10.50-19.40 ppm (av. 15.70 ppm), zinc (Zn): 43.00-95.00 ppm (av. 63.33 ppm) and zircon (Zr) 27.20-57.10 ppm (av. 38.00 ppm).

Medium-grained granular amphibolites consist of barium (Ba) 50.10-256.00 ppm (av. 133.17 ppm), cobalt (Co) 68.40-72.40 ppm (av. 70.13 ppm), chromium (Cr) 20.00-256.00 ppm (av. 683.33 ppm), copper (Cu) 7.00-115.00 ppm (av. 64.00 ppm), hafnium

(Hf) 1.00-2.00 ppm (av. 1.50 ppm), niobium (Nb) 1.00-2.00 ppm (av. 1.50 ppm), nickel (Ni) 24.00-462.00 ppm (av. 221.33 ppm), rubidium (Rb) 2.10-52.20 ppm (av. 20.80 ppm), scandium (Sc) 21.00-80.00 ppm (av. 49.33 ppm), strontium (Sr) 187.00-257.00 ppm (av. 231.67 ppm), thorium (Th) 0.10-3.00 ppm (av. 1.17 ppm), vanadium (V) 197.00-525.00 ppm (av. 370.67 ppm), yttrium (Y) 9.80-19.80 ppm (av. 14.07 ppm), zinc (Zn) 38.00-243.00 ppm (av. 127.67 ppm) and zircon (Zr) 18.80-50.20 ppm (av. 32.90 ppm).

Migmatitic amphibolites consist of barium (Ba) 21.50-97.00 ppm (av. 67.20 ppm), cobalt (Co) 40.30 to 70.90 ppm (av. 59.20 ppm), chromium (Cr) 700.00-770.00 ppm (av. 735.00 ppm), copper (Cu) 19.00-64.00 ppm (av. 43.33 ppm), hafnium (Hf) 1.00-2.00 ppm (av. 1.33 ppm), niobium (Nb) 2.00-4.00 ppm (av. 2.67 ppm), nickel (Ni) 11.00-108.00 ppm (av. 72.67 ppm), rubidium (Rb) 0.70-10.70 ppm (av. 6.70 ppm), scandium (Sc) 21.00-72.00 ppm (av. 47.33 ppm), strontium (Sr) 192.00-642.00 ppm (av. 370.67 ppm), thorium (Th) 0.60-1.10 ppm (av. 1.07 ppm), vanadium (V) 182.00-394.00 ppm (av. 304.00 ppm), yttrium (Y) 14.50-17.60 ppm (av. 16.33 ppm), zinc (Zn) 75.00-95.00 ppm (av. 86.33 ppm) and zircon (Zr) 31.50-47.60 ppm (av. 37.10 ppm).

Layered amphibolites consist of barium (Ba) 221.00-761.00 ppm (av. 860.67 ppm), cobalt (Co) 18.30-99.80 ppm (av. 59.70 ppm), chromium (Cr) about 10.00 ppm, copper (Cu) 12.00 to 207.00 ppm (av. 77.33 ppm), hafnium (Hf) 4.00-6.00 ppm (av. 5.33 ppm), niobium (Nb) 7.00-9.00 ppm (av. 7.67 ppm), nickel (Ni) 10.00-15.00 ppm (av. 12.00 ppm), rubidium (Rb) 2.90-92.90 ppm (av. 44.53 ppm), scandium (Sc) 9.00-15.00 ppm (av. 12.00 ppm), strontium (Sr) 187.00-489.00 ppm (av. 290.67 ppm), thorium (Th) 8.0-12.30 ppm (av. 10.50 ppm), vanadium (V) 13.00-75.00 ppm (av. 44.00 ppm), yttrium (Y) 18.60-29.40 ppm (av. 24.73 ppm), zinc (Zn) 11.00-54.00 ppm (av. 30.33 ppm) and zircon (Zr) 127.00-210.00 ppm (av. 178.67 ppm),

Pyroxenite (only one analysis) consist of barium (Ba) about 113.00 ppm, cobalt (Co) 87.50 ppm, chromium (Cr) 220.00 ppm, copper (Cu) 286.00 ppm, nickel (Ni) 245 ppm, rubidium (Rb) 0.70 ppm, scandium (Sc) 41.00 ppm, strontium (Sr) 129 ppm, thorium (Th) 0.10 ppm, vanadium (V) 192.00 ppm, yttrium (Y) 6.60 ppm, zinc (Zn) 69.00 ppm and zircon (Zr) 9.40 ppm.

Variation (Harker-type) diagrams of selective trace elements plotted against magnesium number ($\#Mg = MgO / (MgO + FeO)$) are shown in Figure 4.2. Magnesium number contents appear to increase from layered amphibolites towards migmatitic amphibolites, granular amphibolites and pyroxenite, respectively. Regarding to Ba, Eu, Rb, Th, Yb and Zr they yield the highest ranges against low #Mg numbers of layered amphibolites; on the other hand they decrease dramatically against increasing #Mg of other amphibolites and pyroxenite which reveal similar ranges of these elements. For Cr and Ni contents, they yield the lowest ranges at low #Mg of layered amphibolite and increase significantly against increasing of #Mg in the other rocks. High Cr concentration (> 200 ppm) may indicate zone of chromite deposit as described in Chapter 3.

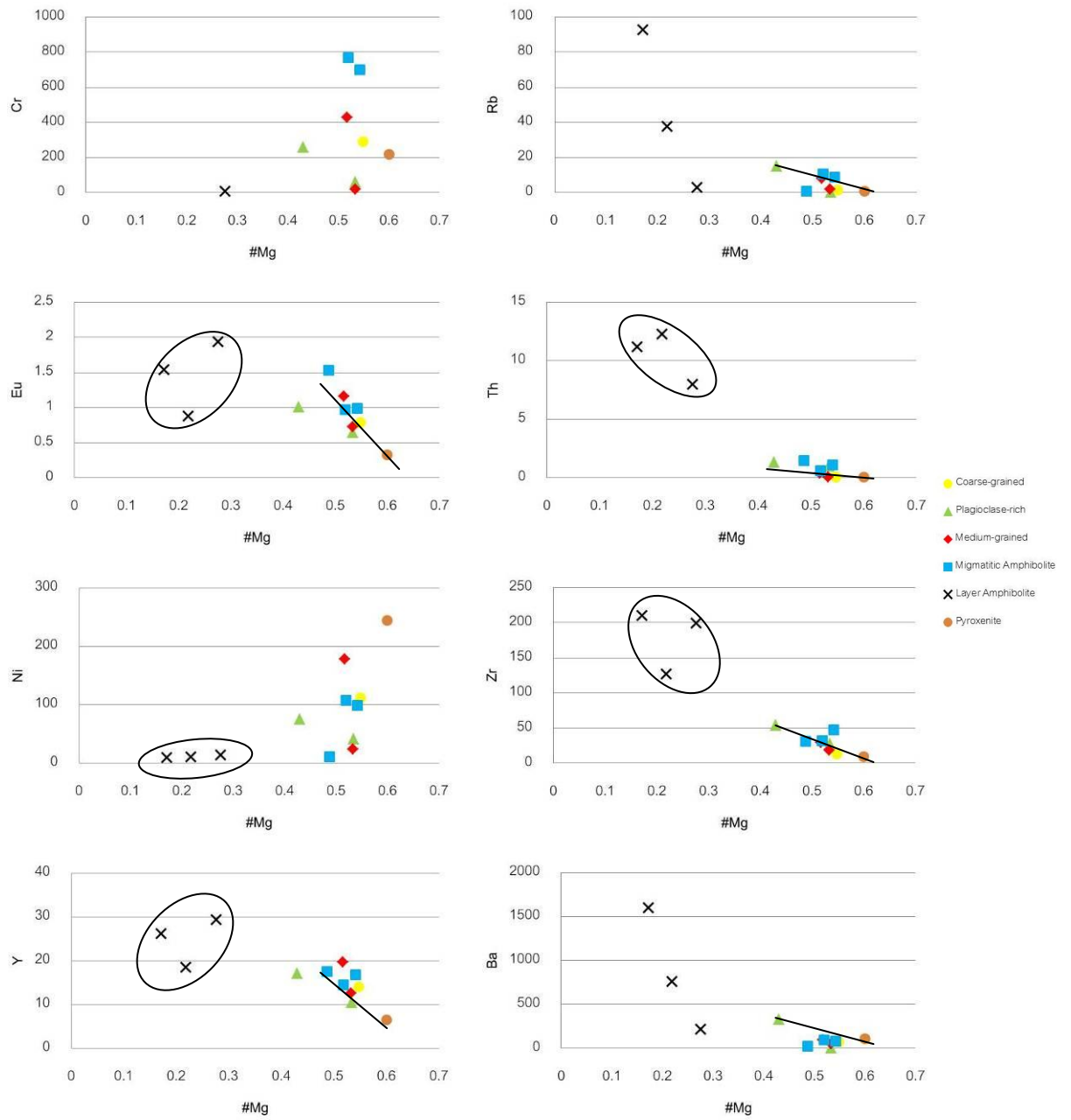


Figure 4.2. Variation diagrams of selective trace elements plotted against magnesium number (#Mg) of amphibolites and pyroxenite from Wang Nam Khiao Area, Nakhon Ratchasima

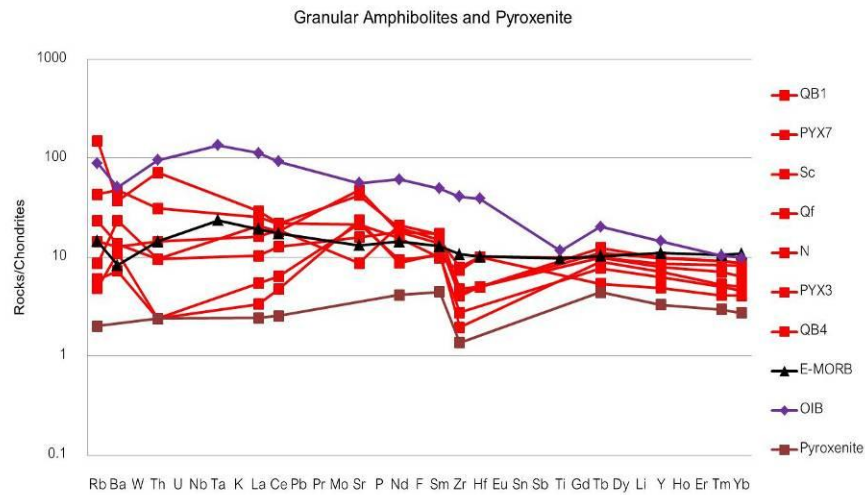


Figure 4.3. Chondrite-normalized spider diagrams of granular amphibolites and pyroxenite from Wang Nam Khiao Area (chondrite's composition and patterns of E-MORB and OIB after Sun and McDonough, 1989)

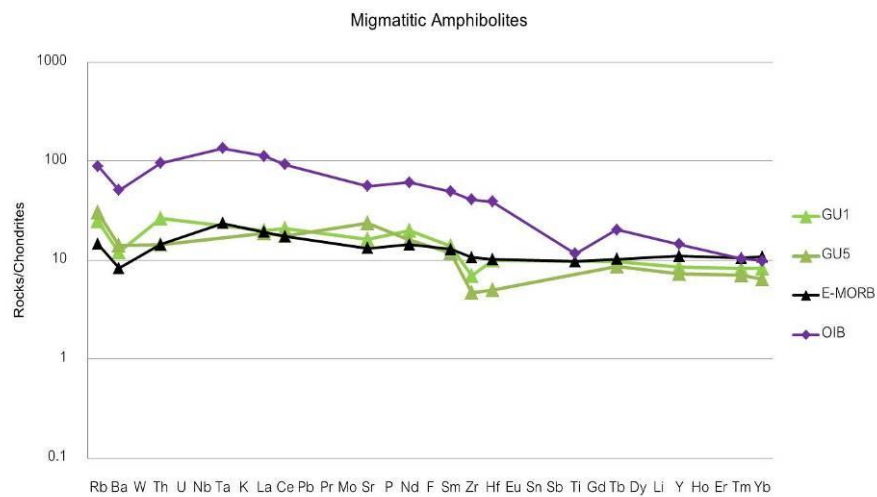


Figure 4.4. Chondrite-normalized spider diagrams of migmatitic amphibolites from Wang Nam Khiao Area (chondrite's composition and patterns of E-MORB and OIB after Sun and McDonough, 1989)

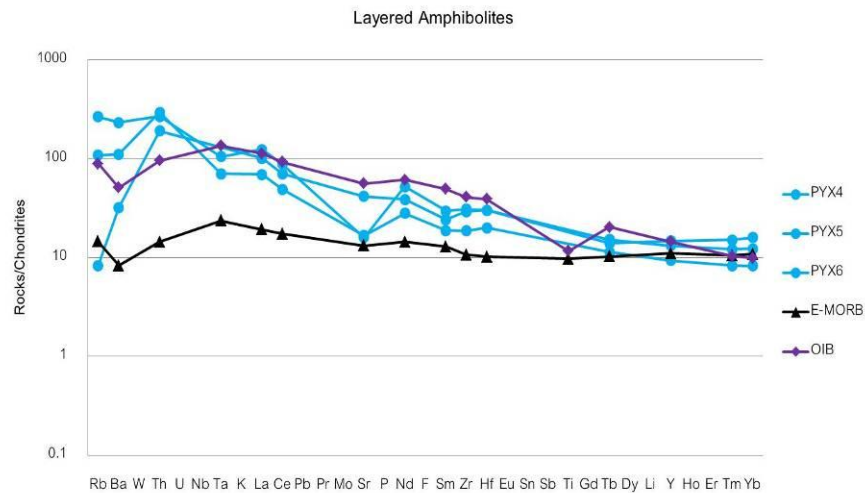


Figure 4.5. Chondrite-normalized spider diagrams of layered amphibolites from Wang Nam Khiao Area (chondrite's composition and patterns of E-MORB and OIB after Sun and McDonough, 1989)

Chondrite-normalized spider diagrams (normalized using chondrite's composition of Sun and McDonough, 1989) usually show zigzag patterns of all rock types; however, there are some differences among these patterns. Patterns of granular amphibolites (Figure 4.3) and migmatitic amphibolites (Figure 4.4) reveal large ion lithophile (LIL) group appear to decreased slightly from Rb to Ti whereas the High field strength (HFS) (Gd to Yb) cations yield closely to flat pattern. These patterns are similar to an E-MORB pattern which is shown in these diagrams for comparison along with a pattern of oceanic island basalt. Pyroxenite's pattern (Figure 4.3) is also close to E-MORB pattern and similar to granular amphibolite patterns; however the whole pattern is lower than those of amphibolites. For layered amphibolites, their patterns are close to a pattern of oceanic island tholiitic basalt (OIB) but they also show negative Ta and Sr and positive Nd and Zr (Figure 4.5). Moreover, the patterns show higher concentrations of

Rb, Ba, W and Th than those of OIB pattern; these may be caused by granite (felsic intrusion) intruded in the north of the study area.

4.1.3 Rare Earth Elements

REE are the series of metals with atomic numbers ranging between 57 and 71 (La and Lu). REE are normally normalized to the reference chondritic composition for presentation so-called chondrite-normalized pattern. REE with even atomic numbers are more stable than one with odd atomic numbers, the usually producing a zig-zag pattern on a composition-abundance diagram (Rollinson, 1993).

Coarse-grained granular amphibolites consist of cerium (Ce) 4.10-6.20 ppm (av. 5.15 ppm), dysprosium (Dy) 2.87-3.53 ppm (av. 3.20 ppm), erbium (Er) 1.50-1.74 ppm (av. 1.74 ppm), europium (Eu) 0.79-0.86 ppm (av. 0.83 ppm), gallium (Ga) 13.00-14.00 ppm (av. 13.50 ppm), gadolinium (Gd) 2.80-3.60 ppm (av. 3.20 ppm), holmium (Ho) 0.56-0.71 ppm (av. 0.64 ppm), lanthanum (La) 110.00-1.80 ppm (av. 1.45 ppm), lutetium (Lu) 0.17-0.22 ppm (av. 0.20 ppm), neodymium (Nd) 5.50-7.40 ppm (av. 6.45 ppm), praseodymium (Pr) 0.92-1.25 ppm (av. 1.09 ppm), samarium (Sm) 2.20-2.70 ppm (av. 2.45 ppm), terbium (Tb) 0.47-0.54 ppm (av. 0.51 ppm), thulium (Tm) 0.18-0.25 ppm (av. 0.22 ppm), tungsten (W) 83.00-139.00 ppm (av. 111.00 ppm) and ytterbium (Yb) 1.10-1.50 ppm (av. 1.30 ppm).

Plagioclase-rich granular amphibolites consist of cerium (Ce) 9.20-18.70 ppm (av. 14.73 ppm), dysprosium (Dy) 2.15-3.86 ppm (av. 3.04 ppm), erbium (Er) 1.14-2.01 ppm (av. 1.70 ppm), europium (Eu) 0.65-1.01 ppm (av. 0.88 ppm), gallium (Ga) 10.00-22.00 ppm (av. 16.00 ppm), gadolinium (Gd) 2.19-3.78 ppm (av. 3.12 ppm), holmium (Ho) 0.42-0.74 ppm (av. 0.60 ppm), lanthanum (La) 3.60-8.30 ppm (av. 5.73 ppm),

lutetium (Lu) 0.15-0.31ppm (av. 0.25 ppm), neodymium (Nd) 7.30-13.20 ppm (av. 11.00 ppm), praseodymium (Pr) 1.44-2.77 ppm (av. 2.31 ppm), samarium (Sm) 1.80-3.40 ppm (av. 2.73 ppm), terbium (Tb) 0.34-0.57 ppm (av. 0.47 ppm), thulium (Tm) 0.60-1.30 ppm (av. 0.25 ppm), tungsten (W) 93.00-243.00 ppm (av. 146.33 ppm) and ytterbium (Yb) 1.00-1.90 ppm (av. 1.57 ppm).

Medium grained granular amphibolites consist of cerium (Ce) 5.50-19.00 ppm (av. 11.83 ppm), dysprosium (Dy) 1.88-3.94 (av. 2.82 ppm), erbium (Er) 1.05-2.29 ppm (av. 1.57 ppm), europium (Eu) 0.53-1.16 ppm (av. 0.81 ppm), gallium (Ga) 13.00-15.00 ppm (av. 14.00 ppm), gadolinium (Gd) 2.03-3.80 ppm (av. 2.73 ppm), holmium (Ho) 0.35-0.82 ppm (av. 0.56 ppm), lanthanum (La) 1.80-9.60 ppm (av. 4.93 ppm), lutetium (Lu) 0.15-0.30 ppm (av. 0.21 ppm), neodymium (Nd) 5.90-11.30 ppm (av. 9.00 ppm), praseodymium (Pr) 1.04-2.38 ppm (av. 1.81 ppm), samarium (Sm) 2.00-3.50 ppm (av. 2.53 ppm), terbium (Tb) 0.28-0.64 ppm (av. 0.44 ppm), thulium (Tm) 0.10-3.00 ppm (av. 0.21 ppm), tungsten (W) 52.00-141.00 ppm (av. 97.00 ppm) and ytterbium (Yb) 0.90-1.90 ppm (av. 1.27 ppm).

Migmatitic amphibolites consist of cerium (Ce) 15.20-28.00 ppm (av. 20.37 ppm), dysprosium (Dy) 2.78-3.87 ppm (av. 3.21 ppm), erbium (Er) 1.62-1.94 ppm (av. 1.82 ppm), europium (Eu) 0.97-1.53 ppm (av. 1.16 ppm), gallium (Ga) 15.00-18.00 ppm (av. 16.67 ppm), gadolinium (Gd) 2.76-4.51 ppm (av. 3.51 ppm), holmium (Ho) 0.55-0.74 ppm (av. 0.63 ppm), lanthanum (La) 6.10-10.70 ppm (av. 7.77 ppm), lutetium (Lu) 0.21-0.27 ppm (av. 0.25 ppm), neodymium (Nd) 10.10-18.90 ppm (av. 13.87 ppm), praseodymium (Pr) 2.18-4.19 ppm (av. 3.01 ppm), samarium (Sm) 2.40-4.70 ppm (av. 3.30 ppm), terbium (Tb) 0.45-0.66 ppm (av. 0.54 ppm), thulium (Tm) 0.60-1.10 ppm (av. 0.28 ppm), tungsten (W) 58.00-219.00 ppm (av. 117.67 ppm) and ytterbium (Yb) 1.40-1.80 ppm (av. 1.57ppm).

Layered amphibolites consist of cerium (Ce) 42.40-76.00 ppm (av. 59.70 ppm), dysprosium (Dy) 3.43-4.94 ppm (av. 4.40 ppm), erbium (Er) 1.88-3.14 ppm (av. 2.65 ppm), europium (Eu) 0.88-1.94ppm (av. 1.45 ppm), gallium (Ga) 10.00-18.00ppm (av. 15.00 ppm), gadolinium (Gd) 3.82-5.25ppm (av. 4.53 ppm), holmium (Ho) 0.67-1.02 ppm (av. 0.89 ppm), lanthanum (La) 22.80-40.50 ppm (av. 32.13 ppm), lutetium (Lu) 0.25-0.47 ppm (av. 0.39 ppm), neodymium (Nd) 17.60-32.70 ppm (av. 24.90 ppm), praseodymium (Pr) 4.79-8.94 ppm (av. 6.81 ppm), samarium (Sm) 3.80-6.00 ppm (av. 4.90 ppm), terbium (Tb) 0.59-0.79 ppm (av. 0.70 ppm), thulium (Tm) 8.00-12.30 ppm (av. 0.40 ppm), tungsten (W) 213.00-938.00ppm (av. 574.33 ppm) and ytterbium (Yb) 1.80-3.50 ppm (av. 2.67 ppm).

Pyroxenite (only one analysis available) consists of cerium (Ce) 2.28 ppm, dysprosium (Dy) 1.40 ppm, erbium (Er) 0.80 ppm, europium (Eu) 0.33 ppm, gallium (Ga) 8.00 ppm, gadolinium (Gd) 1.11 ppm, holmium (Ho) 0.26 ppm, lanthanum (La) 0.80 ppm, lutetium (Lu): 0.10 ppm, neodymium (Nd) 2.60 ppm, praseodymium (Pr) 0.43 ppm, samarium (Sm) 0.90 ppm, terbium (Tb) 0.23 ppm, thulium (Tm) 0.10 ppm, tungsten (W) 64.00 ppm and ytterbium (Yb) 0.60 ppm.

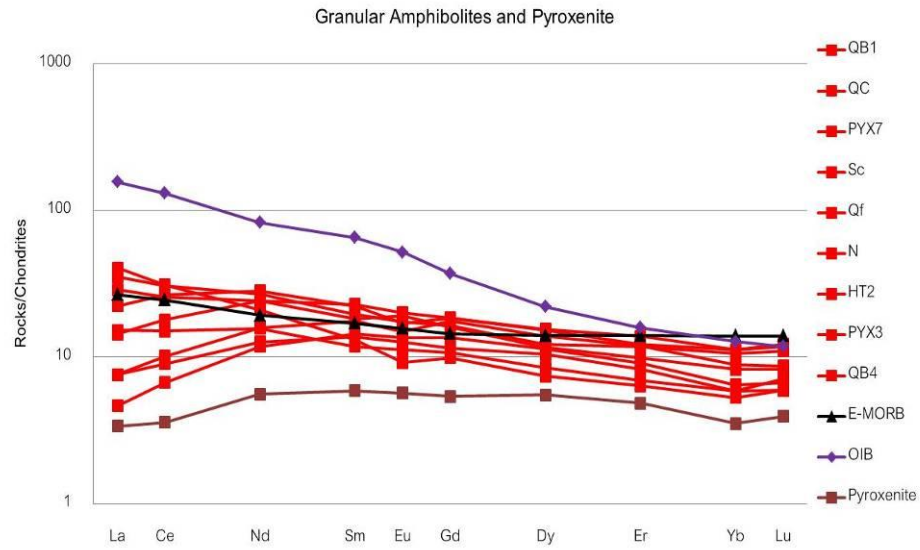


Figure 4.6. Chondrite-normalized REE plots of granular amphibolites and pyroxenite from Wang Nam Khiao Area (chondrite's composition and patterns of E-MORB and OIB after Sun and McDonough, 1989)

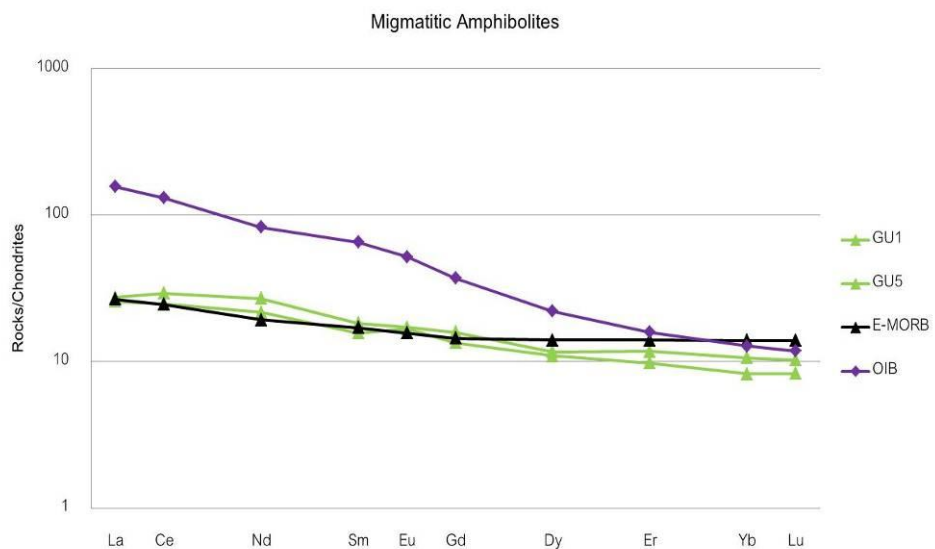


Figure 4.7. Chondrite-normalized REE plots of migmatitic amphibolites from Wang Nam Khiao Area (chondrite's composition and patterns of E-MORB and OIB after Sun and McDonough, 1989)

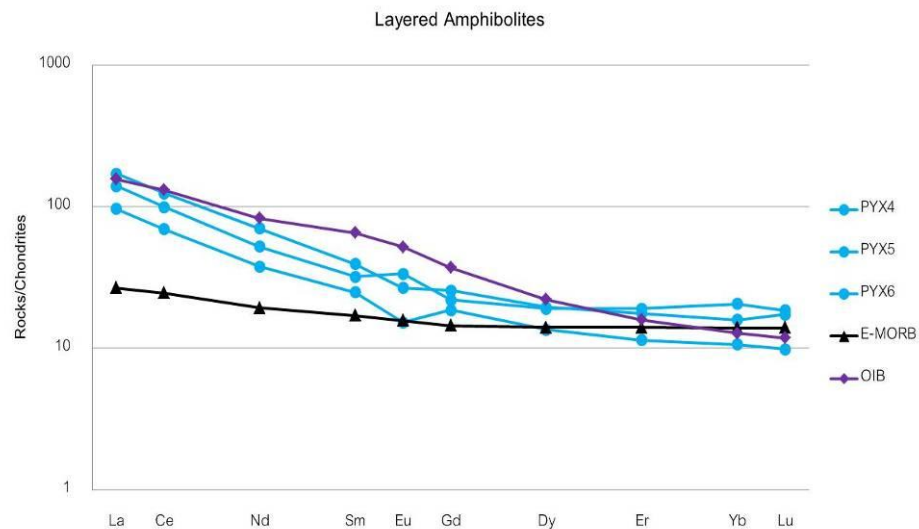


Figure 4.8. Chondrite-normalized REE plots of layered amphibolites from Wang Nam Khiao Area (chondrite's composition and patterns of E-MORB and OIB after Sun and McDonough, 1989)

Chondrites-normalized rare earth elements' patterns show similar patterns of granular amphibolites and migmatitic amphibolites which slightly decrease from La to Lu (Figure 4.6 and 4.7). These patterns are similar to a pattern of E-MORB (Sun and McDonough, 1989) with having low contents of Gd, Dy, Yb and Lu and slightly negative Eu anomaly. Average La/Lu ratios of coarse-grained granular amphibolites, plagioclase-rich granular amphibolites and medium-grained granular amphibolites are about 7, 24 and 30, respectively whereas migmatitic amphibolites yield an average La/Lu ratio of about 30 times. On the other hand, steeper slope of REE patterns (with average La/Lu of 80) belong to layered amphibolites. For pyroxenite, its pattern shows similarly to pattern of E-MORB; however, the whole pattern is lower than ten times. In general, these rocks including most amphibolites and pyroxenite have REE composition similar to E-MORB although some of them appear to have been slightly derived,

probably during metamorphism and uplifting process. Moreover, layered amphibolites may have been modified chemically by later granitic intrusion.

4.2 MINERAL CHEMISTRY

Electron Probe Micro-Analyzer (EPMA), JEOL JXA-8100, was used to analyze chemical compositions of the main mineral phases observed in polished-thin sections. Representative EPMA analyses of amphibole, feldspar and pyroxene are summarized in Tables 4.2 to 4.4. All analyses are collected in Appendix B.

4.2.1 Amphiboles

Amphiboles are the most crucial compositions in all amphibolite groups. The analytical data and their recalculated cation based on 24 oxygen atoms are selectively revealed in Table 4.2.

Coarse-grained granular amphibolites: Amphiboles of this group are composed mainly of 42.40-44.24 %SiO₂, 13.48-14.45 %Al₂O₃, 10.73-12.94 %FeO_{total}, 13.20-14.69 %MgO, 11.33-12.62 %CaO and 1.80-2.37 %Na₂O. The main atomic proportions range between 45.2-50.9 %Mg, 20.9-24.4 %Fe and 28.9-30.5 %Ca which are plotted and present in Figure 4.9.

Plagioclase-rich granular amphibolites: Amphiboles of this group are composed mainly of 42.22-43.77 %SiO₂, 11.43-13.13 %Al₂O₃, 10.27-14.19 %FeO_{total}, 12.90-16.58 %MgO, 12.29-13.42 %CaO and 2.03-2.94 %Na₂O. The main atomic proportions range between 43.3-57.5 %Mg, 18.9-26.8 %Fe and 23.5-30.0 %Ca which are plotted and present in Figure 4.9.

Medium-grain granular amphibolites: Amphiboles of this group are composed mainly of 41.66-45.26 %SiO₂, 11.06-13.89 %Al₂O₃, 13.11-15.97 %FeO_{total}, 11.29-14.61

%MgO, 10.89-13.04 %CaO and 1.09-2.88 %Na₂O. The main atomic proportions range between 38.3-45.3 %Mg, 27.1-35.9 %Fe and 26.8-30.0 %Ca which are plotted and present in Figure 4.9.

Migmatitic amphibolites: Amphiboles of this group are composed mainly of 41.16-47.52 %SiO₂, 11.27-14.83 %Al₂O₃, 7.28-11.86 %FeO_{total}, 16.59-20.95 %MgO, 10.79-13.20 %CaO and 0.09-0.26 %Na₂O. The main atomic proportions range between 53.9-61.6 %Mg, 12.0-19.55 %Fe and 24.9-26.9 %Ca which are plotted and present in Figure 4.9.

Layered amphibolites: Amphiboles of this group are composed mainly of 55.49-58.09 %SiO₂, 2.91-5.95 % Al₂O₃, 11.23-13.74 %FeO_{total}, 15.20-17.38 %MgO, 8.48-8.78 %CaO and 0.12-0.23 %Na₂O. The main atomic proportions range between 52.4-55.0 %Mg, 23.4-26.6 %Fe and 21.1-21.6 %Ca which are plotted and present in Figure 4.9.

In general, Mg-Fe-Ca plots (Figure 4.9) indicate that most amphiboles found coarse-grained, plagioclase-rich and medium-grained granular amphibolites have similar proportions. On the other hand, those of migmatitic amphibolites and layered amphibolites deviate towards higher Mg proportions; moreover, lower Ca proportions of amphiboles are clearly obtained from layered amphibolites. However, these amphiboles still mostly fall within the compositional range of actinolite (Figure 4.9).

Table 4.2 Representative EPMA analyses of amphiboles in rock samples collected from Wang Nam Khiao Area.

Name	Granular Amphibolites												Migmatitic Amphibolites			Layered Amphibolites		
	Coarse-grained			Plagioclase-rich						Medium-grained			GU1-6	GU1-8	GU1-10	PYX4-1	PYX4-2	PYX4-3
	Qc-4	Qc-6	Qc-9	PYX8-3	PYX8-4	PYX8-5	PYX3-1	PYX3-2	PYX3-3	N-2	Scv-1	QBd-1						
SiO ₂	44.24	43.94	43.03	42.51	42.64	42.40	43.77	43.59	42.22	43.21	42.83	44.60	45.41	41.16	47.52	58.09	55.49	56.67
TiO ₂	1.25	0.50	0.48	1.59	1.50	1.53	0.71	0.62	0.12	3.73	1.55	1.63	0.03	0.04	0.00	0.13	0.24	0.19
Al ₂ O ₃	13.68	13.66	14.01	11.56	11.43	11.52	13.13	12.96	12.59	11.75	13.69	11.51	13.11	14.05	14.83	2.91	5.95	4.28
FeO	11.29	12.67	12.05	14.19	14.17	14.12	10.27	10.59	10.93	15.97	14.18	14.96	7.28	11.04	9.54	11.23	13.74	12.21
MnO	0.12	0.13	0.17	0.30	0.28	0.23	0.10	0.15	0.10	0.14	0.18	0.31	0.15	0.32	0.32	0.35	0.33	0.32
MgO	14.42	13.20	14.36	12.92	12.90	12.82	16.02	16.58	16.25	11.29	12.80	12.69	20.95	18.81	16.59	17.38	15.20	16.12
CaO	11.92	12.40	12.51	12.40	12.41	12.29	12.63	12.36	13.42	11.71	11.66	10.89	12.45	12.80	10.79	8.55	8.48	8.78
Na ₂ O	1.80	2.29	2.17	2.73	2.93	2.94	2.03	2.12	2.14	1.87	2.27	1.79	0.14	0.26	0.11	0.12	0.23	0.13
K ₂ O	0.43	0.45	0.30	0.53	0.53	0.53	0.09	0.12	0.03	0.11	0.66	0.51	0.00	0.07	0.07	0.08	0.14	0.08
Total	99.14	99.24	99.09	98.74	98.79	98.37	98.73	99.10	97.81	99.79	99.80	98.89	99.52	98.56	99.77	98.83	99.78	98.78
Si	6.345	6.357	6.229	6.288	6.305	6.294	6.295	6.262	6.193	6.308	6.219	6.516	6.332	5.962	6.586	8.028	7.704	7.886
Ti	0.135	0.054	0.052	0.176	0.166	0.170	0.077	0.067	0.014	0.410	0.169	0.179	0.003	0.005	0.000	0.013	0.025	0.020
Al	2.313	2.331	2.392	2.016	1.992	2.016	2.226	2.195	2.176	2.023	2.344	1.982	2.154	2.399	2.423	0.473	0.973	0.702
Fe ³⁺	0.227	0.185	0.576	0.261	0.189	0.166	0.677	0.803	1.188	0.000	0.181	0.040	0.000	0.000	0.000	0.000	0.000	0.000
Fe ²⁺	1.127	1.348	0.883	1.494	1.563	1.586	0.558	0.469	0.153	1.950	1.541	1.788	0.849	1.338	1.106	1.298	1.595	1.421
Mn	0.014	0.016	0.020	0.038	0.035	0.029	0.012	0.018	0.013	0.017	0.022	0.039	0.018	0.040	0.038	0.041	0.038	0.038
Mg	3.081	2.847	3.098	2.848	2.844	2.837	3.433	3.549	3.552	2.457	2.770	2.764	4.353	4.060	3.427	3.581	3.146	3.342
Ca	1.832	1.922	1.940	1.964	1.966	1.956	1.946	1.902	2.110	1.832	1.814	1.705	1.860	1.987	1.602	1.266	1.261	1.310
Na	0.501	0.644	0.610	0.784	0.840	0.846	0.565	0.592	0.609	0.529	0.639	0.506	0.038	0.073	0.030	0.031	0.062	0.036
K	0.078	0.083	0.056	0.101	0.100	0.100	0.016	0.022	0.005	0.020	0.123	0.095	0.000	0.013	0.012	0.014	0.024	0.015
Total	15.653	15.787	15.856	15.971	16.002	16.000	15.806	15.880	16.013	15.545	15.821	15.614	15.607	15.876	15.223	14.745	14.828	14.769
Atomic (%)																		
Mg	49.2	45.2	47.7	43.4	43.3	43.3	51.9	52.8	50.7	39.4	43.9	43.9	61.6	55.0	55.9	58.3	52.4	55.0
Fe	21.6	24.3	22.5	26.7	26.7	26.8	18.7	18.9	19.1	31.3	27.3	29.0	12.0	18.1	18.0	21.1	26.6	23.4
Ca	29.2	30.5	29.9	29.9	30.0	29.9	29.4	28.3	30.1	29.4	28.8	27.1	26.3	26.9	26.1	20.6	21.0	21.6

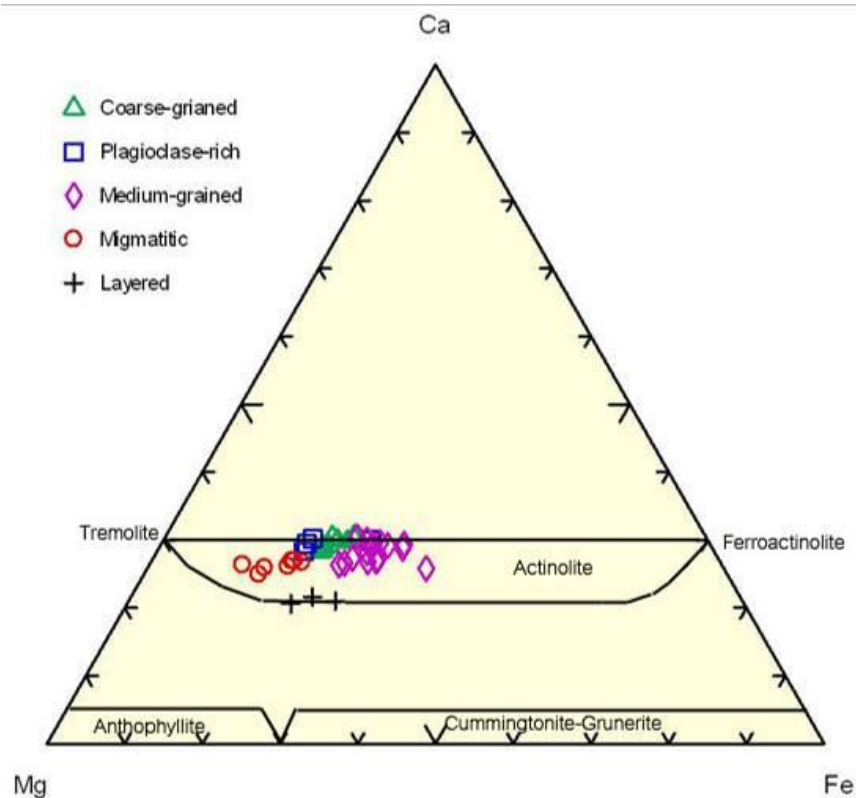


Figure 4.9. Atomic Mg-Fe-Ca plots showing compositions of amphiboles from various rock types collected from Wang Nam Khiao area, Nakhon Ratchasima (classification after Eyuboglu et al., 2011).

4.2.2 Plagioclase

Plagioclase grains found in most amphibolites, i.e., plagioclase-rich amphibolites, migmatitic amphibolites and layered amphibolites, are significantly weathered; however, a few fresh crystals can be observed and analyzed. The selective analytical data and their recalculated cations based on 8 oxygen are presented in Table 4.3. The whole range of analyses is collected in Appendix B.

Plagioclase-rich granular amphibolites: Plagioclases found in this rock type are mainly composed of 61.81-61.97 %SiO₂, 20.00-20.67 %Al₂O₃, 4.91-5.31 %CaO, 11.89-11.95 %Na₂O and 0.07-0.10 %K₂O. Plots of atomic Ca-Na-K proportions (represent to–

anorthite (An), albite (Ab) and orthoclase (Or) end-members) are present in Figure 4.10. They fall within narrow ranges of 18.4-19.7 %An, 80.0-81.1 %Ab and 0.3-0.4 %Or, respectively.

Medium-grained granular amphibolites: Plagioclases found in this rock type are mainly composed of 59.2-60.3 %SiO₂, 24.00-24.69 %Al₂O₃, 5.56-5.84 %CaO, 9.53-9.97 %Na₂O and 0.24-0.31 %K₂O. Plots of atomic Ca-Na-K proportions (represent to–anorthite (An), albite (Ab) and orthoclase (Or) end-members) are present in Figure 4.10. They fall within narrow ranges of 24.0-24.9 %An, 73.7-74.6 %Ab and 1.2-1.6 %Or, respectively.

Migmatitic amphibolites: Plagioclases found in this rock type are mainly composed of 67.14-67.55 %SiO₂, 19.81-20.86 %Al₂O₃, 0.24-0.64 %CaO, 10.08-11.04 %Na₂O and 0.02-0.04 %K₂O. Plots of atomic Ca-Na-K proportions (represent to–anorthite (An), albite (Ab) and orthoclase (Or) end-members) are present in Figure 4.10. They fall within narrow ranges of 1.2-3.3 %An, 96.2-98.5 %Ab and 0.3-0.5 %Or, respectively.

The other plagioclase group composes with 66.16-66.72 %SiO₂, 20.34-20.47 %Al₂O₃, 10.11-10.43 %CaO, 0.88-3.50 %Na₂O and 0.02-0.04 %K₂O. Plots of atomic Ca-Na-K proportions (represent to–anorthite (An), albite (Ab) and orthoclase (Or) end-members) are present in Figure 4.10. They fall within narrow ranges of 61.2-67.1 %An, 32.6-38.6 %Ab and 0.2-0.3 %Or, respectively. These plagioclases show higher percentage of CaO because the rock samples are contained some coarse-grained marble layers.

Layered amphibolites: Plagioclases found in this rock type are mainly composed of 64.52-65.97 %SiO₂, 20.47-21.77 %Al₂O₃, 1.98-3.13 %CaO, 9.46-10.75 %Na₂O and

0.08-0.11 %K₂O. Plots of atomic Ca-Na-K proportions (represent to–anorthite (An), albite (Ab) and orthoclase (Or) end-members) are present in Figure 4.10. They fall within narrow ranges of 9.2-15.4 %An, 84.0-90.3 %Ab and 0.4-0.6 %Or, respectively.

Pyroxenite: Plagioclases found in this rock type are mainly composed of 51.79-56.10 %SiO₂, 27.77-30.77 %Al₂O₃, 11.37-12.36 %CaO , 3.89-5.10 %Na₂O and 0.02-0.14 %K₂O. Plots of atomic Ca-Na-K proportions (represent to–anorthite (An), albite (Ab) and orthoclase (Or) end-members) are present in Figure 4.10. They fall within narrow ranges of 55.1-65.4 %An, 34.5-44.8 %Ab and 0.1-0.3 %Or, respectively.

Figure 4.10 shows widely end-member plots of plagioclases observed in various rock types. In general, these plagioclases are chemically characterized by wide compositional range crucially from albite to labradorite. Plagioclases in plagioclase-rich amphibolites are mostly oligoclase with some albite as well as those occur in layered amphibolites. All plagioclase analyses of medium-grained granular amphibolites fall within oligoclase range. On the other hand, plagioclases in migmatitic amphibolites are mostly characterized by albite composition; however, a few analyses taken from samples closed to coarse-grained marble layers yield extremely high An content up to labradorite-bytownite composition. Plagioclases found in pyroxenite can be divided into labradorite and andesine.

Table 4.3 Representative EPMA analyses of feldspars found in various rock samples from Wang Nam Khiao Area.

Name	Granular Amphibolites						Migmatitic Amphibolites						Layered Amphibolites			Pyroxenite		
	Plagioclase-rich			Medium-grained			GU3-4			GD2-1			PYX4-1			N-a3-1	N-a3-3	N-1-2
	PYX8-1	PYX8-2	PYX8-4	QBd-1	QBd-2	QBd-3	GU3-4	GU3-7	GU3-8	GD2-1	GD2-2	GD2-3	PYX4-1	PYX4-2	PYX4-3	N-a3-1	N-a3-3	N-1-2
SiO ₂	67.31	61.97	61.81	60.31	59.20	60.08	67.33	67.14	67.34	66.42	66.16	66.72	64.66	62.33	64.94	54.61	55.84	52.25
TiO ₂	0.02	0.01	0.00	0.02	0.00	0.04	0.00	0.00	0.00	0.04	0.00	0.00	0.04	0.01	0.00	0.02	0.01	0.03
Al ₂ O ₃	19.27	20.67	20.00	24.10	24.69	24.00	20.85	20.10	20.50	20.47	20.34	20.36	21.71	22.56	21.33	28.56	28.00	30.47
FeO	0.10	0.09	0.04	0.13	0.09	0.09	0.03	0.07	0.04	0.13	0.19	0.29	0.04	0.04	0.07	0.02	0.08	0.30
MnO	0.01	0.00	0.00	0.00	0.00	0.01	0.00	0.00	0.00	0.03	0.00	0.04	0.00	0.00	0.01	0.00	0.00	0.01
MgO	0.01	0.07	0.00	0.00	0.01	0.00	0.00	0.00	0.00	0.03	0.00	0.00	0.00	0.00	0.00	0.00	0.00	0.00
CaO	0.08	5.31	4.91	5.84	5.56	5.84	0.41	0.24	0.41	10.04	10.43	10.11	3.13	4.37	2.94	12.14	11.54	12.18
Na ₂ O	11.34	11.89	11.95	9.97	9.53	9.55	10.57	11.04	11.00	3.50	2.80	0.88	9.46	9.85	9.59	4.34	4.03	4.54
K ₂ O	0.07	0.07	0.10	0.24	0.31	0.28	0.06	0.06	0.07	0.02	0.04	0.03	0.11	0.14	0.08	0.05	0.02	0.03
Total	98.23	100.07	98.80	100.63	99.39	99.89	99.25	98.64	99.36	100.68	99.95	98.42	99.14	99.30	98.95	99.73	99.51	99.82
Si	2.992	2.786	2.811	2.688	2.667	2.694	2.955	2.969	2.958	2.897	2.902	2.942	2.868	2.787	2.884	2.468	2.516	2.373
Ti	0.001	0.000	0.000	0.001	0.000	0.001	0.000	0.000	0.000	0.001	0.000	0.000	0.001	0.000	0.000	0.001	0.000	0.001
Al	1.010	1.096	1.072	1.267	1.311	1.269	1.079	1.048	1.062	1.052	1.052	1.058	1.135	1.189	1.117	1.522	1.487	1.631
Fe	0.004	0.003	0.002	0.005	0.004	0.003	0.001	0.003	0.002	0.005	0.007	0.011	0.001	0.001	0.003	0.001	0.003	0.011
Mn	0.000	0.000	0.000	0.000	0.000	0.000	0.000	0.000	0.000	0.001	0.000	0.001	0.000	0.000	0.001	0.000	0.000	0.000
Mg	0.000	0.004	0.000	0.000	0.001	0.000	0.000	0.000	0.000	0.002	0.000	0.000	0.000	0.000	0.000	0.000	0.000	0.000
Ca	0.004	0.256	0.239	0.279	0.268	0.281	0.019	0.012	0.019	0.469	0.490	0.477	0.149	0.209	0.140	0.588	0.557	0.593
Na	0.977	1.036	1.053	0.862	0.832	0.830	0.900	0.947	0.937	0.296	0.238	0.075	0.813	0.854	0.825	0.380	0.352	0.400
K	0.004	0.004	0.006	0.014	0.018	0.016	0.003	0.003	0.004	0.001	0.002	0.001	0.006	0.008	0.004	0.003	0.001	0.002
Total	4.993	5.186	5.183	5.116	5.102	5.094	4.957	4.982	4.981	4.725	4.691	4.567	4.973	5.049	4.973	4.962	4.917	5.011
Atomic (%)																		
An	0.4	19.7	18.4	24.2	24.0	24.9	2.1	1.2	2.0	61.2	67.1	86.2	15.4	19.5	14.4	60.6	61.2	59.6
Ab	99.2	80.0	81.1	74.6	74.4	73.7	97.5	98.5	97.6	38.6	32.6	13.6	84.0	79.7	85.1	39.2	38.7	40.2
Or	0.4	0.3	0.4	1.2	1.6	1.4	0.4	0.3	0.4	0.2	0.3	0.3	0.6	0.8	0.4	0.3	0.1	0.2

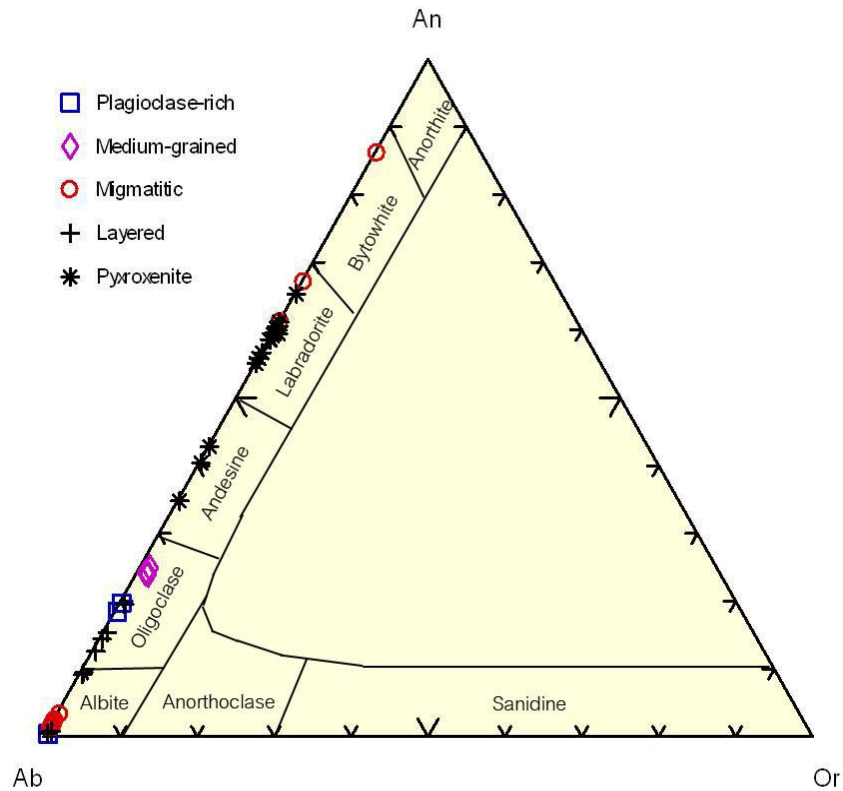


Figure 4.10. Plots of albite–anorthite–orthoclase end-members showing various compositions of plagioclases found in each rock type collected from Wang Nam Khiao area, Nakhon Ratchasima (compositional fields after Deer et al., 1992).

4.2.3 Pyroxene

Pyroxenes are usually altered; however, small fresh pyroxene grains can be observed in most types of amphibolites except coarse-grained granular amphibolites. On the other hand, they are the essential composition of pyroxenite. Analytical data and their calculated cations (based on 6 oxygens) are selectively present in Table 4.4 whereas the other analyses are collected in Appendix B.

Plagioclase-rich granular amphibolites: Pyroxenes found in this rock type contain mainly 49.78-52.37 %SiO₂, 0.91-6.94 %Al₂O₃, 6.83-11.96 %FeO_{total}, 13.52-15.43 %MgO,

and 13.35-23.95 %CaO. Their atomic proportions of Mg, Fe and Ca range from 39.1-49.1%, 11.0-21.6% and 29.4-49.4%, respectively. These proportions are graphically plotted in Figure 4.11.

Medium-grain granular amphibolites: Pyroxenes found in this rock type contain mainly 50.92-54.44 %SiO₂, 4.25-5.98 %Al₂O₃, 9.10-15.38 %FeO_{total}, 14.60-18.72 %MgO and 10.35-12.63 %CaO. Their atomic proportions of Mg, Fe and Ca range from 47.4-56.3%, 15.9-27.2% and 24.3-27.9%, respectively. These proportions are graphically plotted in Figure 4.11.

Migmatitic amphibolites: Pyroxenes found in this rock type contain mainly 53.16-54.9 %SiO₂, 1.27-2.98 %Al₂O₃, 9.01-11.86 %FeO_{total}, 18.40-20.75 %MgO and 11.94-13.20 %CaO. Their atomic proportions of Mg, Fe and Ca range from 54.7-61.6%, 12.0-18.1% and 24.9-27.7%, respectively. These proportions are graphically plotted in Figure 4.11.

Layered amphibolites: Pyroxenes found in this rock type contain mainly 52.61-56.67 %SiO₂, 4.28-5.95 %Al₂O₃, 11.42-13.74 %FeO_{total}, 15.20-16.12 %MgO and 8.78-12.55 %CaO. Their atomic proportions of Mg, Fe and Ca range from 51.0-55.0%, 20.5-26.6% and 21.0-28.5%, respectively. These proportions are graphically plotted in Figure 4.11.

Pyroxenites: Pyroxenes found in this rock type contain mainly 56.84-57.74 %SiO₂, 3.55-4.98 %Al₂O₃, 6.62-7.73w% FeO_{total}, 13.59-15.81 %MgO and 12.65-15.49 %CaO. Their atomic proportions of Mg, Fe and Ca range from 47.4-59.9%, 12.9-17.1% and 23.4-38.8%, respectively. These proportions are graphically plotted in Figure 4.11.

Atomic Ca-Mg-Fe plots as represented CaSiO₃-MgSiO₃-FeSiO₃ end-members of pyroxene analyses show a wide range of composition varying from diopside to augite. In

general, most of pyroxenes in all rock samples are characterized compositionally by augite; however, some analyses of plagioclase-rich granular amphibolites also fall in diopside composition.

Table 4.4 Representative EPMA analyses of pyroxene found in different rock types collected from Wang Nam Khiao Area, Nakhon Ratchasima.

Name	Granular Amphibolites												Migmatitic Amphibolites			Layered Amphibolites			Pyroxenite					
	Plagioclase-rich						Medium-grained						GU1-1	GU1-3	GU3-1	PYX4-1	PYX4-3	PYX4-4	PYX-1	PYX-2	PYX-3	PYX-6	PYX-8	PYX-10
	PYX3-1	PYX3-2	PYX3-3	PYX8-3	PYX8-4	PYX8-6	N-1	N-5	N-3	Qf-3	Qf-4	Qf-5												
SiO ₂	50.60	50.54	49.78	52.35	52.07	52.16	52.37	51.94	53.46	54.89	54.44	53.33	54.94	54.34	54.56	52.61	55.49	56.67	54.03	54.91	54.81	57.74	57.05	56.84
TiO ₂	0.51	0.44	0.63	0.09	0.11	0.05	0.30	0.27	0.18	0.06	0.09	0.04	0.05	0.05	0.00	0.13	0.24	0.19	0.01	0.02	0.00	0.53	0.57	0.50
Al ₂ O ₃	5.22	5.22	6.53	0.99	1.19	1.14	5.80	5.90	4.62	4.25	4.56	5.10	2.93	2.17	1.67	5.18	5.95	4.28	0.07	0.12	0.09	3.55	4.60	4.98
FeO	8.29	7.07	8.27	7.18	7.36	7.42	13.84	15.00	13.20	9.58	9.10	9.29	9.78	9.11	11.54	11.58	13.74	12.21	11.36	11.37	11.28	7.03	6.62	7.06
MnO	0.18	0.14	0.21	0.40	0.39	0.38	0.27	0.31	0.31	0.14	0.15	0.14	0.27	0.22	0.36	0.34	0.33	0.32	0.14	0.11	0.10	0.30	0.17	0.10
MgO	15.43	14.74	14.53	13.92	13.77	13.52	14.93	14.94	15.67	18.72	18.31	18.61	20.46	20.75	19.30	16.12	15.20	16.12	22.22	22.03	22.47	13.59	14.57	14.58
CaO	19.55	21.60	20.13	23.74	23.55	23.41	11.20	10.56	11.01	12.70	12.63	12.61	11.99	11.94	13.20	12.55	8.48	8.78	12.14	12.27	12.11	15.49	14.60	14.72
Na ₂ O	0.31	0.36	0.35	0.46	0.48	0.48	0.77	0.89	0.61	0.22	0.29	0.35	0.24	0.26	0.09	0.52	0.23	0.13	0.07	0.03	0.02	0.07	0.08	0.07
K ₂ O	0.00	0.00	0.01	0.00	0.00	0.02	0.06	0.06	0.02	0.06	0.05	0.11	0.03	0.03	0.02	0.11	0.14	0.08	0.02	0.00	0.00	0.00	0.01	0.00
Total	100.09	100.10	100.43	99.11	98.91	98.57	99.54	99.68	99.08	100.62	99.61	99.56	100.67	98.86	100.75	99.12	99.78	98.78	100.05	100.85	100.86	98.31	98.26	98.86
Si	1.888	1.867	1.836	1.969	1.963	1.973	1.936	1.924	1.975	1.969	1.968	1.936	1.972	1.983	1.984	1.942	2.010	2.057	1.977	1.989	1.984	2.092	2.060	2.045
Ti	0.014	0.012	0.018	0.002	0.003	0.001	0.008	0.008	0.005	0.002	0.002	0.001	0.001	0.001	0.000	0.004	0.006	0.005	0.000	0.001	0.000	0.014	0.015	0.014
Al	0.227	0.227	0.284	0.044	0.053	0.051	0.253	0.258	0.201	0.180	0.195	0.218	0.124	0.094	0.072	0.225	0.254	0.183	0.003	0.005	0.004	0.152	0.196	0.211
Fe ³⁺	0.046	0.061	0.053	0.070	0.074	0.055	0.000	0.000	0.000	0.000	0.000	0.000	0.000	0.000	0.000	0.000	0.000	0.000	0.073	0.028	0.044	0.000	0.000	0.000
Fe ²⁺	0.209	0.157	0.202	0.156	0.158	0.179	0.428	0.465	0.408	0.287	0.275	0.282	0.294	0.278	0.351	0.357	0.416	0.371	0.274	0.316	0.297	0.213	0.200	0.212
Mn	0.006	0.004	0.007	0.013	0.012	0.012	0.009	0.010	0.010	0.004	0.004	0.004	0.008	0.007	0.011	0.010	0.010	0.010	0.004	0.003	0.003	0.009	0.005	0.003
Mg	0.849	0.811	0.798	0.780	0.774	0.762	0.823	0.825	0.863	1.001	0.986	1.007	1.095	1.129	1.046	0.887	0.821	0.872	1.211	1.189	1.212	0.734	0.784	0.782
Ca	0.773	0.855	0.795	0.957	0.952	0.949	0.444	0.419	0.436	0.488	0.489	0.490	0.461	0.467	0.514	0.496	0.329	0.342	0.476	0.476	0.470	0.601	0.565	0.567
Na	0.022	0.026	0.025	0.033	0.035	0.035	0.055	0.064	0.044	0.015	0.020	0.024	0.017	0.018	0.006	0.037	0.016	0.009	0.005	0.002	0.001	0.005	0.005	0.005
K	0.000	0.000	0.000	0.000	0.000	0.001	0.003	0.003	0.001	0.003	0.002	0.005	0.001	0.001	0.001	0.005	0.006	0.004	0.001	0.000	0.000	0.000	0.000	0.000
Total	4.015	4.020	4.018	4.024	4.025	4.019	3.958	3.973	3.942	3.949	3.943	3.968	3.973	3.978	3.984	3.963	3.868	3.853	4.025	4.009	4.015	3.820	3.830	3.839
Atomic (%)																								
Mg	45.2	43.1	43.2	39.7	39.5	39.2	48.6	48.3	50.6	56.3	56.3	56.6	59.2	60.2	54.7	51.0	52.4	55.0	59.5	59.2	59.9	47.4	50.6	50.1
Fe	13.6	11.6	13.8	11.5	11.9	12.1	25.3	27.2	23.9	16.2	15.7	15.9	15.9	14.8	18.4	20.5	26.6	23.4	17.1	17.1	16.9	13.8	12.9	13.6
Ca	41.2	45.3	43.0	48.7	48.6	48.8	26.2	24.5	25.5	27.5	27.9	27.6	24.9	24.9	26.9	28.5	21.0	21.6	23.4	23.7	23.2	38.8	36.5	36.3

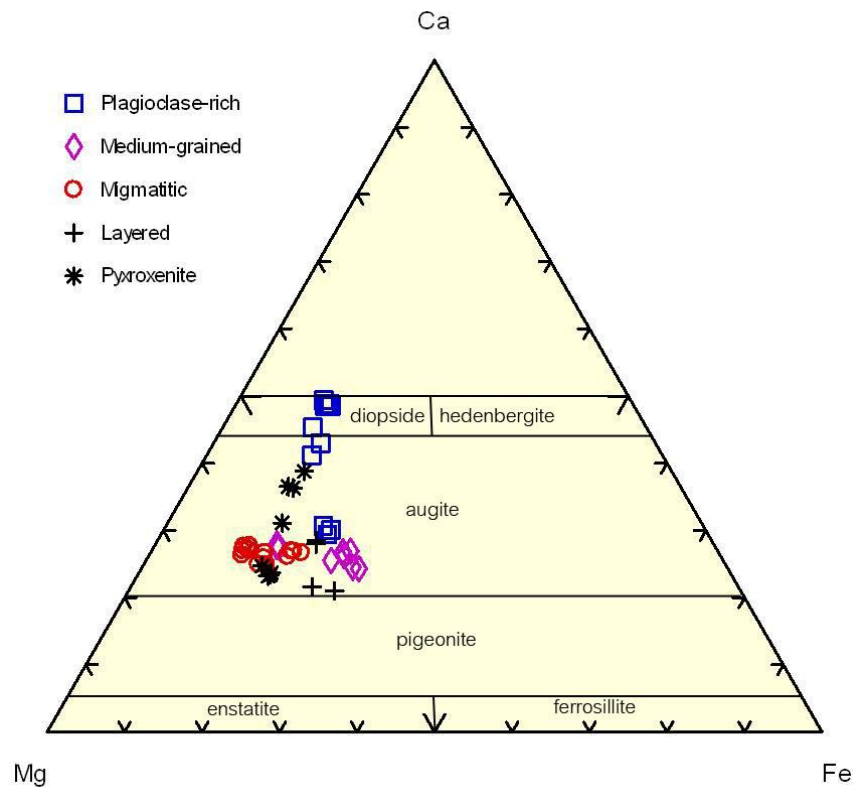


Figure 4.11. Atomic Ca-Mg-Fe plots showing wide compositions (diopside-augite range) of pyroxenes in various rock types collected from Wang Nam Khiao area, Nakhon Ratchasima (fields of classification after Morimoto et al., 1989).

According to mineral chemistry data, amphiboles in all amphibolites groups are significantly characterized by actinolite whereas pyroxenes mostly fall within compositional ranges of augite and diopside. Plagioclases vary from albite to oligoclase compositions with rare labradorite composition. Actinolite is a calc-amphibole (Leake et al., 1997) which usually occurs in high temperature metamorphism and igneous magmatism. It may also occur as an altered product of pyroxene either during the late magmatic stages of crystallizations or during metamorphism (Klein and Hurlbut, 1977). In addition, it is an index mineral of upper green schist facies. Augite is commonly found in igneous rocks while diopside may indicate metamorphism (Klein and Hurlbut, 1977). For

plagioclase, both albite and oligoclase are widely found in metamorphic and igneous rocks while labradorite (found in migmatitic amphibolites) is commonly found in gabbro or basalt (Klein and Hurlbut, 1977). Consequently, it may be concluded, based on mineral chemistry, that all amphibolites are high grade metamorphic rocks which seem to have mafic origin.

CHAPTER V

DISCUSSIONS AND CONCLUSIONS

5.1 Protolith and Initial Provenance of Amphibolite

Based on geochemical data presenting graphically as variation diagrams, discrimination diagrams and tectono-diagrams, chemical compositions of most amphibolite groups and pyroxenite appear to have been originated within the same geochemical environment. However, only layered amphibolites have somewhat differences that may be caused by influence of intrusion on the north. Regarding to discrimination diagram (total alkali versus SiO_2 , TAS diagram) suggested by Le Bas et al. (1986) (Figure 5.1), coarse-grained granular amphibolites, plagioclase-rich granular amphibolites, medium-grained granular amphibolites and migmatitic amphibolites fall obviously in the field of basaltic composition whereas layered amphibolites deviate to the fields of trachytic and rhyolitic compositions. MgO-FeO-alkali plots (Irvine and Baragar, 1971) indicate signature of tholeiitic magma series for both compositions of granular and migmatitic amphibolites; although, a few analyses are close to calc-alkaline series (Figure 5.2). On the other hand, most compositions of layered amphibolites seem to have modified and some analyses disappear in this diagram, consequently. Plots of Ti/1000 versus V designed by Jian et al. (2009) suggest that most compositions of rock samples appear to have related to a provenance of Island Arc Tholeiite (IAT). In addition, Th-Zr-Nb tectono-diagram (after Wood, 1980) indicates that all amphibolites and pyroxenite may have been associated with arc-basalt (Figure 5.4).

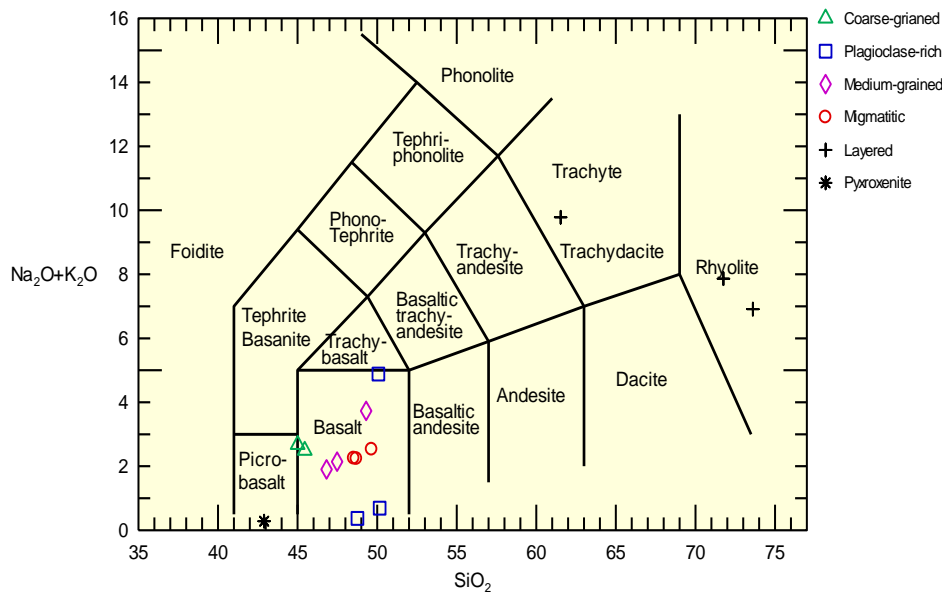


Figure 5.1. TAS diagram (Le Bas et al., 1986) showing compositional plots of whole-rock chemistry of samples collected from Wang Nam Khiao Area, Nakhon Ratchasima.

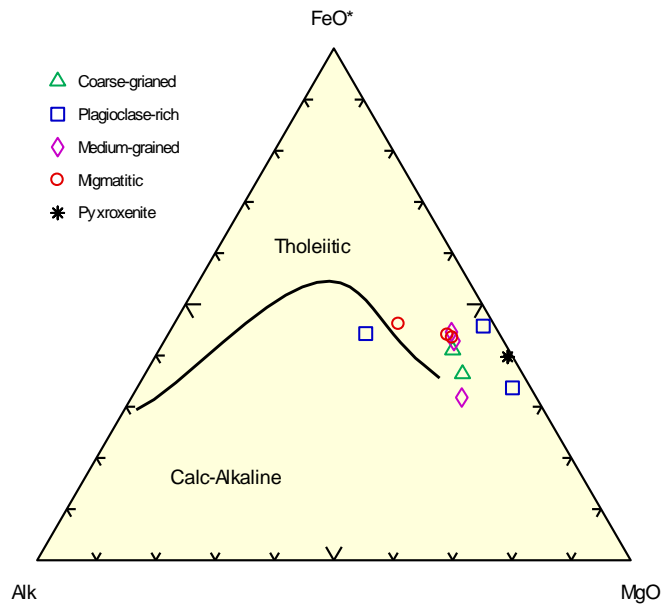


Figure 5.2. Triangular MgO-FeO-Alkali plots (after Irvine and Baragar, 1971) applied to indicate initial magma series of rock samples from Wang Nam Khiao Area, Nakhon Ratchasima.

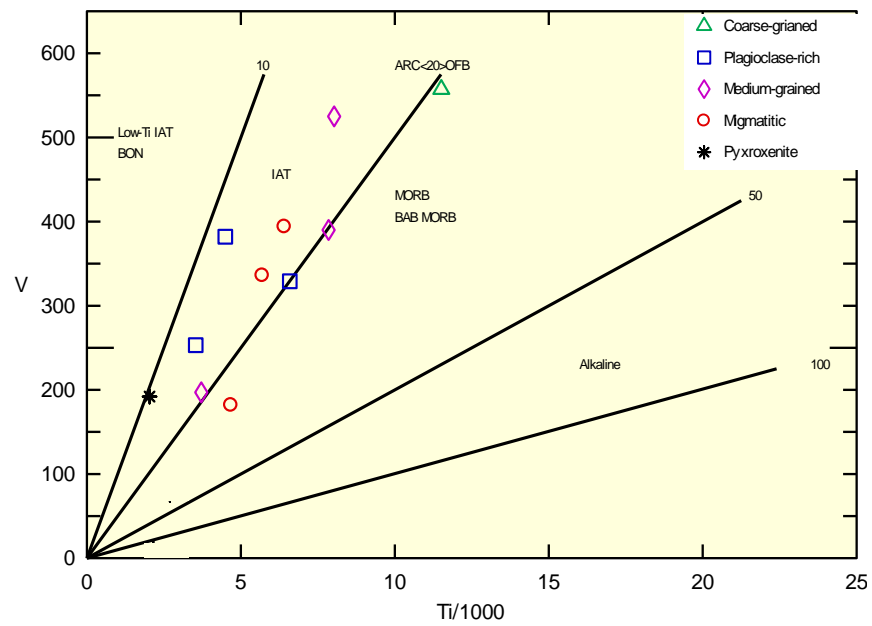


Figure 5.3. Ti-V plots of tectono diagram (after Jian et al., 2009) indicating potentially initial magma series of rock samples from Wang Nam Khiao Area, Nakhon Ratchasima.

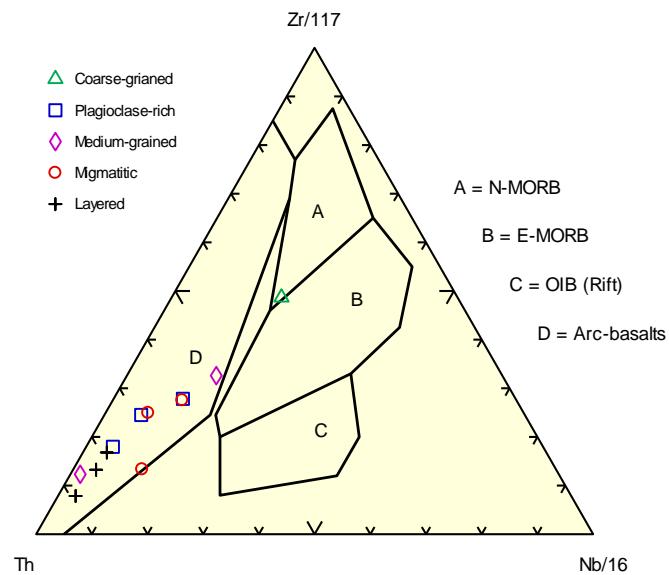


Figure 5.4. Th-Zr-Nb tectono-diagram (after Wood, 1980) indicating significantly most whole-rock analyses of amphibolites geochemically associated with arc-basalt.

According to geochemical analysis as mentioned above, it may imply on the basis of isochemical metamorphic process that the initial composition of all amphibolites including pyroxenite appear to have related to tholeiitic basalt magmas within an ancient island arc provenance.

In addition, chondrite-normalized REE patterns (chondrite composition after Sun and McDonough, 1989) (Figures 5.5-5.7) of all rock types collected under this study are compared with those patterns of normal amphibolites occurred in oceanic domain (after Castro et al., 1996) which present as shaded pattern. Most granular amphibolites (Figure 5.5) and migmatitic amphibolites (Figure 5.6) are similar to such shaded pattern slightly decreasing from LREE to HREE. On the other hand, pyroxenite show rather flat pattern with lower concentration of whole range of REE indicating very low degree of differentiation or partial melting; this may imply mantle remnant of pyroxenite. Moreover, layered amphibolites (Figure 5.7) reveal REE pattern having higher LREE that should support the influence of granitic intrusion.

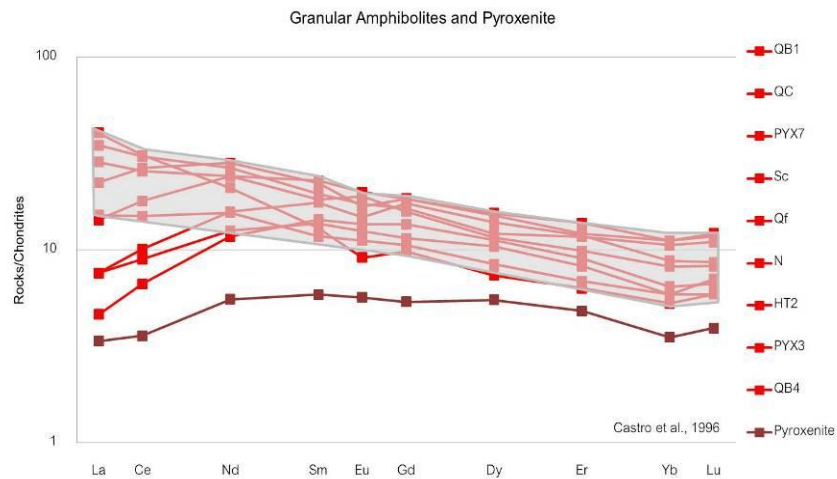


Figure 5.5. Chondrite-normalized REE patterns (chondrite composition after Sun and McDonough, 1989) of granular amphibolites and pyroxenite collected from Wang Nam Khiao Area compared to shaded pattern of normal amphibolites occurred in oceanic domain (after Castro et al., 1996).

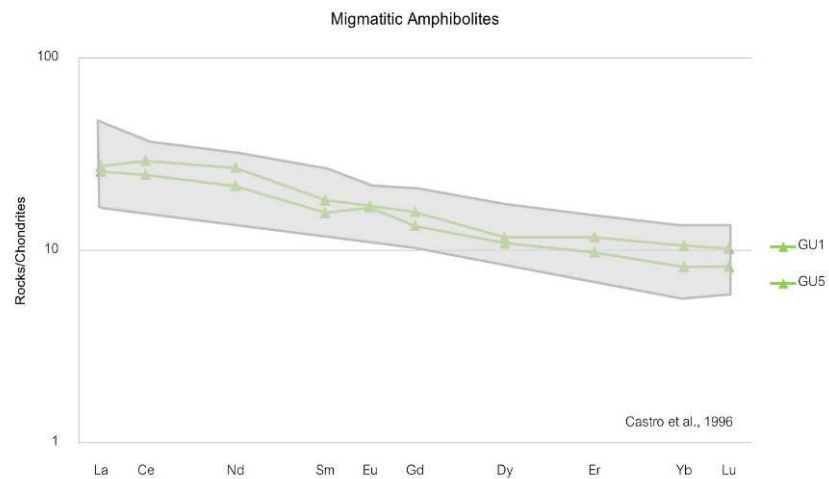


Figure 5.6. Chondrite-normalized REE patterns (chondrite composition after Sun and McDonough, 1989) of migmatitic amphibolites from Wang Nam Khiao Area compared to shaded pattern of normal amphibolites occurred in oceanic domain (after Castro et al., 1996).

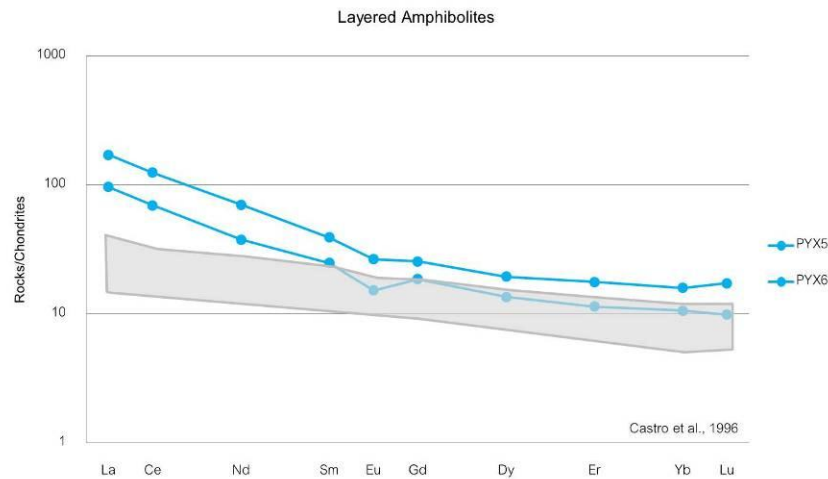


Figure 5.7. Chondrite-normalized REE patterns (chondrite composition after Sun and McDonough, 1989) of layered amphibolites from Wang Nam Khiao Area compared to shaded pattern of normal amphibolites occurred in oceanic domain (after Castro et al., 1996).

5.2 Metamorphism

ACF diagram, plots of mole proportions between A ($\text{Al}_2\text{O}_3 + \text{Fe}_2\text{O}_3 - (\text{Na}_2\text{O} + \text{K}_2\text{O})$), C ($\text{CaO} - 3.33\text{P}_2\text{O}_5$) and F ($\text{FeO} + \text{MgO} + \text{MnO}$), were selected for presentation of metamorphic facies of rock collection, particularly amphibolites, in this study (see Figure 5.8). Consequently, these rocks are significantly corresponding to amphibolites facies, based on their essential mineral assemblage (Nelson, 2011; Woudloper, 2009). The diagrams of individual rock types are shown in Appendix C.

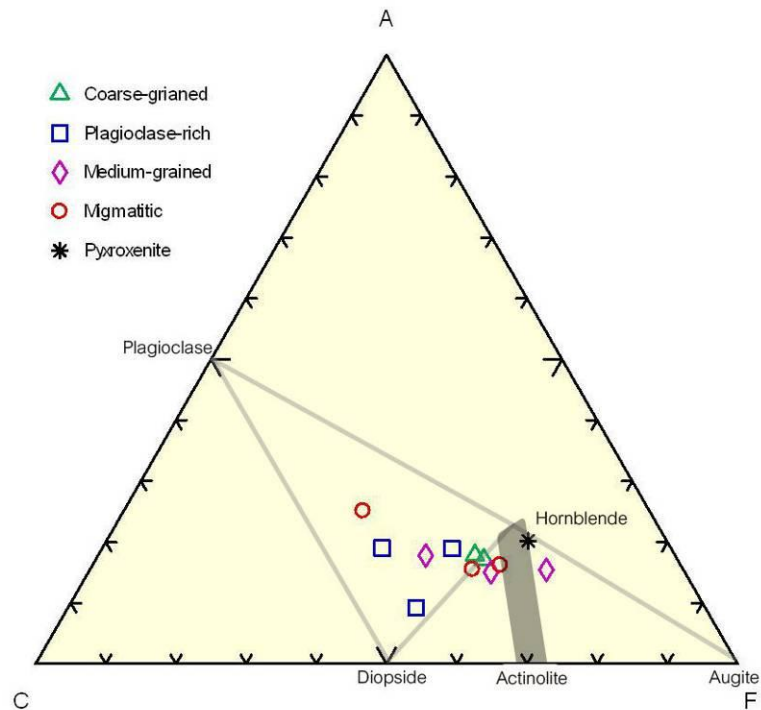


Figure 5.8. ACF diagram showing whole-rock chemical plots against essential mineral assemblages found in each rock type significantly suggesting amphibolite facies.

Amphibole thermobarometer (Amp-TB) was selected for additional investigation for pressure and temperature calculation of peak metamorphism. Amp-TB available for this study has been provided by Ridolfi et al. (2009) which is a spreadsheet operated under Microsoft Excel Office 2003. This spreadsheet allows calculating T-P-H₂O-melt-fO₂ conditions from the composition of calcic amphiboles. It gives reliable results within the ranges of 1064-766K, 73-1000 MPa, $-0.3 < \Delta\text{NNO} < 2.5$, H₂O-melt 3.4-10.6 wt%. Results of P-T calculation from amphibole analyses of all rock types are summarized in Table 5.1 and details are reported below. However, major compositions analyzed by EPMA should be selected prior to calculation using such spreadsheet which is recommended for the suitable ranges of 14-20% Al₂O₃, 1-13% CaO, <14% MgO, <12% FeO and < 2% TiO₂.

Table 5.1. P-T estimation of amphibolites from Wang Nam Khiao Area, using Amp-TB of Ridolfi et al. (2009).

Samples	Granular Amphibolites								
	Coarse-grained			Plagioclase-rich			Medium-grained		
	Qc-1	Qc-2	Qc-3	PYX8-3	PYX8-4	PYX8-5	Qf-7	Qf-8	Qf-9
SiO ₂ (wt.%)	42.41	42.53	42.56	42.51	42.64	42.4	42.23	41.52	41.98
TiO ₂ (wt.%)	2.21	2.1	2.09	1.59	1.5	1.53	2.1	2.25	2.55
Al ₂ O ₃ (wt.%)	14.45	14.44	14.33	11.56	11.43	11.52	12.17	12.81	12.5
FeO (wt.%)	10.85	10.73	10.85	14.19	14.17	14.12	13.42	13.91	13.11
MnO (wt.%)	0.14	0.12	0.19	0.3	0.28	0.23	0.2	0.17	0.16
MgO (wt.%)	14.33	14.69	14.53	12.92	12.9	12.82	14.61	14.3	14.82
CaO (wt.%)	11.52	11.33	11.36	12.4	12.41	12.29	11.16	11.52	11.03
Na ₂ O (wt.%)	2.32	2.28	2.4	2.73	2.93	2.94	2.43	2.41	2.47
K ₂ O (wt.%)	0.61	0.6	0.61	0.53	0.53	0.53	0.42	0.41	0.36
Check composition									
H ₂ O _{amp} (wt.%)	1.96	1.96	1.96	1.91	1.91	1.91	1.93	1.93	1.94
Fe ₂ O ₃ (wt.%)	7.81	9.29	8.62	3.86	3.04	3.15	12.46	12.25	13.09
FeO (wt.%)	3.82	2.37	3.1	10.72	11.44	11.29	2.21	2.89	1.33
O=F,Cl (wt.%)	0	0	0	0	0	0	0	0	0
Al#	0.18	0.17	0.17	0.11	0.12	0.12	0.03	0.02	0.01
Physical-chemical conditions									
uncertainty (σ_{est})	22	22	22	22	22	22	22	22	22
T (°C)	726	722	721	685	683	685	689	710	699
P (Kbar)	6.19	6.08	5.96	3.39	3.3	3.41	3.62	4.21	3.86
oceanic depth (km)	21.9	21.4	21	12	11.6	12	12.8	14.9	13.6
continental depth (km)	23.4	23	22.5	12.8	12.5	12.9	13.7	15.9	14.6

Based on suggested compositional ranges as mentioned above, analyses of amphiboles found in coarse-grained, plagioclase-rich and medium-grained granular amphibolites are more appropriate for this amphibole thermobarometer; on the other hand, those in migmatitic amphibolite, layered amphibolites and pyroxenite are invalid (see Appendix D). Compositions of amphibole in layered amphibolites appear to have more felsic composition whereas those in pyroxenite have more mafic composition but are mostly weathered. For migmatitic amphibolites, they must have higher temperature and pressure over the mafic solidus curve under water saturation of mafic composition (see Figure 5.9); then partial melting may have been taken place as suggested by many researchers (e.g., Schnetger, 1994; Brown et al., 1995; Hartek and Pattison, 1996; Jung et al., 1998). Therefore, amphiboles occurred in these rocks should have been modified their compositions, accordingly. Table 5.1 shows P-T conditions of all available rock

samples. Coarse-grained granular amphibolites yield 721-726°C and 5.96-6.19 Kbar; plagioclase-rich granular amphibolites fall within 683-685°C and 3.3-3.41 Kbar; medium-grained granular amphibolites yield 689-710°C and 3.62-4.61 Kbar. In general, these amphibolite may have equilibrated within a narrow range of $686.4 \pm 31.78^\circ\text{C}$ and 4.218 ± 1.0775 Kbar.

All temperature and pressure results calculated from Amp-TB are also plotted in a P-T path as shown in Figure 5.9. It clearly indicates that all of these amphibolites mainly belong to amphibolite facies and forwarding to granulite facies. Moreover, a few analyses of coarse-grained amphibolites are very close to melting curve of water-saturated basalt at higher pressure. Migmatitic amphibolites which their amphiboles are invalid this Amp-TB clearly indicate partial melting process of this amphibolites. For layered amphibolites, their compositions are partially involved by granite intrusion; therefore, their amphiboles are not suitable for this calculation. However, they may have been undertaken the same metamorphic condition prior to influence of igneous intrusion.

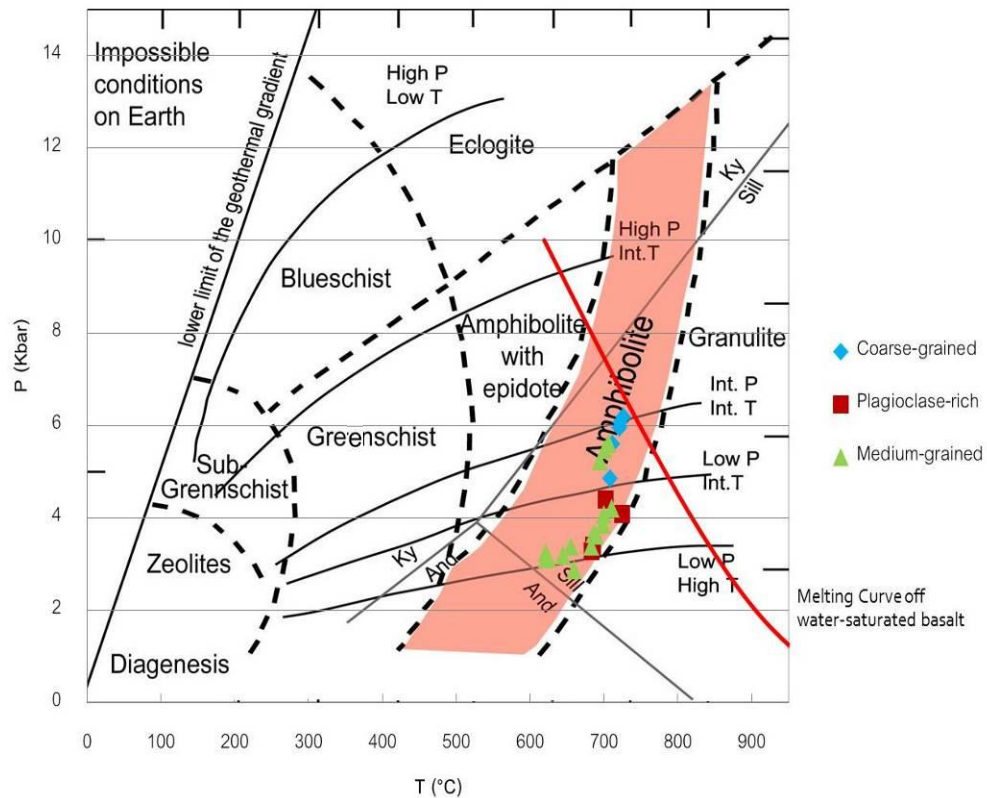


Figure 5.9. Plots of pressure and temperature (P-T) of amphiboles available under this study in correlation with metamorphic facies after Cambeses (2011). The red line is a melting curve of water saturated basalt (after Yoder and Tilley, 1962).

5.3 Ancient Tectonic Setting

Petrochemical data of amphibolites and related rocks indicate initial tholeiitic affinity prior to metamorphism. Trace elements and REE also show compositional signature of enriched mid-oceanic ridge basalt (E-MORB) composition as well as their spider patterns are similar to normal amphibolites in southwest Spain (Castro et al., 1996) in which they have been reported as MORB-derived composition in oceanic remnant. This E-MORB signature and tholeiite arc affinity may be associated with oceanic plate and convection current affected zone (Steven, 2002; Donnelly, 2004).

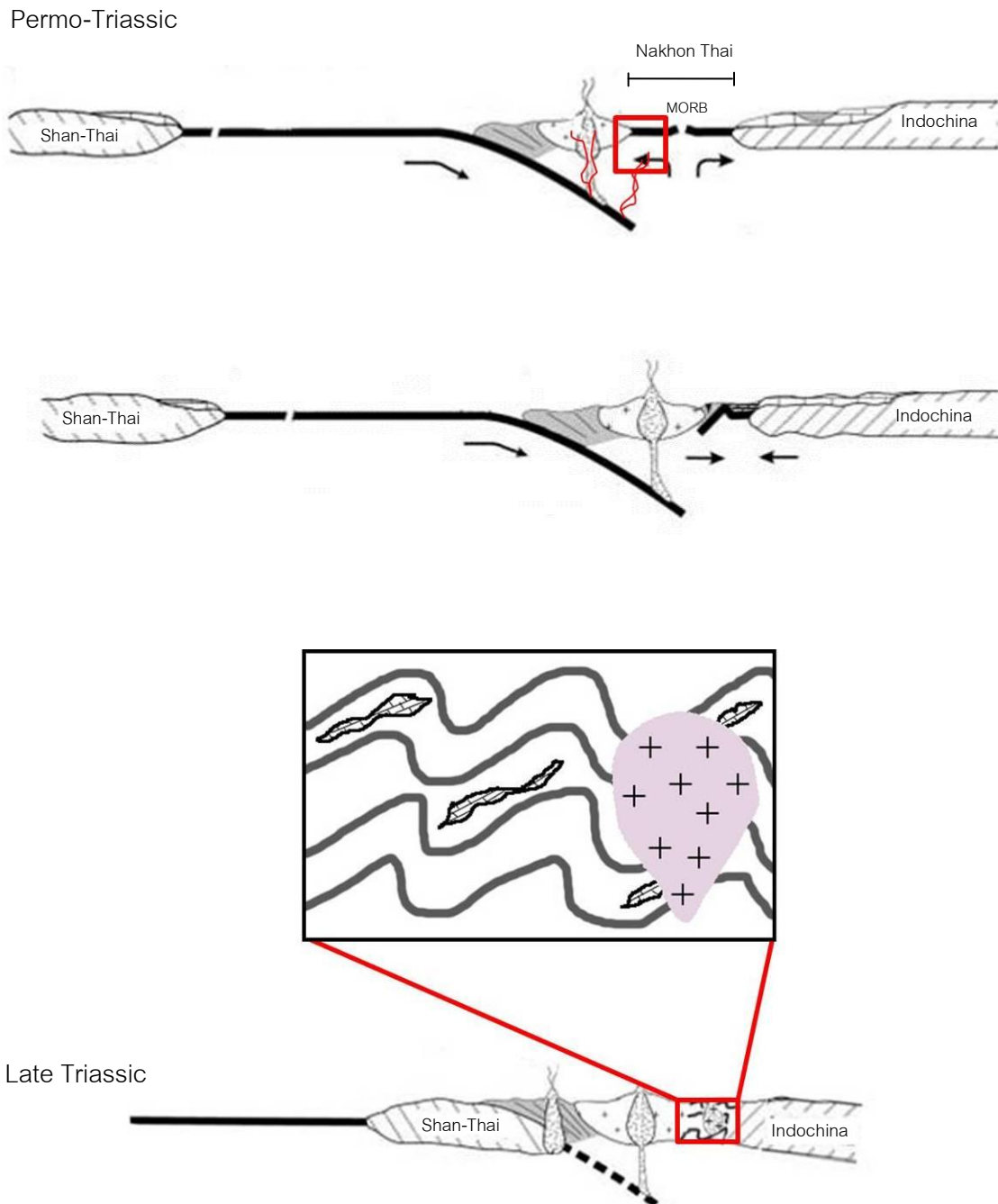


Figure 5.10. Ancient tectonic model of the study area as in red rectangular (modified after Sone and Metcalfe, 2008). Starting with E-MORB-involved tholeiitic arc terrane occurred in Permo-Triassic as a part of Nakhon Thai oceanic plate (Charusiri et al., 1997). Subsequently, Shan-Thai moved eastwards; consequently, its connected oceanic

plate (Lampang-Chiang Rai named by Charusiri et al., 1997) subducted into the Nakhon Thai, Compressional strength appear to have effected to Nakhonthai plates, continuously until ending of collision between Shan-Thai and Indochina microcontinents in Late Triassic (Charusiri et al., 1997). During the collision, it may introduce peak metamorphism to the study area. Subsequently, granite may have intruded into the study area as a consequence of partial melting caused by decompressional relaxation after collision.

During Permo-Triassic period, mantle plume and convection current has occurred and caused ancient subduction-related volcanic arc as well as sea floor spreading within back-arc basin yielding E-MORB involvement with arc tholeiitic magma suite of the study area. This original rock (protolith) may have occurred in Permo-Triassic (Ridd and Morley, 2011) along oceanic plate of Nakhon-Thai ocean floor laying between Shan-Thai and Indochina microcontinents (Charusiri et al., 1997). After the collision between Shan-Thai and Indochina microcontinents during late Triassic, this protolith may have metamorphosed under high pressure and temperature (see P-T path in Figure 5.9); consequently, various types of amphibolites have been equilibrated as peak metamorphism (see Figure 5.10). Granite intrusion in the northern area may subsequently take place in Triassic (Charusiri et al., 1993). These granites have been studied by Booncharoen (2011) and they also suggested oceanic island arc affinity of granite.

5.4 Conclusions

1. Amphibolites and related rocks (e.g., serpentized pyroxenite, granite, gabbro and phyllitic shale) have spread around an area of Ban Yup I Pun and Ban Nong Mai

Dang with. Amphibolites can be divided into five groups according to their physical properties, petrographic description, whole-rock geochemistry and mineral chemistry. They are composed of coarse-grained granular amphibolites, plagioclase-rich granular amphibolites, medium-grained granular amphibolites, migmatitic amphibolites and layered amphibolites.

2. Coarse-grained, plagioclase-rich and medium-grained granular amphibolites are different in grain size but they have the same mineral assemblage, mainly consisting actinolite and albite-oligoclase plagioclase. Geochemically, their major and minor oxides, trace elements and REE fall within the similar ranges assuming that they may have the same protolith before undertaking metamorphism and reaching amphibolite facies.

3. Migmatitic amphibolites are found associated with some coarse-grained marble in the study area. Their mineral assemblages and grain size are similar to medium-grained amphibolites. In addition, their whole-rock geochemistry is also quite similar but amphiboles occurred with both rock types have somewhat different composition caused by temperature and pressure higher than the water-saturated melting curve of basalt.

4. Layered amphibolites are associated with pink granite in the north of study area; therefore, its compositions appear to have been modified by metasomatism.

5. All amphibolites appear to have occurred in oceanic plate area, part of Nakhon Thai. Metamorphism caused by compression collision between Shan Thai and Indochina microcontinents during late Triassic would impact indirectly to E-MORB-involved tholeiitic in ancient arc terrane yielding different types of amphibolites.

REFERENCES

- Booncharoen, P. Petrography and geochemistry of granite from Ban Nong Mai Daeng, Tambon Wang Mee, Amphoe Wang Nam Keaw, Changwat Nakhon Ratchasima. Bachelor's Thesis, Department of Geology, Faculty of Science, Chulalongkorn University, 2011.
- Brown, M., Averkin, Y.A., McLellan, E.L., and Sawyer, E.W. Melt segregation in migmatites. Journal of Geophysical Research 15 (1995) : 15655-15679.
- Cambeses, A. Metamorphic facies diagram: Thin films of amphibolite (Sample ACEB-2). WeSapiens/Geologia [Online] 2011. Available from : http://www.wesapiens.org/static/image/geology/metamorphic_petrology/amphibolite_facies.jpg [2012, September 7]
- Castro, A., Fernandez, C., Rosa, J.D., Ventas, I.M., and Roger, G. Significance of MORB-derived Amphibolites from the Aracena Metamorphic Belt, Southwest Spain. Journal of Petrology (1996) : 235-260.
- Charusiri, P., Clark, A.H., Farrar, E., Archibald, D., and Charusiri, B. Granite belts in Thailand: evidence from the $^{40}\text{Ar}/^{39}\text{Ar}$ geochronological and geological syntheses. Journal of Southeast Asian Earth Sciences 14 (1993) : 127-136.
- Charusiri, P., Kosuwan, S., and Imsamut, S. Tectonic Evolution of Thailand: From Bunopas (1981)'s to a new scenario. International Conference on Stratigraphy and Tectonic Evolution of Southeast Asia and the South Pacific (1997) : 414-419.
- Chutakositkanon, V., and Hisada, K. Tectono-stratigraphy of the Sa Kaeo-Chanthaburi Accretionary Complex, eastern Thailand: reconstruction of tectonic evolution of

oceanic plate-Indochina collision. Proceedings of the International Symposia on Geoscience Resources and Environments of Asia Terranes (GREAT 2008), 4th IGCP 516, and 5th APSEG (November 2008) : 330-338.

Deer W.A., Howie, R.A., and Zussman, J. An Introduction to the Rock-forming Minerals. Addison Wesley Longman Limited, 1992.

Donnelly, K.E, Goldsteina, S.L., Langmuir, C.H., and Spiegelmana, M. Origin of enriched ocean ridge basalts and implications for mantle dynamics. Earth and Planetary Science Letters 226 (2004) : 347– 366.

Eyuboglu, Y., Santosh, M., Bektas S., and Chung S.L. Late Triassic subduction-related ultramafic–mafic magmatism in the Amasya region (eastern Pontides, N. Turkey): Implications for the ophiolite conundrum in Eastern Mediterranean. Journal of Asian Earth Sciences (2011) : 234–257.

Hartak, T.H.D., and Pattison, D.R.M. Genesis of the Kapuskasing (Ontario) migmatitic mafic granulites by dehydration melting of amphibolite: the importance of quartz to reaction progress. Journal of Metamorphic Geol (1996) : 591–611.

Hisada, K. Sugiyama, M., Ueno, K., and Charusiri, P. Missing Ophiolitic rocks along the Mae Yuam Fault as the Gondwana-Tethys divide in north-west Thailand. Island Arc 13 (2004) : 119-127.

Hutchison, C.S. Ophiolites in Southeast Asia. Geological Society of American Bulletin 6 (1975) : 797-806.

Irvine, T. N., and Baragar, W.R. A. A guide to the chemical classification of the common volcanic rocks. Can. J. Earth Sci (1971) : 523-548.

- Jian, P., and others. Devonian to Permian plate tectonic cycle of the Paleo-Tethys Orogen in southwest China (I): Geochemistry of ophiolites, arc/back-arc assemblages and within-plate igneous rocks. Lithos 113 (2008) : 748-765.
- Jung, S., Mezger, K., Masberg, P., Hoffer, E., and Hoernes, S. Petrology of an intrusion-related high-grade migmatite: implications for partial melting of metasedimentary rocks and leucosome-forming processes. Journal of Metamorphic Geol (1998) : 425–445.
- Klein, C., and Hurlbut, C.S. Manual of Mineralogy 20th edition 1977.
- Koroteev, V.A., Ogorodnikov, V.N., Sazonov, V.N., and Polenov, Y.A. Alkaline and acid metasomatism rocks in gneiss-amphibolite complexes of the Urals: a case history of the Ufaiei metamorphic block, southern Urals. Doklady Earth Science (2007) : 1160-1163.
- Kumalachan, P., and Yoemniyom, S. Emery. Department of Mineral Resources. 1978. (in Thai)
- Leake, B.E. 1997 Nomenclature of amphiboles : report of the subcommittee amphiboles of the international mineralogical association, commission on new minerals and mineral names. The Canadian Mineralogist 35 : 219-246.
- LeBas, M.J., LeMaitre, R.W., Streckeisen, A., and Zanettin, B. A chemical classification of volcanic rocks based on the total alkali silica diagram. J. Pet 27 (1986) : 745-750.
- Leblanc, M., and Temagout, A. Chromite pods in a lherzolite massif (Colla, Algeria): Evidence of oceanic-type mantle rocks along the West Mediterranean Alpine Belt. Lithos 23 (1989) : 153-162.

- Monroe, J.S., Wicander, R., and Hazlett, R. Physical Geology: Exploring the Earth, Sixth Edition. Thomson Brooks/Cole, 2007.
- Morimoto, N. Nomenclature of pyroxenes. Canadian Mineralogist. 27 (1989) : 143-156.
- Nelson, S.A. Metamorphic facies & metamorphism and plate tectonics. Earth Materials [Online]. 2004. Available from : http://www.tulane.edu/metamorphic_facies. [2012, September 7]
- Putthaphiban, P., Vichidchalerpong, A., and Boonprasert, T. Geologic Map of Thailand 1:50000 Ban Tha I Som (5337IV) and Ban Sap Bon (5337I). Department of Mineral Resources, 1981. (in Thai)
- Putthaphiban, P., Vichidchalerpong, A., and Boonprasert, T. Geologic Map of Thailand 1:50000 Ban Tha I Som (5337IV) and Ban Sap Bon (5337I). Department of Mineral Resources, 1989. (in Thai)
- Orberger, B., Lorand, J.P., Girardeau, J., Mercier, J.C.C., and Pitragool, S. Petrogenesis of ultramafic rocks and associated chromitites in the Nan-Uttaradit Ophiolite, northern Thailand. Lithos 35 (1995) : 153-182.
- Qasim, J.M. Geochemistry of amphibolites from the southern part of the Kohistom arc, north Pakistan. Mineralogical Magazine 52 (April 1988) : 147-159.
- Ravikant, V., Pal, T., and Das, D. Chromites from the Nidar ophiolite and Karzok complex, Transhimalaya, eastern Ladakh : their magmatic evolution. Journal of Asian Earth Sciences 24 (2004) : 177-184.
- Ridd, M.F., and Morley, C.K. The Khao Yai Fault on the southern margin of the Khorat Plateau, and the pattern of faulting in Southeast Thailand. Proceedings of the Geologists' Association 122 (2011) : 143-156.

- Ridolfi, F., Renzulli, A., and Puerini, M. Stability and chemical equilibrium of amphibole in calc-alkaline magmas: an overview, new thermobarometric formulations and application to subduction-related volcanoes. Contrib Mineral Petrol. (2009)
- Rollinson, H.R. Using geochemical data: evaluation, presentation and interpretation. Harlow: Longman Scientific and Technical Ltd., 1993.
- Salayapongse, S. Metamorphic rocks of Thailand. The Symposium on Geology of Thailand (Aug 2002) : 253-260.
- Schnetger, B. Partial melting during the evolution of the amphibolite- to granulite-facies gneisses of the Ivrea Zone, northern Italy. Chemical Geology 113 (1994) : 71-101.
- Seusutthiya K., and Maopeth, N. Petrography and Geochemistry of Ultramafic rocks at Ban Bun Tan, Suwankuha Subdistrict, NongBua Lamphu Province Bachelor's project, Department of Geology, Faculty of Science, Chulalongkorn University, 2001.
- Shi, R., and others. Melt/mentle mixing produces podiform chromite deposits in ophiolites: Implications of Re-Os systematics in the Dongqiao Neo-tethyan ophiolite, northern Tibet. Gondwana Research 21 (2012) : 194-206.
- Sone, M., and Metcalfe, I. Parallel Tethyan sutures in mainland Southeast Asia: New insights for Palaeo-Tethys closure and implications for the Indosinian orogeny. C.R.Geoscience 340 (2008) : 166-179.
- Steven, E. EMORB-sea floor basalt in the wrong place at the wrong time. Earth Science News [Online]. 2002. Available from : <http://www.records.viu.ca/earles/emorb-jan02.htm> [2002, September 23].

- Sun, S.S. and McDonough, W.F. Chemical and isotopic systematics of oceanic basalts: implications for mantle composition and processes. London: Geol. Soc. Spec. Publ., 1989.
- Sutthirat, C. Origin of mafic and ultramafic rocks and relation to geological sutures in Thailand. Final research report, Thailand Research Fund, Chulalongkorn University, 2009.
- Ueno, K., and Hisada, K. The Nan-Uttaradit-Sa Kaeo Sutures as a main Paleo-Tethyan suture in Thailand: Is it real? Gondwana Research 4 (2001) : 804-805.
- Wang, W.L., Aitchison, J.C., Lo, C.H., and Zeng Q.G. Geochemistry and geochronology of the amphibolite blocks in ophiolitic mélanges along Banong-Nujaing suture, central Tibet. Journal of Asian Earth Sciences (2008) : 122-138.
- Wimooktanun, V., Sopha, V., and Ratchasri D. Topographic map of Thailand scale 1:50,000 Ban Sub Bon. Department of Mineral Resources, 1989. (in Thai)
- Wimooktanun, V., Sopha, V., and Ratchasri D. Topographic map of Thailand scale 1:50,000 Ban Tha E Som. Department of Mineral Resources. Bangkok, 1989. (in Thai)
- Winter, JD. An introduction to igneous and metamorphic petrology. 2001.
- Wood, D.A. The application of a Th-Hf-Ta diagram to problems of tectonomagmatic classification and to establishing the nature of crustal contamination of basaltic lavas of the British Tertiary volcanic province. Earth Planet. Sc. Lett (1980)
- Woudloper. ACF diagram of Metamorphic facies. Wikipedia [Online]. 2009. Available from : http://en.wikipedia.org/wiki/File:ACFtriangles_EN.svg [2012, September 7]

Yoder, H.S. Jr., and C.E., Tilley. The melting curves for water-saturated basalts. Journal of Petrology 3 (1962)

APPENDICES

APPENDIX A

Whole-rock analyses of amphibolites and pyroxenite from Wang Nam Khiao, Nakhon Ratchasima. Major and minor oxides (% wt) yielded from XRF analysis and trace elements (ppm) obtained from ICP-MS analysis.

Name	Granular Amphibolite								Migmatitic Amphibolite			Layer Amphibolite			Pyroxenite
	Coarse		Plagioclase-rich				Medium		GU1	GU3	GU5	PYX4	PYX5	PYX6	PYX1
	QB1	QC	HT2	PYX3	QB4	PYX7	Sc	Qf							
Major Oxide (%)															
SiO ₂	45.45	45.01	48.76	50.16	50.08	47.49	46.82	49.31	48.53	49.65	48.70	61.53	73.61	71.76	42.90
Al ₂ O ₃	11.12	10.92	9.31	5.37	13.47	9.52	10.78	10.25	9.56	12.25	9.67	19.70	14.18	15.95	11.75
Fe ₂ O ₃	10.77	11.12	8.62	7.60	9.67	12.07	9.76	9.60	11.87	7.40	11.18	3.02	1.96	2.38	12.95
MgO	13.00	14.08	9.83	14.18	7.21	12.88	11.11	16.56	13.07	5.98	11.96	1.15	0.43	0.46	19.36
CaO	13.26	13.94	21.21	21.33	11.76	13.22	17.68	9.27	12.10	18.17	13.99	4.04	2.28	0.85	12.18
MnO	0.10	0.11	0.11	0.13	0.09	0.15	0.10	0.14	0.19	0.13	0.16	0.03	bdl	bdl	0.21
K ₂ O	0.72	0.78	0.21	0.15	1.02	0.88	0.60	2.39	0.80	0.21	0.94	0.40	2.60	3.92	0.06
Na ₂ O	1.77	1.89	0.16	0.54	3.86	1.26	1.30	1.34	1.45	2.32	1.30	9.38	4.31	3.94	0.22
TiO ₂	1.92	2.05	0.75	0.59	1.10	1.31	1.34	0.62	0.95	0.78	1.07	0.45	0.36	0.49	0.34
P ₂ O ₅	bdl	0.02	0.04	bdl	0.29	bdl	0.04	0.16	0.07	0.84	bdl	0.06	bdl	bdl	bdl
LOI	1.40	0.61	1.15	0.76	1.90	1.42	0.79	2.04	1.71	1.39	1.89	0.69	1.27	1.23	0.89
SUM	99.51	100.53	100.15	100.81	100.45	100.20	100.32	101.68	100.30	99.12	100.86	100.45	101.00	100.98	100.86
Elements (ppm)															
Ba	75.80	77.10	2.70	87.00	327.00	93.40	50.10	256.00	83.10	21.50	97.00	221.00	761.00	1600.00	113.00
Ce	4.10	6.20	9.20	16.30	18.70	11.00	5.50	19.00	17.90	28.00	15.20	60.70	42.40	76.00	2.20
Co	78.90	77.30	48.40	49.50	48.70	69.60	68.40	72.40	70.90	40.30	66.40	18.30	61.00	99.80	87.50
Cr	290.00	190.00	60.00	580.00	260.00	430.00	20.00	1600.00	700.00	bdl	770.00	10.00	bdl	bdl	220.00
Cu	83.00	129.00	8.00	7.00	25.00	115.00	70.00	7.00	47.00	19.00	64.00	207.00	13.00	12.00	286.00
Dy	2.87	3.53	2.15	3.86	3.10	3.94	2.65	1.88	2.97	3.87	2.78	4.83	3.43	4.94	1.40
Er	1.50	1.97	1.14	2.01	1.94	2.29	1.37	1.05	1.94	1.90	1.62	3.14	1.88	2.92	0.80
Eu	0.79	0.86	0.65	0.98	1.01	1.16	0.73	0.53	0.99	1.53	0.97	1.94	0.88	1.54	0.33
Ga	13.00	14.00	22.00	10.00	16.00	15.00	13.00	14.00	17.00	18.00	15.00	18.00	10.00	17.00	8.00
Gd	2.80	3.60	2.19	3.78	3.38	3.80	2.37	2.03	3.26	4.51	2.76	4.51	3.82	5.25	1.11
Hf	bdl	bdl	1.00	1.00	2.00	1.00	bdl	2.00	2.00	1.00	1.00	6.00	4.00	6.00	bdl
Ho	0.56	0.71	0.42	0.74	0.63	0.82	0.52	0.35	0.61	0.74	0.55	1.02	0.67	0.98	0.26
La	1.10	1.80	3.60	5.30	8.30	3.40	1.80	9.60	6.50	10.70	6.10	33.10	22.80	40.50	0.80
Lu	0.17	0.22	0.15	0.31	0.28	0.30	0.18	0.15	0.26	0.27	0.21	0.47	0.25	0.44	0.10
Nb	bdl	1.00	1.00	2.00	2.00	2.00	bdl	1.00	2.00	4.00	2.00	7.00	7.00	9.00	bdl
Nd	5.50	7.40	7.30	13.20	12.50	11.30	5.90	9.80	12.60	18.90	10.10	24.40	17.60	32.70	2.60
Ni	112.00	67.00	42.00	84.00	75.00	178.00	24.00	462.00	99.00	11.00	108.00	15.00	11.00	10.00	245.00
Pr	0.92	1.25	1.44	2.72	2.77	2.01	1.04	2.38	2.66	4.19	2.18	6.69	4.79	8.94	0.43
Rb	1.70	2.00	0.20	5.00	15.10	8.10	2.10	52.20	8.70	0.70	10.70	2.90	37.80	92.90	0.70
Sc	89.00	103.00	37.00	54.00	32.00	47.00	80.00	21.00	49.00	21.00	72.00	15.00	bdl	9.00	41.00
Sm	2.20	2.70	1.80	3.40	3.00	3.50	2.10	2.00	2.80	4.70	2.40	4.90	3.80	6.00	0.90
Sr	278.00	219.00	438.00	102.00	497.00	187.00	257.00	251.00	192.00	642.00	278.00	489.00	196.00	187.00	129.00
Tb	0.47	0.54	0.34	0.57	0.51	0.64	0.40	0.28	0.50	0.66	0.45	0.72	0.59	0.79	0.23
Th	0.10	0.10	1.00	0.60	1.30	0.40	0.10	3.00	1.10	1.50	0.60	8.00	12.30	11.20	0.10
Tm	0.18	0.25	0.16	0.31	0.28	0.31	0.17	0.14	0.28	0.31	0.24	0.51	0.28	0.41	0.10
Ti	11508.46	12287.68	4495.49	3536.45	6593.39	7852.13	8031.95	3716.27	5694.29	4675.31	6413.57	2697.30	2157.84	2937.06	2037.96
V	557.00	680.00	382.00	253.00	329.00	390.00	525.00	197.00	336.00	182.00	394.00	75.00	13.00	bdl	192.00
W	139.00	83.00	243.00	93.00	103.00	98.00	141.00	52.00	76.00	219.00	58.00	213.00	572.00	938.00	64.00
Y	14.10	17.60	10.50	19.40	17.20	19.80	12.60	9.80	16.90	17.60	14.50	29.40	18.60	26.20	6.60
Yb	1.10	1.50	1.00	1.90	1.80	1.90	1.00	0.90	1.80	1.50	1.40	3.50	1.80	2.70	0.60
Zn	36.00	74.00	43.00	95.00	52.00	102.00	38.00	243.00	95.00	89.00	75.00	11.00	26.00	54.00	69.00
Zr	13.30	18.00	27.20	32.70	54.10	29.70	18.80	50.20	47.60	31.50	32.20	199.00	127.00	210.00	9.40

* bdl = below detection limit

APPENDIX B

EPMA analyses of amphiboles in coarse-grained and plagioclase-rich granular amphibolites collected from Wang Nam Khiao Area.

Name	Granular Amphibolites														
	Coarse-grained									Plagioclase-rich					
	Qc-1	Qc-2	Qc-3	Qc-4	Qc-5	Qc-6	Qc-7	Qc-8	Qc-9	PYX8-3	PYX8-4	PYX8-5	PYX3-1	PYX3-2	PYX3-3
SiO ₂	42.41	42.53	42.56	44.24	43.65	43.94	43.30	42.40	43.03	42.51	42.64	42.40	43.77	43.59	42.22
TiO ₂	2.21	2.10	2.09	1.25	0.46	0.50	0.41	0.45	0.48	1.59	1.50	1.53	0.71	0.62	0.12
Al ₂ O ₃	14.45	14.44	14.33	13.68	13.18	13.66	13.41	13.24	14.01	11.56	11.43	11.52	13.13	12.96	12.59
FeO	10.85	10.73	10.85	11.29	11.44	12.67	12.78	12.94	12.05	14.19	14.17	14.12	10.27	10.59	10.93
MnO	0.14	0.12	0.19	0.12	0.13	0.13	0.17	0.13	0.17	0.30	0.28	0.23	0.10	0.15	0.10
MgO	14.33	14.69	14.53	14.42	14.35	13.20	13.32	14.14	14.36	12.92	12.90	12.82	16.02	16.58	16.25
CaO	11.52	11.33	11.36	11.92	12.62	12.40	12.34	12.59	12.51	12.40	12.41	12.29	12.63	12.36	13.42
Na ₂ O	2.32	2.28	2.40	1.80	2.00	2.29	2.37	2.32	2.17	2.73	2.93	2.94	2.03	2.12	2.14
K ₂ O	0.61	0.60	0.61	0.43	0.73	0.45	0.41	0.35	0.30	0.53	0.53	0.53	0.09	0.12	0.03
Total	98.83	98.80	98.93	99.14	98.56	99.24	98.51	98.54	99.09	98.74	98.79	98.37	98.73	99.10	97.81
Si	6.127	6.136	6.141	6.345	6.343	6.357	6.327	6.217	6.229	6.288	6.305	6.294	6.295	6.262	6.193
Ti	0.240	0.228	0.227	0.135	0.050	0.054	0.045	0.050	0.052	0.176	0.166	0.170	0.077	0.067	0.014
Al	2.460	2.455	2.438	2.313	2.258	2.331	2.311	2.289	2.392	2.016	1.992	2.016	2.226	2.195	2.176
Fe ³⁺	0.069	0.109	0.062	0.227	0.390	0.185	0.300	0.685	0.576	0.261	0.189	0.166	0.677	0.803	1.188
Fe ²⁺	1.242	1.186	1.247	1.127	1.000	1.348	1.262	0.901	0.883	1.494	1.563	1.586	0.558	0.469	0.153
Mn	0.017	0.014	0.024	0.014	0.016	0.016	0.020	0.016	0.020	0.038	0.035	0.029	0.012	0.018	0.013
Mg	3.084	3.157	3.124	3.081	3.107	2.847	2.901	3.090	3.098	2.848	2.844	2.837	3.433	3.549	3.552
Ca	1.784	1.751	1.757	1.832	1.964	1.922	1.933	1.978	1.940	1.964	1.966	1.956	1.946	1.902	2.110
Na	0.651	0.637	0.672	0.501	0.562	0.644	0.672	0.658	0.610	0.784	0.840	0.846	0.565	0.592	0.609
K	0.111	0.110	0.113	0.078	0.136	0.083	0.076	0.065	0.056	0.101	0.100	0.100	0.016	0.022	0.005
Total	15.785	15.782	15.805	15.653	15.826	15.787	15.847	15.950	15.856	15.971	16.002	16.000	15.806	15.880	16.013
Atomic (%)															
Mg	49.9	50.9	50.5	49.2	48.1	45.2	45.4	46.4	47.7	43.4	43.3	43.3	51.9	52.8	50.7
Fe	21.2	20.9	21.2	21.6	21.5	24.3	24.4	23.8	22.5	26.7	26.7	26.8	18.7	18.9	19.1
Ca	28.9	28.2	28.4	29.2	30.4	30.5	30.2	29.7	29.9	29.9	30.0	29.9	29.4	28.3	30.1

EPMA analyses of amphiboles in medium-grained granular amphibolites collected from Wang Nam Khiao Area.

Name	Medium-grained granular amphibolites												
	Qf-2	Qf-3	Qf-5	Qf-7	Qf-8	Qf-9	N-1	N-2	N-4	N-5	Scv-1	Scv-2	Scv-3
SiO ₂	41.96	41.66	42.56	42.23	41.52	41.98	42.67	43.21	52.02	52.02	42.83	42.60	42.68
TiO ₂	0.77	1.54	1.02	2.10	2.25	2.55	3.15	3.73	0.39	0.39	1.55	1.57	1.57
Al ₂ O ₃	11.49	11.82	12.50	12.17	12.81	12.50	11.33	11.75	10.96	10.96	13.69	13.82	13.89
FeO	15.12	15.47	13.59	13.42	13.91	13.11	15.94	15.97	16.16	16.16	14.18	14.09	13.50
MnO	0.45	0.28	0.14	0.20	0.17	0.16	0.23	0.14	0.24	0.24	0.18	0.19	0.22
MgO	12.78	12.32	13.82	14.61	14.30	14.82	11.35	11.29	9.69	9.69	12.80	12.62	12.70
CaO	12.44	12.02	13.04	11.16	11.52	11.03	11.44	11.71	9.07	9.07	11.66	11.88	12.08
Na ₂ O	2.78	2.77	2.20	2.43	2.41	2.47	1.09	1.87	0.33	0.33	2.27	2.32	2.31
K ₂ O	0.34	0.24	0.04	0.42	0.41	0.36	1.33	0.11	0.21	0.21	0.66	0.65	0.64
Total	98.12	98.11	98.92	98.74	99.30	98.97	98.52	99.79	99.07	99.07	99.80	99.74	99.58
Si	6.279	6.231	6.236	6.191	6.079	6.130	6.343	6.308	7.370	7.370	6.219	6.196	6.202
Ti	0.087	0.173	0.112	0.232	0.247	0.280	0.352	0.410	0.041	0.041	0.169	0.171	0.172
Al	2.026	2.083	2.159	2.103	2.211	2.151	1.986	2.023	1.831	1.831	2.344	2.370	2.380
Fe ³⁺	0.561	0.398	0.769	0.427	0.573	0.404	0.088	0.000	0.000	0.000	0.181	0.188	0.158
Fe ²⁺	1.330	1.537	0.896	1.219	1.130	1.198	1.894	1.950	1.915	1.915	1.541	1.526	1.483
Mn	0.057	0.036	0.017	0.025	0.022	0.020	0.029	0.017	0.029	0.029	0.022	0.023	0.027
Mg	2.850	2.747	3.017	3.191	3.121	3.226	2.515	2.457	2.045	2.045	2.770	2.736	2.750
Ca	1.994	1.927	2.048	1.753	1.807	1.725	1.822	1.832	1.377	1.377	1.814	1.852	1.881
Na	0.808	0.802	0.626	0.691	0.683	0.698	0.314	0.529	0.090	0.090	0.639	0.653	0.652
K	0.064	0.046	0.008	0.078	0.076	0.067	0.253	0.020	0.039	0.039	0.123	0.120	0.118
Total	16.057	15.979	15.889	15.910	15.948	15.897	15.595	15.545	14.738	14.738	15.821	15.835	15.822
Atomic (%)													
Mg	42.3	41.6	44.8	48.4	47.1	49.2	39.8	39.4	38.3	38.3	43.9	43.4	43.8
Fe	28.1	29.3	24.7	25.0	25.7	24.4	31.4	31.3	35.9	35.9	27.3	27.2	26.2
Ca	29.6	29.2	30.4	26.6	27.3	26.3	28.8	29.4	25.8	25.8	28.8	29.4	30.0

EPMA analyses of amphiboles in migmatitic amphibolites and layered amphibolites collected from Wang Nam Khiao Area.

Name	Migmatitic Amphibolites									Layered Amphibolites		
	GU1-4	GU1-5	GU1-6	GU1-8	GU1-9	GU1-10	GU1-11	GU1-12	GU1-13	PYX4-1	PYX4-2	PYX4-3
SiO ₂	44.33	44.34	45.41	41.16	41.83	47.52	44.56	43.16	43.83	58.09	55.49	56.67
TiO ₂	0.00	0.05	0.03	0.04	0.00	0.00	0.00	0.04	0.00	0.13	0.24	0.19
Al ₂ O ₃	12.98	12.17	13.11	14.05	13.27	14.83	11.67	12.05	11.27	2.91	5.95	4.28
FeO	9.01	9.11	7.28	11.04	11.86	9.54	11.54	11.04	11.86	11.23	13.74	12.21
MnO	0.26	0.22	0.15	0.32	0.34	0.32	0.36	0.32	0.34	0.35	0.33	0.32
MgO	19.83	20.75	20.95	18.81	18.40	16.59	19.30	18.81	18.40	17.38	15.20	16.12
CaO	12.08	11.94	12.45	12.80	12.66	10.79	13.20	12.80	12.66	8.55	8.48	8.78
Na ₂ O	0.19	0.26	0.14	0.26	0.17	0.11	0.09	0.26	0.17	0.12	0.23	0.13
K ₂ O	0.03	0.03	0.00	0.07	0.03	0.07	0.02	0.07	0.03	0.08	0.14	0.08
Total	98.70	98.86	99.52	98.56	98.55	99.77	100.75	98.56	98.55	98.83	99.78	98.78
Si	6.292	6.292	6.332	5.962	6.070	6.586	6.298	6.234	6.342	8.028	7.704	7.886
Ti	0.000	0.005	0.003	0.005	0.000	0.000	0.000	0.005	0.000	0.013	0.025	0.020
Al	2.171	2.037	2.154	2.399	2.270	2.423	1.944	2.052	1.922	0.473	0.973	0.702
Fe ³⁺	0.000	0.000	0.000	0.000	0.000	0.000	0.000	0.000	0.000	0.000	0.000	0.000
Fe ²⁺	1.069	1.081	0.849	1.338	1.439	1.106	1.364	1.334	1.435	1.298	1.595	1.421
Mn	0.031	0.026	0.018	0.040	0.042	0.038	0.044	0.039	0.042	0.041	0.038	0.038
Mg	4.194	4.390	4.353	4.060	3.979	3.427	4.066	4.049	3.967	3.581	3.146	3.342
Ca	1.837	1.815	1.860	1.987	1.969	1.602	1.999	1.981	1.963	1.266	1.261	1.310
Na	0.052	0.072	0.038	0.073	0.048	0.030	0.023	0.073	0.048	0.031	0.062	0.036
K	0.005	0.005	0.000	0.013	0.005	0.012	0.004	0.013	0.005	0.014	0.024	0.015
Total	15.651	15.723	15.607	15.876	15.821	15.223	15.743	15.778	15.723	14.745	14.828	14.769
Atomic (%)												
Mg	59.1	60.2	61.6	55.0	53.9	55.9	54.7	55.0	53.9	58.3	52.4	55.0
Fe	15.1	14.8	12.0	18.1	19.5	18.0	18.4	18.1	19.5	21.1	26.6	23.4
Ca	25.9	24.9	26.3	26.9	26.7	26.1	26.9	26.9	26.7	20.6	21.0	21.6

EPMA analyses of plagioclase in plagioclase-rich granular amphibolites, medium-grained granular amphibolites and migmatitic amphibolites collected from Wang Nam Khiao Area.

Name	Granular Amphibolites						Migmatitic Amphibolites											
	Plagioclase-rich			Medium-grained														
	PYX8-1	PYX8-2	PYX8-4	QBd-1	QBd-2	QBd-3	GU3-2	GU3-3	GU3-4	GU3-5	GU3-6	GU3-7	GU3-8	GU3-9	GU3-10	GD2-1	GD2-2	GD2-3
SiO ₂	67.31	61.97	61.81	60.31	59.20	60.08	67.15	67.54	67.33	67.55	67.48	67.14	67.34	67.09	67.03	66.42	66.16	66.72
TiO ₂	0.02	0.01	0.00	0.02	0.00	0.04	0.08	0.03	0.00	0.02	0.00	0.00	0.00	0.00	0.02	0.04	0.00	0.00
Al ₂ O ₃	19.27	20.67	20.00	24.10	24.69	24.00	20.12	20.86	20.85	19.81	19.96	20.10	20.50	20.00	20.10	20.47	20.34	20.36
FeO	0.10	0.09	0.04	0.13	0.09	0.09	0.03	0.00	0.03	0.04	0.00	0.07	0.04	0.05	0.04	0.13	0.19	0.29
MnO	0.01	0.00	0.00	0.00	0.00	0.01	0.01	0.00	0.00	0.00	0.01	0.00	0.00	0.00	0.00	0.03	0.00	0.04
MgO	0.01	0.07	0.00	0.00	0.01	0.00	0.01	0.00	0.00	0.00	0.00	0.00	0.00	0.00	0.05	0.03	0.00	0.00
CaO	0.08	5.31	4.91	5.84	5.56	5.84	0.39	0.39	0.41	0.35	0.64	0.24	0.41	0.49	0.24	10.04	10.43	10.11
Na ₂ O	11.34	11.89	11.95	9.97	9.53	9.55	10.45	10.08	10.57	10.81	10.36	11.04	11.00	10.71	10.56	3.50	2.80	0.88
K ₂ O	0.07	0.07	0.10	0.24	0.31	0.28	0.05	0.05	0.06	0.05	0.09	0.06	0.07	0.05	0.09	0.02	0.04	0.03
Total	98.23	100.07	98.80	100.63	99.39	99.89	98.30	98.94	99.25	98.63	98.53	98.64	99.36	98.39	98.12	100.68	99.95	98.42
Si	2.992	2.786	2.811	2.688	2.667	2.694	2.974	2.965	2.955	2.984	2.982	2.969	2.958	2.973	2.974	2.897	2.902	2.942
Ti	0.001	0.000	0.000	0.001	0.000	0.001	0.003	0.001	0.000	0.001	0.000	0.000	0.000	0.000	0.001	0.001	0.000	0.000
Al	1.010	1.096	1.072	1.267	1.311	1.269	1.051	1.080	1.079	1.032	1.040	1.048	1.062	1.045	1.052	1.052	1.052	1.058
Fe	0.004	0.003	0.002	0.005	0.004	0.003	0.001	0.000	0.001	0.002	0.000	0.003	0.002	0.002	0.001	0.005	0.007	0.011
Mn	0.000	0.000	0.000	0.000	0.000	0.000	0.000	0.000	0.000	0.000	0.000	0.000	0.000	0.000	0.000	0.001	0.000	0.001
Mg	0.000	0.004	0.000	0.000	0.001	0.000	0.001	0.000	0.000	0.000	0.000	0.000	0.000	0.000	0.003	0.002	0.000	0.000
Ca	0.004	0.256	0.239	0.279	0.268	0.281	0.019	0.018	0.019	0.016	0.030	0.012	0.019	0.023	0.011	0.469	0.490	0.477
Na	0.977	1.036	1.053	0.862	0.832	0.830	0.898	0.858	0.900	0.926	0.887	0.947	0.937	0.920	0.908	0.296	0.238	0.075
K	0.004	0.004	0.006	0.014	0.018	0.016	0.003	0.003	0.003	0.003	0.005	0.003	0.004	0.003	0.005	0.001	0.002	0.001
Total	4.993	5.186	5.183	5.116	5.102	5.094	4.949	4.925	4.957	4.964	4.944	4.982	4.981	4.966	4.956	4.725	4.691	4.567
Atomic (%)																		
An	0.4	19.7	18.4	24.2	24.0	24.9	2.0	2.1	2.1	1.7	3.3	1.2	2.0	2.4	1.2	61.2	67.1	86.2
Ab	99.2	80.0	81.1	74.6	74.4	73.7	97.6	97.6	97.5	98.0	96.2	98.5	97.6	97.2	98.2	38.6	32.6	13.6
Or	0.4	0.3	0.4	1.2	1.6	1.4	0.3	0.3	0.4	0.3	0.5	0.3	0.4	0.3	0.5	0.2	0.3	0.3

EPMA analyses of plagioclase in layered amphibolites and pyroxenite collected from Wang Nam Khiao Area.

Name	Layered Amphibolites								Pyroxenite										
	PYX4-1	PYX4-2	PYX4-3	PYX4-4	PYX4-5	PYX4-6	PYX6-1	PYX6-2	N-a3-1	N-a3-3	N-u1-1	N-u1-2	N-u1-3	N-u2-1	N-u2-2	N-u2-3	N-1-1	N-1-2	N-1-3
SiO ₂	64.66	62.33	64.94	65.97	64.52	65.91	67.66	67.84	54.61	55.84	55.54	55.16	54.85	55.18	53.31	54.88	51.79	52.25	52.79
TiO ₂	0.04	0.01	0.00	0.00	0.00	0.03	0.00	0.05	0.02	0.01	0.00	0.00	0.00	0.00	0.03	0.04	0.01	0.03	0.08
Al ₂ O ₃	21.71	22.56	21.33	20.47	20.77	20.50	19.95	19.73	28.56	28.00	28.47	28.54	28.65	29.34	30.36	29.45	29.92	30.47	29.22
FeO	0.04	0.04	0.07	0.01	0.11	0.04	0.12	0.46	0.02	0.08	0.09	0.05	0.00	0.09	0.09	0.09	0.20	0.30	0.09
MnO	0.00	0.00	0.01	0.00	0.00	0.03	0.04	0.00	0.00	0.00	0.00	0.00	0.02	0.01	0.00	0.00	0.01	0.01	0.00
MgO	0.00	0.00	0.00	0.01	0.00	0.01	0.00	0.02	0.00	0.00	0.00	0.00	0.00	0.00	0.01	0.01	0.02	0.00	0.01
CaO	3.13	4.37	2.94	1.98	2.78	2.02	0.10	0.16	12.14	11.54	11.68	11.73	12.21	12.03	13.34	12.36	12.14	12.18	11.58
Na ₂ O	9.46	9.85	9.59	10.75	10.65	10.54	10.77	10.49	4.34	4.03	4.54	4.95	4.44	4.68	3.89	4.56	4.57	4.54	5.05
K ₂ O	0.11	0.14	0.08	0.09	0.09	0.09	0.04	0.09	0.05	0.02	0.02	0.02	0.02	0.04	0.03	0.14	0.03	0.03	0.03
Total	99.14	99.30	98.95	99.27	98.93	99.16	98.67	98.84	99.73	99.51	100.33	100.46	100.19	101.37	101.05	101.52	98.68	99.82	98.85
Si	2.868	2.787	2.884	2.920	2.880	2.919	2.986	2.991	2.468	2.516	2.490	2.476	2.468	2.455	2.389	2.443	2.379	2.373	2.416
Ti	0.001	0.000	0.000	0.000	0.000	0.001	0.000	0.002	0.001	0.000	0.000	0.000	0.000	0.000	0.001	0.001	0.000	0.001	0.003
Al	1.135	1.189	1.117	1.068	1.093	1.071	1.038	1.026	1.522	1.487	1.505	1.510	1.520	1.539	1.604	1.545	1.620	1.631	1.577
Fe	0.001	0.001	0.003	0.000	0.004	0.001	0.004	0.017	0.001	0.003	0.003	0.002	0.000	0.003	0.004	0.003	0.008	0.011	0.004
Mn	0.000	0.000	0.001	0.000	0.000	0.001	0.001	0.000	0.000	0.000	0.000	0.000	0.001	0.000	0.000	0.000	0.000	0.000	0.000
Mg	0.000	0.000	0.000	0.001	0.000	0.001	0.000	0.001	0.000	0.000	0.000	0.000	0.000	0.000	0.001	0.001	0.001	0.000	0.001
Ca	0.149	0.209	0.140	0.094	0.133	0.096	0.004	0.007	0.588	0.557	0.561	0.564	0.589	0.574	0.640	0.589	0.598	0.593	0.568
Na	0.813	0.854	0.825	0.922	0.921	0.905	0.921	0.897	0.380	0.352	0.395	0.431	0.387	0.404	0.338	0.393	0.407	0.400	0.449
K	0.006	0.008	0.004	0.005	0.005	0.005	0.002	0.005	0.003	0.001	0.001	0.001	0.001	0.002	0.002	0.008	0.002	0.002	0.001
Total	4.973	5.049	4.973	5.010	5.037	5.000	4.957	4.946	4.962	4.917	4.955	4.985	4.966	4.978	4.978	4.984	5.015	5.011	5.018
Atomic (%)																			
An	15.4	19.5	14.4	9.2	12.6	9.5	0.5	0.8	60.6	61.2	58.6	56.6	60.2	58.5	65.4	59.5	59.4	59.6	55.8
Ab	84.0	79.7	85.1	90.3	87.0	90.0	99.2	98.6	39.2	38.7	41.3	43.2	39.6	41.2	34.5	39.7	40.4	40.2	44.1
Or	0.6	0.8	0.4	0.5	0.5	0.5	0.3	0.6	0.3	0.1	0.1	0.1	0.1	0.2	0.2	0.8	0.2	0.2	0.1

EPMA analyses of pyroxenes in plagioclase-rich granular amphibolites and medium-grained granular amphibolites collected from Wang Nam Khiao Area.

Name	Granular Amphibolites																	
	Plagioclase-rich									Medium-grained								
	PYX3-1	PYX3-2	PYX3-3	PYX8-1	PYX8-2	PYX8-3	PYX8-4	PYX8-5	PYX8-6	Qf-1	Qf-2	Qf-3	Qf-4	Qf-5	N-1	N-2	N-3	N-5
SiO ₂	50.60	50.54	49.78	52.37	52.22	52.35	52.07	52.01	52.16	51.24	50.92	54.89	54.44	53.33	52.37	52.00	53.46	51.94
TiO ₂	0.51	0.44	0.63	0.04	0.03	0.09	0.11	0.09	0.05	0.04	0.09	0.06	0.09	0.04	0.30	0.28	0.18	0.27
Al ₂ O ₃	5.22	5.22	6.53	0.91	0.98	0.99	1.19	1.20	1.14	5.22	5.63	4.25	4.56	5.10	5.80	5.98	4.62	5.90
FeO	8.29	7.07	8.27	7.27	6.83	7.18	7.36	7.77	7.42	14.51	14.72	9.58	9.10	9.29	13.84	15.38	13.20	15.00
MnO	0.18	0.14	0.21	0.41	0.43	0.40	0.39	0.44	0.38	0.26	0.28	0.14	0.15	0.14	0.27	0.33	0.31	0.31
MgO	15.43	14.74	14.53	14.00	13.82	13.92	13.77	13.70	13.52	15.92	15.23	18.72	18.31	18.61	14.93	14.60	15.67	14.94
CaO	19.55	21.60	20.13	23.71	23.95	23.74	23.55	23.63	23.41	12.24	12.03	12.70	12.63	12.61	11.20	10.35	11.01	10.56
Na ₂ O	0.31	0.36	0.35	0.39	0.49	0.46	0.48	0.51	0.48	0.64	0.96	0.22	0.29	0.35	0.77	0.77	0.61	0.89
K ₂ O	0.00	0.00	0.01	0.00	0.00	0.00	0.00	0.00	0.02	0.17	0.18	0.06	0.05	0.11	0.06	0.06	0.02	0.06
Total	100.09	100.10	100.43	99.09	98.74	99.11	98.91	99.36	98.57	100.23	100.04	100.62	99.61	99.56	99.54	99.76	99.08	99.88
Si	1.868	1.867	1.836	1.970	1.970	1.969	1.963	1.958	1.973	1.902	1.896	1.969	1.968	1.936	1.936	1.929	1.975	1.924
Ti	0.014	0.012	0.018	0.001	0.001	0.002	0.003	0.002	0.001	0.001	0.003	0.002	0.002	0.001	0.008	0.008	0.005	0.008
Al	0.227	0.227	0.284	0.040	0.044	0.044	0.053	0.053	0.051	0.228	0.247	0.180	0.195	0.218	0.253	0.261	0.201	0.258
Fe ³⁺	0.046	0.061	0.053	0.068	0.074	0.070	0.074	0.094	0.055	0.031	0.049	0.000	0.000	0.000	0.000	0.000	0.000	0.000
Fe ²⁺	0.209	0.157	0.202	0.161	0.142	0.156	0.158	0.151	0.179	0.420	0.409	0.287	0.275	0.282	0.428	0.477	0.408	0.465
Mn	0.006	0.004	0.007	0.013	0.014	0.013	0.012	0.014	0.012	0.008	0.009	0.004	0.004	0.004	0.009	0.010	0.010	0.010
Mg	0.849	0.811	0.798	0.785	0.777	0.780	0.774	0.769	0.762	0.880	0.845	1.001	0.986	1.007	0.823	0.807	0.863	0.825
Ca	0.773	0.855	0.795	0.956	0.968	0.957	0.952	0.953	0.949	0.487	0.480	0.488	0.489	0.490	0.444	0.411	0.436	0.419
Na	0.022	0.026	0.025	0.028	0.035	0.033	0.035	0.037	0.035	0.046	0.069	0.015	0.020	0.024	0.055	0.056	0.044	0.064
K	0.000	0.000	0.000	0.000	0.000	0.000	0.000	0.000	0.001	0.008	0.009	0.003	0.002	0.005	0.003	0.003	0.001	0.003
Total	4.015	4.020	4.018	4.023	4.025	4.024	4.025	4.031	4.019	4.010	4.016	3.949	3.943	3.968	3.958	3.962	3.942	3.973
Atomic (%)																		
Mg	45.2	43.1	43.2	39.9	39.6	39.7	39.5	39.1	39.2	48.4	47.4	56.3	56.3	56.6	48.6	47.6	50.6	48.3
Fe	13.6	11.6	13.8	11.6	11.0	11.5	11.9	12.4	12.1	24.8	25.7	16.2	15.7	15.9	25.3	28.1	23.9	27.2
Ca	41.2	45.3	43.0	48.5	49.4	48.7	48.6	48.5	48.8	26.8	26.9	27.5	27.9	27.6	26.2	24.3	25.5	24.5

EPMA analyses of pyroxenes in migmatitic amphibolites collected from Wang Nam Khiao Area.

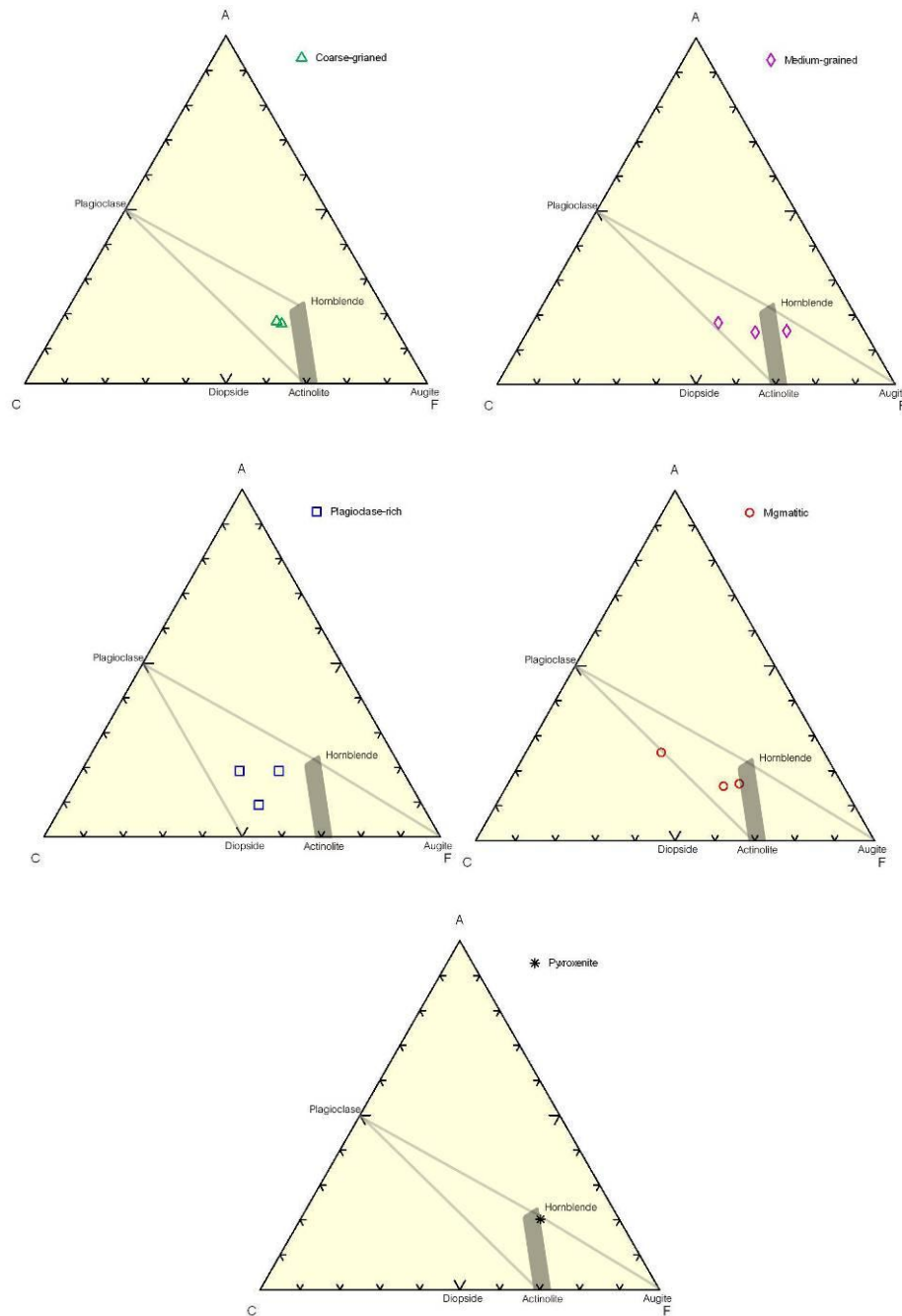
Name	Migmatitic Amphibolites														
	GU1-1	GU1-2	GU1-3	GU1-4	GU1-5	GU1-6	GU1-7	GU1-8	GU1-9	GU3-1	GU3-2	GU3-3	GU3-4	GU3-5	GU3-6
SiO ₂	54.94	54.33	54.34	57.41	58.11	57.27	59.50	59.43	58.16	54.56	53.16	53.83	59.39	60.84	59.39
TiO ₂	0.05	0.00	0.05	0.03	0.03	0.04	0.03	0.02	0.06	0.00	0.04	0.00	0.00	0.00	0.00
Al ₂ O ₃	2.93	2.98	2.17	1.11	0.87	1.12	0.95	0.76	1.32	1.67	2.05	1.27	2.83	1.12	2.83
FeO	9.78	9.01	9.11	7.28	7.09	6.95	7.09	7.13	7.40	11.54	11.04	11.86	9.54	7.90	9.54
MnO	0.27	0.26	0.22	0.15	0.15	0.12	0.15	0.18	0.17	0.36	0.32	0.34	0.32	0.32	0.32
MgO	20.46	19.83	20.75	20.95	20.75	20.36	19.39	19.48	20.16	19.30	18.81	18.40	16.59	17.56	16.59
CaO	11.99	12.08	11.94	12.45	12.69	12.88	12.44	12.49	12.58	13.20	12.80	12.66	10.79	11.14	10.79
Na ₂ O	0.24	0.19	0.26	0.14	0.20	0.09	0.19	0.11	0.33	0.09	0.26	0.17	0.11	0.02	0.11
K ₂ O	0.03	0.03	0.03	0.00	0.02	0.03	0.02	0.00	0.06	0.02	0.07	0.03	0.07	0.03	0.07
Total	100.67	98.70	98.86	99.52	99.90	98.87	99.76	99.61	100.24	100.75	98.56	98.55	99.63	98.94	99.63
Si	1.972	1.983	1.983	2.054	2.068	2.061	2.110	2.112	2.065	1.984	1.974	2.003	2.115	2.164	2.115
Ti	0.001	0.000	0.001	0.001	0.001	0.001	0.001	0.001	0.001	0.000	0.001	0.000	0.000	0.000	0.000
Al	0.124	0.128	0.094	0.047	0.036	0.048	0.040	0.032	0.055	0.072	0.090	0.056	0.119	0.047	0.119
Fe ³⁺	0.000	0.000	0.000	0.000	0.000	0.000	0.000	0.000	0.000	0.000	0.000	0.000	0.000	0.000	0.000
Fe ²⁺	0.294	0.275	0.278	0.218	0.211	0.209	0.210	0.212	0.220	0.351	0.343	0.369	0.284	0.235	0.284
Mn	0.008	0.008	0.007	0.005	0.005	0.004	0.005	0.005	0.005	0.011	0.010	0.011	0.010	0.010	0.010
Mg	1.095	1.079	1.129	1.117	1.101	1.092	1.025	1.031	1.067	1.046	1.041	1.020	0.880	0.931	0.880
Ca	0.461	0.472	0.467	0.477	0.484	0.497	0.473	0.476	0.479	0.514	0.509	0.505	0.412	0.424	0.412
Na	0.017	0.013	0.018	0.010	0.013	0.007	0.013	0.008	0.023	0.006	0.019	0.012	0.008	0.002	0.008
K	0.001	0.001	0.001	0.000	0.001	0.001	0.001	0.000	0.003	0.001	0.003	0.001	0.003	0.001	0.003
Total	3.973	3.960	3.978	3.927	3.920	3.918	3.876	3.876	3.918	3.984	3.991	3.976	3.831	3.814	3.831
Atomic (%)															
Mg	59.2	59.1	60.2	61.6	61.3	60.7	60.0	60.0	60.4	54.7	55.0	53.9	55.9	58.5	55.9
Fe	15.9	15.1	14.8	12.0	11.8	11.6	12.3	12.3	12.4	18.4	18.1	19.5	18.0	14.8	18.0
Ca	24.9	25.9	24.9	26.3	27.0	27.6	27.7	27.7	27.1	26.9	26.9	26.7	26.1	26.7	26.1

EPMA analyses of pyroxenes in layered amphibolites and pyroxenite collected from Wang Nam Khiao Area.

Name	Layered Amphibolites				Pyroxenite											
	PYX4-1	PYX4-2	PYX4-3	PYX4-4	PYX-1	PYX-2	PYX-3	PYX-6	PYX-7	PYX-8	PYX-9	PYX-10	PYX-11	PYX-12		
SiO ₂	52.61	52.66	55.49	56.67	54.03	54.91	54.81	57.74	51.74	57.05	57.16	56.84	57.74	57.05		
TiO ₂	0.13	0.14	0.24	0.19	0.01	0.02	0.00	0.53	0.74	0.57	0.39	0.50	0.53	0.57		
Al ₂ O ₃	5.18	5.14	5.95	4.28	0.07	0.12	0.09	3.55	4.72	4.60	4.77	4.98	3.55	4.60		
FeO	11.58	11.42	13.74	12.21	11.36	11.37	11.28	7.03	9.75	6.62	7.73	7.06	7.03	6.62		
MnO	0.34	0.32	0.33	0.32	0.14	0.11	0.10	0.30	0.09	0.17	0.19	0.10	0.30	0.17		
MgO	16.12	15.85	15.20	16.12	22.22	22.03	22.47	13.59	21.34	14.57	15.81	14.58	13.59	14.57		
CaO	12.55	12.03	8.48	8.78	12.14	12.27	12.11	15.49	12.24	14.60	12.65	14.72	15.49	14.60		
Na ₂ O	0.52	0.59	0.23	0.13	0.07	0.03	0.02	0.07	0.04	0.08	0.15	0.07	0.07	0.08		
K ₂ O	0.11	0.10	0.14	0.08	0.02	0.00	0.00	0.00	0.05	0.01	0.01	0.00	0.00	0.01		
Total	99.12	98.24	99.78	98.78	100.05	100.85	100.86	98.31	100.70	98.26	98.86	98.86	98.31	98.26		
Si	1.942	1.955	2.010	2.057	1.977	1.989	1.984	2.092	1.869	2.060	2.051	2.045	2.092	2.060		
Ti	0.004	0.004	0.006	0.005	0.000	0.001	0.000	0.014	0.020	0.015	0.010	0.014	0.014	0.015		
Al	0.225	0.225	0.254	0.183	0.003	0.005	0.004	0.152	0.201	0.196	0.202	0.211	0.152	0.196		
Fe ³⁺	0.000	0.000	0.000	0.000	0.073	0.028	0.044	0.000	0.041	0.000	0.000	0.000	0.000	0.000		
Fe ²⁺	0.357	0.355	0.416	0.371	0.274	0.316	0.297	0.213	0.254	0.200	0.232	0.212	0.213	0.200		
Mn	0.010	0.010	0.010	0.010	0.004	0.003	0.003	0.009	0.003	0.005	0.006	0.003	0.009	0.005		
Mg	0.887	0.877	0.821	0.872	1.211	1.189	1.212	0.734	1.148	0.784	0.846	0.782	0.734	0.784		
Ca	0.496	0.479	0.329	0.342	0.476	0.476	0.470	0.601	0.473	0.565	0.486	0.567	0.601	0.565		
Na	0.037	0.042	0.016	0.009	0.005	0.002	0.001	0.005	0.003	0.005	0.010	0.005	0.005	0.005		
K	0.005	0.005	0.006	0.004	0.001	0.000	0.000	0.000	0.002	0.000	0.000	0.000	0.000	0.000		
Total	3.963	3.952	3.868	3.853	4.025	4.009	4.015	3.820	4.014	3.830	3.843	3.839	3.820	3.830		
Atomic (%)																
Mg	51.0	51.3	52.4	55.0	59.5	59.2	59.9	47.4	59.9	50.6	54.1	50.1	47.4	50.6		
Fe	20.5	20.7	26.6	23.4	17.1	17.1	16.9	13.8	15.4	12.9	14.8	13.6	13.8	12.9		
Ca	28.5	28.0	21.0	21.6	23.4	23.7	23.2	38.8	24.7	36.5	31.1	36.3	38.8	36.5		

APPENDIX C

Metamorphic facies diagram of coarse-grained, plagioclase-rich, medium-grained granular amphibolites, migmatitic amphibolites, layered amphibolites and pyroxenite



P-T calculation of medium-grained granular amphibolites from Wang Nam Khiao Area (Amp-TB of Ridolfi et al., 2009)

Sample	Medium-grained Granular Amphibolites																					
	Qf-2	Qf-3	Qf-5	Qf-7	Qf-8	Qf-9	Qf-10	Qf-11	Qf-12	Qf-13	Qf-14	N-1	N-2	N-4	N-5	Scv-1	Scv-2	Scv-3	QBd-1	QBd-2	QBd-3	QBd-5
SiO ₂ (wt.%)	41.96	41.66	42.56	42.23	41.52	41.98	53.13	51.4	49.62	49.94	49.95	42.67	43.21	52.02	52.02	42.83	42.6	42.68	44.6	44.17	45.26	43.31
TiO ₂ (wt.%)	0.77	1.54	1.02	2.1	2.25	2.55	0.02	0.14	0.24	0.12	0.24	3.15	3.73	0.39	0.39	1.55	1.57	1.57	1.63	1	1	0
Al ₂ O ₃ (wt.%)	11.49	11.82	12.5	12.17	12.81	12.5	10.71	11.25	11.24	11.57	11.29	11.33	11.75	10.96	10.96	13.69	13.82	13.89	11.51	11.5	11.9	11.06
FeO (wt.%)	15.12	15.47	13.59	13.42	13.91	13.11	8.15	9.17	8.94	9.2	8.63	15.94	15.97	16.16	16.16	14.18	14.09	13.5	14.96	15.11	14.72	15.14
MnO (wt.%)	0.45	0.28	0.14	0.2	0.17	0.16	0.14	0.19	0.18	0.21	0.17	0.23	0.14	0.24	0.24	0.18	0.19	0.22	0.31	0.26	0.31	0
MgO (wt.%)	12.78	12.32	13.82	14.61	14.3	14.82	18	17.93	19.25	17.56	17.46	11.35	11.29	9.69	9.69	12.8	12.62	12.7	12.69	12.96	13.4	14
CaO (wt.%)	12.44	12.02	13.04	11.16	11.52	11.03	9.25	8.13	9.93	10.76	10.68	11.44	11.71	9.07	9.07	11.66	11.88	12.08	10.89	10.96	11.02	12.25
Na ₂ O (wt.%)	2.78	2.77	2.2	2.43	2.41	2.47	0.14	0.19	0.14	0.25	0.24	1.09	1.87	0.33	0.33	2.27	2.32	2.31	1.79	1.81	1.73	2.88
K ₂ O (wt.%)	0.34	0.24	0.04	0.42	0.41	0.36	0.09	0.38	0.41	0.18	0.27	1.33	0.11	0.21	0.21	0.66	0.65	0.64	0.51	0.49	0.36	0.1
Check composition																						
H ₂ O _{amp} (wt.%)	1.89	1.89	1.93	1.93	1.93	1.94	2.08	2.05	2.05	2.05	2.04	1.9	1.94	2	2	1.95	1.95	1.95	1.94	1.92	1.96	1.92
Fe ₂ O ₃ (wt.%)	6.02	6.42	6.7	12.46	12.25	13.09	0	0	5.13	17.1	15.55	6.54	5.29	0	0	7.96	6.78	5.55	9.9	11.23	11.91	8.85
FeO (wt.%)	9.71	9.69	7.56	2.21	2.89	1.33	8.15	9.17	4.32	-6.18	-5.36	10.06	11.21	16.16	16.16	7.02	7.99	8.51	6.05	5.01	4	7.18
O=F,Cl (wt.%)	0	0	0	0	0	0	0	0	0	0	0	0	0	0	0	0	0	0	0	0	0	0
Physical-chemical conditions																						
uncertainty (σ_{est})	22	22	22	22	22	22	invalid	invalid	invalid	invalid	invalid	22	22	invalid	invalid	22	22	22	22	22	22	22
T (°C)	683	686	700	689	710	699	invalid	invalid	invalid	invalid	invalid	645	655	invalid	invalid	694	701	706	621	624	621	659
P (Kbar)	3.39	3.67	4.08	3.62	4.21	3.86	invalid	invalid	invalid	invalid	invalid	3.19	3.39	invalid	invalid	5.24	5.49	5.62	3.11	3.14	3.26	2.89
oceanic depth (km)	12	12.9	14.4	12.8	14.9	13.6	invalid	invalid	invalid	invalid	invalid	11.3	12	invalid	invalid	18.5	19.4	19.8	11	11.1	11.5	10.2
continental depth (km)	12.8	13.9	15.4	13.7	15.9	14.6	invalid	invalid	invalid	invalid	invalid	12	12.8	invalid	invalid	19.8	20.7	21.2	11.7	11.9	12.3	10.9

BIOGRAPHY

Miss Vanachawan Hunyek was born in Trang, Thailand on 2nd February 1987. She completed high school from Buranarumluk School, Trang in 2004. After finished the high school, she was studying at Department of Geology, Faculty of Science, and Chulalongkorn University and got a scholarship from the Development and Promotion of Science and Technology Talents project (DPST). She graduated her Bachelor's Degree (B.Sc.) in Geology in 2008 focused on small foraminiferas in tsunami sediments. After completed the B.Sc., she got the DPST's scholarship and continued to start her Master's Degree Program in Geology at Chulalongkorn University. Her research has been focused on amphibolites in Amphoe Wang Nam Khiao Area, Changwat Nakhon Ratchasima, Thailand and published in Proceedings for the 7th Conference on Science and Technology for Youth 2012; 51-62.